POLYMERIZED SILICONE MICROEMULSIONS

THE POLYMERIZATION AND APPLICATION OF SILICONE MICROEMULSIONS IN THE DEVELOPMENT OF NANOSTRUCTURED MATERIALS

By Marlena E. Whinton, H.B.Sc

A thesis

Submitted to the School of Graduate Studies

In Partial Fulfillment of the Requirements for the Degree of

Doctor of Philosophy

McMaster University Doctor of Philosophy (2015) Hamilton, Ontario

(Chemical Biology)

TITLE: The Polymerization and Application of Silicone Microemulsions in the Development of Nanostructured Materials

AUTHOR: Marlena E. Whinton, H.B.Sc. (McMaster University)

SUPERVISOR: Professor Michael A. Brook

NUMBER OF PAGES: xv, 132

Lay Abstract

This thesis is about the chemical modification and polymerization of nanostructured liquids in the form of silicone microemulsions to create nanoporous silicone elastomers (nano is one billionth, 10^{-9}, so 1 nanometer = 1 billionth of meter). Despite the highly prevalent commercial use of silicones and the utility of silicone elastomers, little is known about the polymerization of silicone microemulsions to create nanoporous materials. The first goal of this thesis was to polymerize silicone microemulsions, using methods that have been previously used in the polymerization of hydrocarbon microemulsions. Silicone microemulsions were successfully polymerized using a reactive surfactant and rigidification of the oil phase was achieved using common silicone crosslinking chemistry. The second goal was to understand how the type of chemistry affects changes in structure upon transition from liquid microemulsion to solid polymer. Nanostructuring was retained in polymerized microemulsions both with and without oil phase polymerization. Finally, the third goal was to exploit silicone microemulsion domains to control titanium dioxide particle formation. Particle formation was slowed as a result of domain constricted particle growth.

Abstract

Microemulsions are nanostructured dispersions that have unique properties, which make them attractive for applications such as biomaterials, drug delivery, and nanoparticle synthesis. The behaviour of hydrocarbon microemulsions and their applications have been extensively studied, however, there have been very few studies in the preparation or the polymerization of silicone microemulsions. Silicone microemulsions offer a unique template by which to create novel nanoporous silicone elastomers and/or hydrogels. The prevalent use of silicones in biomaterials, coatings, and personal care (to name a few) make the development of silicone-based microemulsions of particular interest.

The aim of thesis research was to polymerize silicone microemulsions and to understand the factors that contribute to retaining initial template morphology in the polymeric product. Chapter Two of this thesis focuses on the preparation of silicone microemulsions containing a non-polymerizable and polymerizable trisiloxane surfactant, respectively. Formulations were prepared and characterized by electrical conductivity to determine the microemulsion structure type. Formulations located in the bicontinuous region of the phase diagram were polymerized, producing transparent silicone elastomers.

The focus of Chapter Three was to determine the tolerance of silicone microemulsions to selected chemistry that is relevant to silicone polymers. Previous work done in the field of polymerizing silicone microemulsions has been based on radical polymerization processes. There are no reports that examine the polymerization of a silicone microemulsion by room temperature vulcanization (RTV), a common process for creating

silicone elastomers. We aimed to better understand the effects of RTV cure on morphology retention from the liquid to polymeric product to determine if this type of chemistry could be used in the formation of nanoporous silicone elastomers either on its own or in conjunction with a radical polymerization process. In order to understand the effects of an RTV process on polymer structure, we examined the effect of the variable components (necessary for the RTV cure) on the silicone microemulsion template. Small angle X-ray scattering (SAXS) and transmission electron microscopy (TEM) were used as tools to characterize materials prior to and after cure. Silicone microemulsions that were cured using the RTV process produced nanoporous polymeric elastomers, however, the initial bicontinuous microemulsion template was not retained. RTV cured microemulsions retained the bicontinuous structure if the RTV cure was preceded by a photopolymerization reaction to "lock-in" surfactant monomers at the oil/water interface.

Chapter Four explores the use of silicone microemulsions as a reaction vehicle in the formation of nano-TiO_2 particles. The focus of this chapter was the exploitation of microemulsion droplets and bicontinuous structures that were designed to retard TiO_2 particle formation in situ. Titanium isopropoxide (TTIP) was incorporated into silicone microemulsions containing varying amounts of water. Interactions between TTIP and the trisiloxane polyether surfactant result in the formation of a compound containing a Ti^{4+}, coordinated to silicone surfactant molecules via a polyether linkage. Titania forms in situ as water is titrated into the surfactant/oil mixture, resulting in the formation of a microemulsion. The formation of TiO_2 was monitored by UV-Vis spectroscopy and the TiO_2 particles were characterized using transmission electron microscopy.

Acknowledgements

I would first, and foremost, like to acknowledge my Ph.D. supervisor, Dr. Michael A. Brook, whom has provided endless support and patience through my studies. His enthusiasm and passion for research has been exceptionally motivating over the years. Mike has provided countless professional opportunities through conferences and collaborations. In addition, he was instrumental in helping me reach my own career aspirations and for that, I will always be grateful. I feel fortunate that have been part of the Brook Group and I could not have asked for a better graduate supervisor. I would also like to thank my committee members, Dr. Kalai Saravanamuttu and Dr. Todd Hoare, for all their suggestions. They've helped me to see alternative perspectives and to be a scientist outside of my comfort zone.

I would like to thank Marcia Reid of the Electron Microscopy Facility for all her help over the years. She has always enthusiastically helped me with preparing and imaging samples that were neither easy to prepare nor easy to image. A special thanks also goes to Tammy Feher who has always gone above and beyond to help me with any administrative challenge, question, or need. I've also always enjoyed our conversations!

Of course I have to thank my group members. I would do individual shout-outs, but you've all been equally fantastic. I've loved our coffee breaks, educational (and non educational) chats, and all the help you've provided throughout the years. I could always turn to my group members for any problem I needed help, guidance, or advice on. Dr. Dan Chen, you captain that ship and you do it well. Ok, so I lied. I did do a shout-out.

I have to thank my family for all their support. My mom and dad have rarely ever let me pay for a dinner out on account of my “student” status. I suppose I have a lot of dinners that I will need to make up for now. I couldn’t have survived the last five years without their encouragement and loving words.

Finally, I have to thank my husband who, up until this point, has probably thought that I completely forgot to acknowledge him. Well Mr. Mark Kyle McGrath, I always save the best for last. You have been on this journey with me since 2011 and I can’t thank you enough for the support, understanding, patience, and love that you have shown me. We met, fell in love, and got married, all while I was still working towards completing my degree. I know there are times when you thought it would never end. This Ph.D. thesis is also your Ph.D. thesis. I love you and thank-you.

Table of Contents

1. CHAPTER 1: INTRODUCTION 1

1.1. Overview 1

1.1.1. Silicone Fluids 1

1.1.2. Functional Silicones 2

1.1.3. Siloxane Surfactants 4

1.2. Silicone Crosslinking 8

1.3. Silicones in Nano & Biomaterials 12

1.4. Microemulsions 14

1.4.1. Microemulsion Structure 15

1.4.2. Phase Behaviour 16

1.4.3. Microemulsion Stability 18

1.4.4. Silicone Microemulsions 20

1.5. Microemulsion Polymerization 23

1.5.1. Microemulsion Polymerization to form Latex Particles 24

1.5.2. Nanoporous Solids from Microemulsion Polymerization 25

1.5.3. Polymerization in Silicone Microemulsions 27

1.6. Microemulsion Characterization 29

1.6.1. Electron Microscopy & Preparation Techniques 29

1.6.2. Electrical Conductivity 31

1.6.3. Small Angle X-ray Scattering (SAXS) 32

1.7. Applications of Microemulsions 33

1.8. Thesis Focus 37

1.9. References 39

2. CHAPTER 2: ELASTOMERIC HYDROGELS BY POLYMERIZATION SILICONE MICROEMULSIONS 47

2.1. Abstract 47

2.2. Introduction 47

2.3. Results & Discussion 49

2.4. Conclusion & Acknowledgements 56

2.5. Experimental 56

2.5.1. Materials 56

2.5.2. Formation of Microemulsions 57

2.6. References & Notes 59

3. CHAPTER 3: SILICONE MICROEMULSION STRUCTURES ARE MAINTAINED DURING POLYMERIZATION USING REACTIVE SURFACTANTS 61

3.1. Abstract 61

3.2. Introduction 62

3.3. Experimental 65

3.3.1. Materials 65

3.3.2. Microemulsion Formulation 66

3.3.3. Conductivity Measurements 67

3.3.4. Microemulsion Formulations Prepared for Polymerization 67

3.3.5. RTV Silicone Cure 67

3.3.6. Photopolymerization 68

3.3.7. Structural Determination by Small Angle X-ray Scattering (SAXS) 69

3.3.8. Transmission Electron Microscopy 71

3.4. Results 72

3.4.1. Effect of RTV Additives on Microemulsion Morphology 72

3.4.2. RTV (Condensation) Polymerization of Silicone Microemulsions 74

3.4.3. Photopolymerization of Silicone Microemulsions 74

3.4.4. Dual Polymerization of Silicone Microemulsions: RTV Cure & Photopolymerization 76

3.4.5. Transmission Electron Microscopy of Polymerized Materials 77

3.5. Discussion 78

3.6. Conclusion 83

3.7. Acknowledgments 83

3.8. References 84

4. CHAPTER 4: VERY SLOW FORMATION OF TIO_2 NANOPARTICLES BY HYDROLYSIS OF AN ALKOXYTITANATE WITHIN A BICONTINUOUS SILICONE/WATER MICROEMULSION 87

4.1. Abstract 87

4.2. Introduction 87

4.3. Experimental Section 90

4.3.1. Materials 90
4.3.2. Methods 90

4.4. Results 92

4.4.1 Particle Size Distribution 97

4.5. Discussion 99

4.6. Conclusion 105

4.7. Supporting Information 106

4.8. Acknowledgements 107

4.9. References 107

5. CHAPTER 5: GENERAL CONCLUSIONS 109

6. CHAPTER 6: APPENDIX 116

6.1. Supporting Information for CHAPTER 2: Elastomeric hydrogels by polymerizing silicone microemulsions 116

6.1.1. Characterization 117

6.2. Supporting Information for CHAPTER 3: Silicone Microemulsion Structures are maintained during Microemulsion Polymerization using Reactive Surfactants 120

6.3. Supporting Information for CHAPTER 4: Very slow formation of TiO_2 nanoparticles by hydrolysis of an alkoxytitanate within a bicontinuous silicone/water microemulsion 121

6.3.1. General Methods 121
6.3.2. Microemulsion Formulations with Mass Quantities 126
6.3.3. Additional UV-Vis Absorbance Spectra 128
6.3.4. Transmission Electron Microscopy 128

LIST OF FIGURES, TABLES & CHARTS

FIGURE 1.1.1: THE FORMATION OF SILICONE POLYMER FROM DIMETHYLDICHLOROSILANE BY ACID/BASE EQUILIBRATION 1
FIGURE 1.1.2: FORMATION OF HYDRIDE FUNCTIONALIZED PDMS FROM AN EQUILIBRATION REACTION 3
FIGURE 1.1.3: SILOXANE SURFACTANT ARCHITECTURES 4
FIGURE 1.2.1: CROSSLINKING OF SILICONES BY TETRAFUNCTIONAL SILANES OR FUNCTIONALLY-TERMINATED PDMS 8
FIGURE 1.2.2: SILICONE CROSSLINKING VIA RADICAL AND PLATINUM-CATALYZED HYDROSILYLATION REACTION 9
FIGURE 1.2.3: FORMATION OF HYDROXYL METAL CATALYST AND CROSSLINKING OF SILICONE WITH TETRAFUNCTIONAL SILANE 11
FIGURE 1.4.1: A: WINSOR I, III, II MICROEMULSIONS AND B: POSSIBLE STRUCTURES OF WINSOR TYPE IV MICROEMULSIONS 15
FIGURE 1.6.1: A REPRESENTATIVE CONDUCTIVITY CURVE FOR THE STRUCTURAL TRANSITIONS BETWEEN W/O-BICONTINUOUS-O/W IN A MICROEMULSION. 32
FIGURE 1.7.1: MICELLIZATION OF TITANIUM ALKOXIDE AND SUBSEQUENT NUCLEATION AND FORMATION OF PRIMARY TITANIA PARTICLES 35
FIGURE 2.3.1: SILSURF A008-UP, **2**: SILMER ACR A008-UP (N~8), A: FORMATION OF SILICA UNDER THE SAME REACTION CONDITIONS, B: CONDENSATION CURE OF SILICONES 50
FIGURE 2.3.2: PHASE DIAGRAMS ACCORDING TO ENTRY 6, TABLE 2.3.1. 51
FIGURE 2.3.3: TOP VIEW OF POLYMERIZED MICROEMULSION AFTER A DE/REHYDRATION CYCLE (VIAL DIAMETER ~ 1 CM). 53
FIGURE 2.3.4: POLYMERIZED MICROEMULSION ABSORPTION OF PHENOL RED OVER TIME (HOURS) (VIAL DIAMETER ~ 1.5 CM). 53
A 55
FIGURE 2.3.5: MODEL OF THE INTERNAL WATER/SILICONE OIL INTERFACE DURING CROSSLINKING/PHOTOPOLYMERIZATION. 55
FIGURE 3.3.1: PHASE DIAGRAM FOR ACR A008-UP/OH-PDMS/30WT% HEMA-WATER. THE BICONTINUOUS ZONE IS SHOWN IN RED. 66
FIGURE 3.3.2: PHOTOPOLYMERIZATION OF SURFACTANT WITH HYDROPHILIC MONOMER, HEMA. 69
$q = 4\pi\lambda\mathrm{SIN}\theta 2$ 70
FIGURE 3.4.1: TEM MICROGRAPHS OF SELECTED CURED MICROEMULSIONS A: PHOTOPOLYMERIZED MICROEMULSION (TABLE 3.3.1, FORMULATION 6); B: PHOTOPOLYMERIZED & RTV MICROEMULSION (TABLE 3.3.1, FORMULATION 8); C: RTV CURE MICROEMULSION (TABLE 3.3.1, FORMULATION 3). 78
FIGURE 4.3.1: SILSURF A008-UP. 90
FIGURE 4.4.1: FORMATION OF TIO$_2$ PARTICLES IN MICROEMULSION: A: TRANSETHERIFICATION OF TTIP WITH THE SURFACTANT SILSURF A008 UP. B: HYDROLYSIS AND C: CONDENSATION/MICELLIZATION D: FORMATION OF TIO$_2$ PARTICLES THAT ADSORB ONTO THE SURFACE OF A E: W/O OR F: BICONTINUOUS MICROEMULSION 94
FIGURE 4.5.1: MODEL SHOWING BICONTINUOUS MICROEMULSION DOMAINS CONSTRAINING TIO$_2$ PARTICLE AGGREGATION INITIALLY TO THE SIZE OF THE AQUEOUS DOMAINS. A: HYDROLYSIS AND CONDENSATION LEADING TO MICELLES AND TIO$_2$ PARTICLES. B: EXPANSION OF DOMAINS OVER TIME, WHICH REQUIRES REORGANIZATION OF THE DOMAINS, ALLOWS PARTICLE AGGREGATION. 105
FIGURE 6.1.1: CONDUCTIVITY PLOT FOR μE BASED ON WATER TITRATION INTO SURFACTANT/OIL MIXTURE USING SURFACTANT:OIL RATIO FROM FORMULATION 1 (TABLE 6.1.1, ENTRY 1). 118

FIGURE 6.1.2: PHASE DIAGRAMS FOR μE FORMED WITH: A: WATER, 15-35 CST SILICONE OIL + 1, B: 10% HEMA IN WATER, 45-85 CST SILICONE OIL + 1. X INDICATES HIGH WATER/LOW SURFACTANT ZONES THAT WERE SEEN ONLY WITH SURFACTANT 1. 118
FIGURE 6.1.3: SEM IMAGES USING GOLD COATING OF THE MICROGEL (TABLE 2.5.3.5.1, ENTRY 10) AT THREE MAGNIFICATIONS. SCALE BAR = 10 μM, 100 NM AND 100 NM. 119
FIGURE 6.1.4: RELEASE CURVE FOR PHENOL RED IN THE MICROGEL (, ENTRY 10). C_0: RELEASED CONCENTRATION; C: TOTAL CONCENTRATION. 119
FIGURE 6.3.1: RAW MATERIAL INTERACTIONS BETWEEN TTIP AND SURFACTANT MONOMER RESULTING IN THE SYNTHESIS OF A004-UP-TITANIUM ALKOXIDES 1-3 WITH PREDICTED SUBSTITUTION ON TITANIUM CENTER. 122
FIGURE 6.3.2: ^{1}H NMR OF 1 123
FIGURE 6.3.3: ^{1}H NMR OF 2 124
FIGURE 6.3.4: ^{1}H NMR OF 3 125
FIGURE 6.3.5: ^{1}H NMR OF SURFACTANT A004-UP. 126
FIGURE 6.3.6: ISOLATED PARTICLES FROM MEDIUM WATER CONTENT MICROEMULSION 4 HOURS AFTER INITIAL TTIP MICROEMULSION PREPARATION. 129
FIGURE 6.3.7: ISOLATED PARTICLES FROM MEDIUM WATER CONTENT MICROEMULSION 24 HOURS AFTER INITIAL TTIP MICROEMULSION PREPARATION. 129
FIGURE 6.3.8: ISOLATED PARTICLES FROM MEDIUM WATER CONTENT MICROEMULSION 48 HOURS AFTER INITIAL TTIP MICROEMULSION PREPARATION. 130
FIGURE 6.3.9: EDX OF ISOLATED PARTICLES FROM MEDIUM WATER CONTENT MICROEMULSION AFTER A: 4, B: 24 AND C: 48 HOURS. 131
FIGURE 6.3.10: IMAGE ANALYSIS STEPS FOR PARTICLE SIZE DETERMINATION AT 10000X MAGNIFICATION. 132
TABLE 2.3.1: MICROEMULSION FORMULATIONS 54
TABLE 3.3.1: FORMULATIONS LEADING TO POLYMERIZED MICROEMULSIONS^A 69
TABLE 3.4.1: STRUCTURAL PARAMETERS DETERMINED FROM THE TEUBNER-STREY MODEL 73
TABLE 4.3.1: MICROEMULSION FORMULATIONS USING TRISILOXANE-PEG SURFACTANT SILSURF A008-UP WITH AND WITHOUT TTIP^A 92
TABLE 6.1.1: FULL MICROEMULSION FORMULATIONS WITH MASSES (SURFACTANT PHASE) 116
TABLE 6.3.1: FORMULATIONS AND ASSOCIATED MASSES USED FOR UV ABSORPTION MEASUREMENTS BETWEEN QUARTZ SLIDES FOLLOWING THE UV ABSORPTION OF TTIP AND TIO_2 126
TABLE 6.3.2: MICROEMULSION STRUCTURAL PARAMETERS DETERMINED BY TEUBNER-STREY ANALYSIS OF ACQUIRED SCATTERING DATA. 127
CHART 3.4.1: ACQUIRED SAXS CURVE AND FITTED TEUBNER-STREY MODEL (BLACK CURVE) FOR MICROEMULSION FORMULATIONS 73
CHART 4.4.1: TTIP MICROEMULSIONS. A: OIL-IN-WATER WITH A TOTAL WATER CONTENT 34.73WT% (224:1 MOLE RATIO $[H_2O]$:[TI(SILSURF)$_4$]). B-C: BICONTINUOUS WITH A TOTAL WATER CONTENT 18.25WT% (94:1 MOLE RATIO $[H_2O]$:[TI(SILSURF)$_4$) AND 13.37WT% (66:1 MOLE RATIO $[H_2O]$:[TI(SILSURF)$_4$]), RESPECTIVELY. D: WATER-IN-OIL WITH A TOTAL WATER CONTENT OF 7.67WT% (35:1 MOLE RATIO $[H_2O]$:[TI(SILSURF)$_4$]). 96
CHART 6.3.1: SAXS CHARACTERIZATION OF MICROEMULSION FORMULATION 6 OF TABLE 6.3.1 127
CHART 6.3.2: DIFFERENCES IN UV-VIS ABSORPTION OF A008-UP/TTIP MIXTURE AND TTIP IN IPA. 128

LIST OF SYMBOLS & ABBREVIATIONS

ΔA	change in interfacial area
A	amplitude
d	domain size
f_a	amphiphilicity factor
ΔG_{form}	free energy of formation
I	intensity
N_A	number of surfactant molecules
n_s	moles of surfactant
n_{CO}	moles of co-surfactant
q	scattering vector
ΔS_{config}	change in entropy
μE	microemulsion
γ_{12}	interfacial tension between phase 1 & 2
ξ	correlation length
AFM	atomic force microscopy
AIBN	azobisisobutyronitrile
AOT (Aerosol OT)	dioctyl sodium sulfosuccinate
AUDMAA	((acryloyloxy)undecyl)dimethylammonium acetate
AUTMAB	((acryloyloxy)undecyl)trimethylammonium bromide
Cryo-TEM	cryogenic transmission electron microscopy
cSt	centistokes
CTAB	cetyltrimethylammonium bromide
CTVB	cetyltrimethylammonium 4-vinylbenzoate
D_4	octamethylcyclotetrasiloxane
DBK	dibenzyl ketone

DBTDL	dibutyltin dilaurate
DDAB	didodecyldimethylammonium bromide
DMPA	2,2-dimethyoxy-2-phenylacetophenone
DTAB	dodecyltrimethylammonium bromide
EDX	energy-dispersive X-ray spectroscopy
EO	ethylene oxide
FF-TEM	freeze fracture transmission electron microscopy
FTIR	Fourier transform infrared spectroscopy
HEMA	2-hydroxyethyl methacrylate
HLB	hydrophilic-lipophilic balance
HMP	2-hydroxy-2-methylpropiophenone
HTV	high temperature vulcanization
keV	kiloelectron-volts
LEDs	light emitting diodes
M	monofunctional silane
MEHQ	mono methyl ether hydroquinone
mNm^{-1}	milliNewtons per metre
MTSM	methacrylate-terminated silicone macromonomer
Na-DEHSS	sodium bis(2-ethylhexyl) sulfosuccinate (synonymous to Aerosol OT)
OAc	acetoxy group
OMe	methoxy group
O/W	oil-in-water
PDMS	polydimethylsiloxane
PEO	poly(ethylene oxide)
POSS	polyhedral silsesquioxanes
Q	tetrafunctional silane
RTV	room temperature vulcanization

SANS	small angle neutron scattering
SAXS	small angle X-ray scattering
SDS	sodium dodecyl sulfate
SEM	scanning electron microscopy
SiO_2	silicon dioxide
T	temperature
TEM	transmission electron microscopy
TEOS	tetraethyl orthosilicate (tetraethoxysilane)
$Ti(O\text{-}i\text{Pr})_4$	titanium isopropoxide
TiO_2	titanium dioxide
TTB	titanium tetrabutoxide
UV-Vis	ultraviolet-visible
W/O	water-in-oil

1. Chapter 1: Introduction

1.1. Overview

This thesis is about microemulsions, and the exploitation of their nanostructuring before and after polymerization of either or both water and oil phases. The microemulsions of particular interest in this thesis are based on (crosslinked) silicones and on acrylic polymers formed within the aqueous phase of a microemulsion. Therefore, prior to examining microemulsions, a brief introduction to silicone polymers and the crosslinking of silicones will be provided.

1.1.1. Silicone Fluids

Small cyclic and linear oligomers consisting of repeating units of silicon and oxygen are formed upon the hydrolysis of chlorosilanes[1,2,3] (Figure 1.1.1) The polymerization of these small cyclic and linear compounds by acid or base equilibration leads to the formation of long silicone polymers[4] of generic structure $(R_2SiO)_n$, where R can encompass a range of carbon-based substituents, such as methyl, phenyl, vinyl, etc.[2]

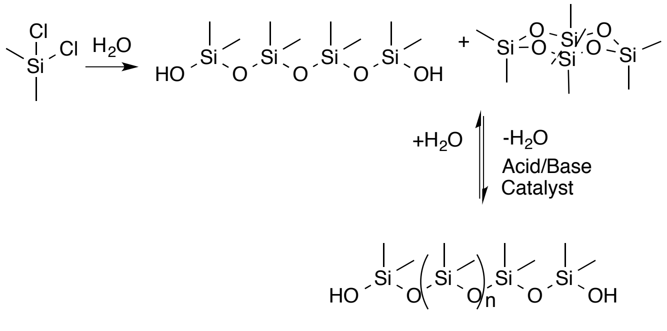

Figure 1.1.1: The formation of silicone polymer from dimethyldichlorosilane by acid/base equilibration

Silicone polymers range from a few repeat units up to several tens of thousand repeating units while retaining fluidity, a property that is unique to silicones. Hydrocarbons of high alkyl chain length form solids after 18 carbon units[5] (~260 g/mol), whereas silicones always remain as fluid oil, despite reaching molecular weights of up to 1 million g/mol. This unique property arises from the flexibility of the silicon-oxygen backbone, which is a consequence of larger bond angles and bond lengths between the silicon-oxygen bond when compared to either the carbon-carbon bond or the carbon-oxygen bond. In addition, the silicon-oxygen bond is more stable than the analogous carbon-oxygen bond.[1] The flexibility and strength of the silicon-oxygen backbone is responsible for thermal stability, electrical resistance, oxygen permeability, oxidative stability, and hydrophobic properties of the polymer.[2] The hydrophobicity of silicones is, in part, due to the methyl groups situated along the polymer backbone which, owing to the flexibility of the polymer backbone, can always be oriented towards an interface.[2,6] The presence of methyl groups along the polymer backbone also results in silicones having low surface tensions (between 16 and 21 mNm^{-1}), giving them excellent spreading capabilities.[6,7]

1.1.2. Functional Silicones

Silicones can be functionalized with side chains in order to alter the physical properties of the original PDMS structure. A silicone polymeric structure normally consists of a silicon-oxygen repeat unit with methyl groups branched off of each silicon atom, however, other pendent groups can be introduced along the backbone: functional groups including vinyl and hydride are particularly important. In addition to the functionalization of silicone polymers along the backbone, polymers can also be mono or di-functionalized at the polymer chain ends.[2] In order to functionalize a silicone polymer at the end of the chain, a hydride-terminated PDMS is typically first prepared by the equilibration reaction of octamethylcyclotetrasiloxane (D_4) with 1,1,3,3-tetramethyldisiloxane (Figure 1.1.2). Hydride-terminated PDMS can undergo hydrosilylation of the Si-H groups to lead to a variety of end-group structures.[2] Pendent functionalized PDMS is achieved in a similar manner; however, the starting cyclic silicone is heptamethylcyclotetrasiloxane, which contains a hydride group in place of a methyl.

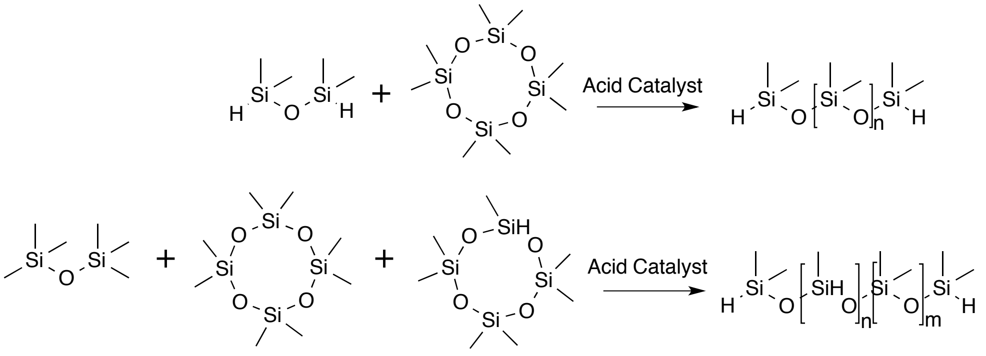

Figure 1.1.2: Formation of hydride functionalized PDMS from an equilibration reaction

Functionalization of silicones with a hydrophile can lead to polymers with amphiphilic character. Common hydrophilic moieties include polymers of ethylene oxide and copolymers of ethylene oxide/propylene oxide.[6] Attachment of a polyether hydrophile to a siloxane backbone can be achieved through transetherfication, hydrosilylation, or by a reaction with reactive pendent groups previously functionalized onto the silicone backbone.[7]

Incorporation of hydrophilic moieties onto silicone polymers leads to amphiphilic copolymers (silicone surfactants) with different architectures (Figure 1.1.3). The three main structure types are rake-type (sometimes referred to as comb or graft), ABA copolymers (middle silicone unit is terminated with hydrophilic portion), and trisiloxane surfactants.[7,8]

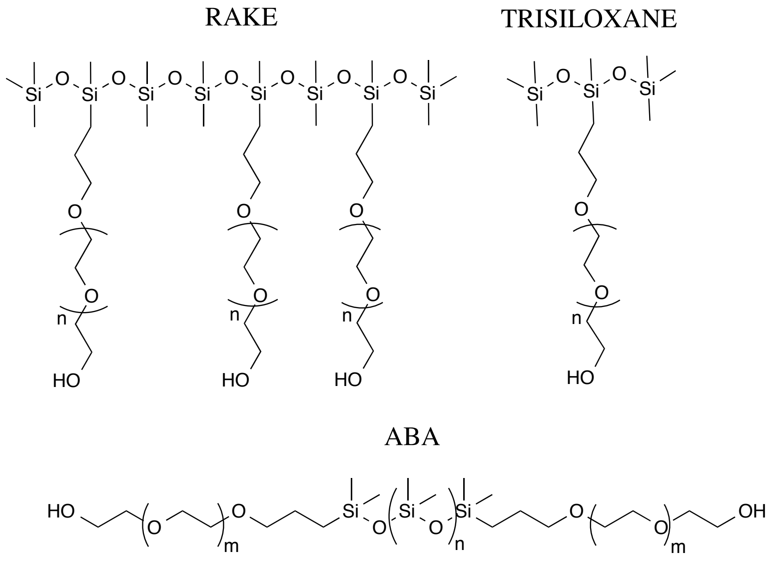

Figure 1.1.3: Siloxane surfactant architectures

1.1.3. Siloxane Surfactants

Trisiloxane surfactants are unique in that the silicone portion comes from a small silicone oligomer (heptamethyltrisiloxane) instead of a polydisperse silicone chain. In this regard, only the polyether portion of trisiloxane surfactants is not monodisperse.[7] Along with the different silicone surfactant architectures, properties of these copolymers can depend on the type and length of the hydrophile and the ratio of polyether to silicone in the copolymer.[6] Silicone copolymers of low molecular weight are generally excellent wetting agents, while increasing molecular weight results in copolymers that act as emulsifiers.[9]

Due to their unique properties and super spreading capabilities[8,10,11], trisiloxane surfactants have been extensively studied and reported in the literature[12,13], although their behaviour is still not fully understood.[12, 14] The wetting properties of these surfactants promote the spreading of aqueous solutions on hydrophobic surfaces to near zero contact angles, a function known as superwetting.[15]

Trisiloxane surfactants can form unique structures (bilayers, micellar layers, monolayers) on solid substrates depending on the surface substrate. The aggregate structures and adsorption behaviour of trisiloxane surfactants of varying polyether length were analyzed by AFM and compared to non-ionic hydrocarbon surfactants of the type C_mE_n.[16] The hydrophobicity of the trisiloxane group is comparable to $C_{12}H_{25}$, however, the length and volume is significantly different.[7,17] Hill found that trisiloxane surfactant of EO=6 is equivalent in phase behaviour to surfactant type $C_{12}E_4$.[7,8] Similarly, trisiloxane surfactants of EO=8 and EO=12 were found to be equivalent to surfactant types $C_{12}E_5$ and $C_{12}E_6$, respectively.[16,18]

The phase behaviour of trisiloxane surfactant solutions has also been extensively studied and has been found to be correlated to the length of the polyether chain and the temperature of the system.[8,18] Linear trisiloxane surfactants of EO=8 at high concentration (>60%) have lamellar regions and at low concentrations (<1% in water), dispersions of bilayer vesicles are formed. Surprisingly, identical phase behaviour was observed for the branched version of the trisiloxane EO=8 surfactant, an observation that has been explained by the high flexibility of the silicone chain.[7] Decreasing the length of the polyether chain to four units results in a reverse micellar solution at all surfactant concentrations[17], however, increasing the number of polyether units results in more complex structures. Trisiloxane surfactants with chain length between 6 to 12 ethylene oxide units result in the formation of lamellar liquid crystalline phase in excess water between 0.2 to 0.8 wt% surfactant in water and, at polyether lengths greater than 12 units, surfactants begin to form hexagonal liquid crystal phases mixed with rod-type micellar solution.[8,19] The exact concentrations in which these structures are formed vary, depending on the exact number of EO units.[17]

Polymeric silicone surfactants (rake type and ABA) have polydisperse siloxane units and can vary in a number of ways: molecular weight of the siloxane chain, the average number of hydrophilic groups, the chain length of the hydrophile, and, for copolymer hydrophiles, the ratio of ethylene oxide units to propylene oxide units.[7] Phase studies on rake type silicone surfactants of type $MD_{22}(D'E_8)_2M$ show that over a wide temperature range (0-70 °C) the surfactant forms an inverse hexagonal phase up to concentrations of 80 wt% in water. Increasing the hydrophilic properties of the surfactant by the addition of 4 EO units per chain to form a 12 EO hydrophile results in the formation of a lamellar phase liquid crystal over a wide temperature range at all concentrations. At low concentrations (<5wt%) these surfactants form dispersions of micelles with a diversity of shapes such as wormlike, globular, tubular, and multi-lamellar vesicles.[7] Investigations into AB type block silicone-PEO copolymer surfactants by Kunieda et al. have shown that both hydrophobic and hydrophilic chain length affect surfactant curvature, and therefore, phase behaviour. For surfactants of the same siloxane length, increasing the number of polyether units results in a change of structure from a discontinuous inverse cubic phase, to the reverse hexagonal phase, and finally to the lamellar liquid crystal phase.[20] The phase changes observed upon increasing the polyether chain lengths are similar to the transitions observed for rake-type copolymer structures (hexagonal phase to lamellar).

The unique properties and superior wetting behaviour of siloxane surfactants have resulted in their use in a broad range of applications that span different industries. They are used as additives in polyurethane foam manufacturing in order to stabilize foam and to promote emulsification of polyols and isocyanates. They are also used to facilitate fibre production by enabling the efficient spread of lubricants on fibres. This is essential for reducing friction and, therefore, reducing overheating during high-speed production. Trisiloxane spreading capability is also put to use in agriculture, where siloxane surfactants are used as adjuvants to enhance the spreading of herbicides and insecticides on plants.[21] In the personal care and cosmetic industry, hydrophobic silicone surfactants are used to improve the spreading of organic oils and waxes, whereas water-soluble siloxane surfactants are used in aqueous formulations, such as shampoos and shower gels.[7] The interfacial properties of trisiloxane surfactants have also attracted attention for use in the formulation of microemulsions. Kunieda et al. examined the phase behaviour of a microemulsion consisting of equal amounts of water and oil (decane). The effect of polyether length on microemulsion phases were investigated and it was determined that the three phase body is formed when the surfactant contains 9 ethylene oxide units, indicated a balanced microemulsion with a net surfactant curvature of zero.[17]

1.2. Silicone Crosslinking

Silicone polymers can be converted into elastomers through a variety of different mechanisms that result from the crosslinking of silicones. There are two common types of crosslinking. The first type is the incorporation of a tri- or tetrafunctional silane, which bridges two or more polymeric chains. The second type of crosslinking involves the use of end group functionality (vinyl- or hydrogen-terminated polymers) that can react with each other to form silicon-carbon bonds.[2]

The incorporation of a tri- or tetrafunctional silane typically results in the formation of a siloxane network that is composed entirely of Si-O linkages (Figure 1.2.1), while the use of end-group functionality to create a silicone network normally results in organic segments that link silicone chains (Figure 1.2.2)

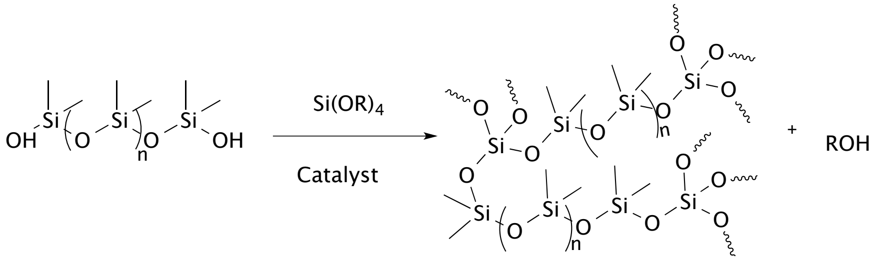

Figure 1.2.1: Crosslinking of silicones by tetrafunctional silanes or functionally-terminated PDMS

The three most common mechanisms used commercially to crosslink silicones are hydrosilylation (addition) crosslinking, room-temperature vulcanization (RTV), and high temperature vulcanization (HTV).[2]

Hydrosilylation results in the formation of a carbon-silicon bond from a reaction between two functionalized silicone polymers. One polymer contains Si-H functionality and the other polymer contains Si-CH=CH_2 (vinyl) groups.[2,22] There are two types of hydrosilylation processes: a radical process and a transition metal catalyzed process.[2,23] In the radical process, an azo or peroxide compound typically provides the radical source, causing proton abstraction from the Si-H functionalized silicone.[24] The hydride-functionalized polymer now has a radical on the silicon atom that readily reacts with the alkene of a vinyl functionalized PDMS, resulting in the formation of a carbon-silicon bond. A new radical is now formed at the carbon atom of the newly formed bond, which can repeat the process of hydrogen abstraction from the Si-H functional silicone (Figure 1.2.2).

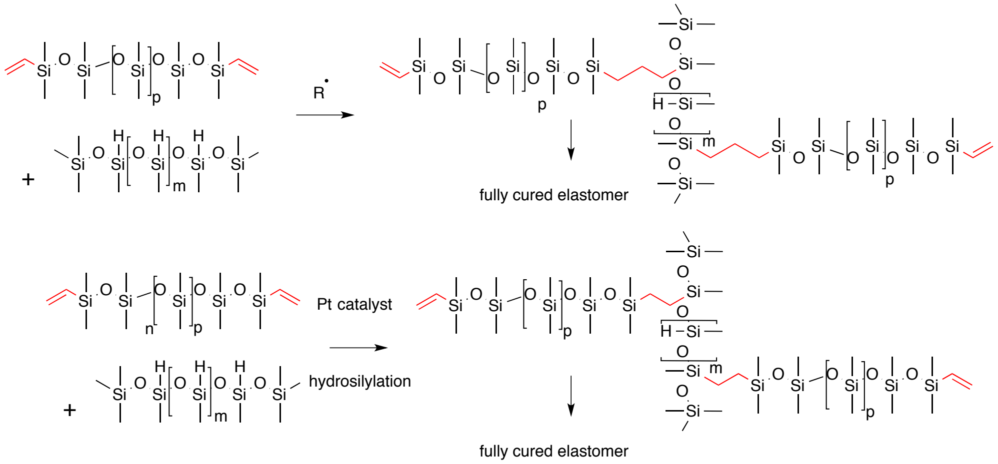

Figure 1.2.2: Silicone crosslinking via radical and platinum-catalyzed hydrosilylation reaction

Hydrosilylation can also proceed through a transition metal catalyzed mechanism. Platinum catalysts (Karstedt's catalyst and Speier's catalyst)[2,23] are most commonly used. The first step in this catalytic mechanism with Speier's catalyst is the reduction of the platinum(IV) catalysts to a platinum(II) state by the complexation/ligand exchange of the alkene with the platinum centre: Karstedt's is already at the Pt(0) state. The addition of an Si-H compound results in the oxidation of the platinum centre to the original platinum(IV) state and the conversion of the alkene π complexation with platinum to a σ complex. Reductive syn elimination occurs, forming a new silicon-carbon bond, and the platinum(II) state is regenerated.[2]

The RTV process is one of the most common methods for crosslinking silicones. It is a condensation polymerization process and is commonly used in applications such as silicon caulking, coatings, sealants, mold making, automotive applications, biomaterials, etc.[25,26] RTV involves a nucleophilic substitution reaction at the silicon atom of a tri/tetra-substituted silane by the hydroxyl group of a hydroxyl-terminated silicone. In addition to substituted silanes, titanium alkoxides can also function as crosslinkers. Titanium alkoxides are much more reactive than tetra-substituted silanes to nucleophilic substitution by silanol PDMS and will occur in the absence of catalyst. However, the extreme reactivity of the titanium centre results in a readily hydrolyzed titanium-oxygen bond at the newly formed crosslinking sight.[27] Note that alkoxytitanium compounds also serve as catalysts for the process (see below).

The rate of substitution is dependent on the type of leaving group present on the crosslinking silane, which can consist of halides, carboxylates, or alkoxides.[2] For example, an acetoxy group has a faster rate of hydrolysis than a methoxy group, which is faster than an ethoxy group. The rate at which these groups hydrolyze from the crosslinker determines the ultimate rate of cure.[2]

The nucleophilic substitution of the silanol-terminated PDMS with a silane crosslinker requires a catalyst, which can be an acid, base, or metal (tin or titanium alkoxy derivative). Protonation of the alkoxy leaving group (of the silane) from an acid catalyst accelerates nucleophilic substitution by improving the leaving group. Deprotonation of the silanol (nucleophile) by a base catalyst improves nucleophilicity of the oxygen atom, which also increases the reaction rate.[2] Acid and base catalysts are less effective than metal catalysts at crosslinking silicones. Metal catalysts, such as titanates or tin-derived esters, require water as a co-catalyst, which results in the hydrolysis of the titanate or tin ester to form a hydroxyl metal catalyst (Figure 1.2.3). The hydroxyl-metal catalyst reacts with the silane crosslinker to create an activated silicon centre for attack by the nucleophilic silanol group of hydroxyl-terminated PDMS.

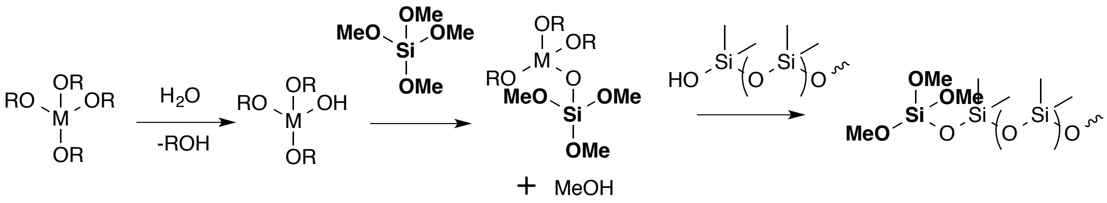

Figure 1.2.3: Formation of hydroxyl metal catalyst and crosslinking of silicone with tetrafunctional silane

1.3. Silicones in Nano & Biomaterials

Silicones have been used in biomaterial applications since the 1940’s where they were first used in bile duct repair.[28] Since then, silicones have been used extensively in biomedical applications, such as long-term and short-term implants, lubrication for syringe coatings, adhesives for wound dressings, and in scar reduction treatments.[29] With current advances in nanotechnology, silicones are finding an even greater range of utility; combined with a desire to improve upon existing biomaterial properties.[30] The increasing availability of oligomeric silsesquioxanes (e.g., polyhedral silsesquioxanes, POSS) has led to the development of nanostructured polymeric materials with improved chemical and physical properties, which can be used for superior cardiovascular implants.[31] In addition to biomaterials applications, silicone-based nanomaterials are of increasing interest in LEDs, photocatalysts, and coatings.[32,33,34,35]

Silicones are incorporated into nanomaterials in a variety of ways, such as matrix polymers for nanoparticle encapsulation or as a suspension medium for nanoparticles in solution. They are also used in nanoparticle modification and grafted onto a particle surface to improve particle properties.

Silicone MQ resins are products of the condensation reaction between a monofunctional silane (M) and a tetrafunctional silane (Q).[36] They have a three dimensional silicone network structure and possess desirable properties, such as high hardness, antifriction, and radiation resistance.[37] The molecular weight of the MQ resin can be adjusted by changing the concentration of acid catalyst, the ratio of M to Q units, and the reaction time.[38] Increasing any of the mentioned parameters will result in an increase in molecular weight.[36]

MQ resins can be used to form inorganic-organic nanocomposites. Xiang et al. prepared nanocomposites of MQ resins and titania by incorporating a titanium butoxide solution into the MQ matrix.[37] The composite resin was characterized with FT-IR and UV-Vis, which showed new IR absorption peaks that correspond to Ti-O-Si bonds and new UV peaks at 237nm that correspond to the absorption of TiO_2.[37]

Yoshii et al. characterized the morphology of a MQ resin containing a vinyl-functionalized M unit by TEM. The vinyl M unit was reacted with a M^H unit via a platinum-catalyzed hydrosilylation reaction. Unreacted vinyl groups were stained with osmium tetroxide and the resulting TEM images showed nanoporous regions of approximately 2nm in size.[39] The characterization of MQ resin morphology and the incorporation of particles to create MQ resin composites highlight the use of silicones to create structured interfaces on nanometer length scales. MQ resins are an example of a silicone material that is inherently nanostructured, however, there are other more indirect approaches to the incorporation of silicones in nanomaterials.

Silicone nanoparticle composites have been prepared that do not contain MQ resins. Crick et al. prepared silicone-nanoparticle composites consisting of iron oxide, nickel, titania, cobalt, and gold nanoparticles embedded in a Sylgard silicone elastomer in a desire to create highly photocatalytic superhydrophobic thin-film materials.[33] Li et al. used silicone to improve the dispersion of TiO_2 nanoparticles in silicone oil by grafting phosphate-modified PDMS onto the nanoparticle surface. The dispersion and encapsulation of silicone nanoparticles has become of interest for LED applications towards improving light-extraction efficiency by reducing total internal reflection between the encapsulated matrix and LED chip.[32]

RTV silicone elastomers, often used as protective coatings, may be susceptible to environmental aging, which can result in a decrease in hydrophobicity over time, leading to erosion and further aging. The incorporation of nano-silica into RTV silicone elastomers was shown to mitigate the loss of hydrophobicity due to aging compared to the control and was also shown to have improved thermal degradation properties. The improved performance of nanocomposite RTV silicones is attributed to the superior ability of nano-silica to reflect ultraviolet radiation.[34] Environmental aging is also a significant issue in facial prostheses, which resulted in a decreased lifetime for a facial prosthetic device. The incorporation of titanium, zinc, or cerium nano-oxides was found to improve the mechanical properties of the prostheses within certain concentration limits.[40]

The incorporation of nanoparticles into a silicone matrix to create novel silicone nanocomposites, the direct modification of nanoparticles with silicone polymers for improved dispersion, or the preparation of superior biomaterials based on the incorporation of a small siloxane oligomer are just a few examples of how silicones have been utilized in nanotechnology to create better, more robust materials.

1.4. Microemulsions

Microemulsions are a unique type of nanomaterial, an isotropic nanostructured dispersion consisting of oil, water, and surfactant. Schulman & Hoar first described microemulsions in 1943 as a spontaneous emulsion that had formed in the presence of a surfactant,[41] although the term microemulsions wasn't explicitly coined until the late 1950's. Schulman et al. reported on the formation of a completely transparent solution that occurred upon the addition of a short chain alcohol to a translucent/hazy dispersion water, benzene, hexanol, and potassium oleate.[42] He proposed that the addition of alcohol resulted in negative (or near negative) interfacial tension owing to preferential interfacial packing, resulting in the spontaneous formation of these mixtures.[43,44]

1.4.1. Microemulsion Structure

Microemulsions can exhibit different types of nanostructuring, depending on factors such as salinity, temperature, or ratio of components. They can exist in equilibrium with an oil or water phase, depending on structure type, or can exist as a single homogeneous phase (Figure 1.4.1).

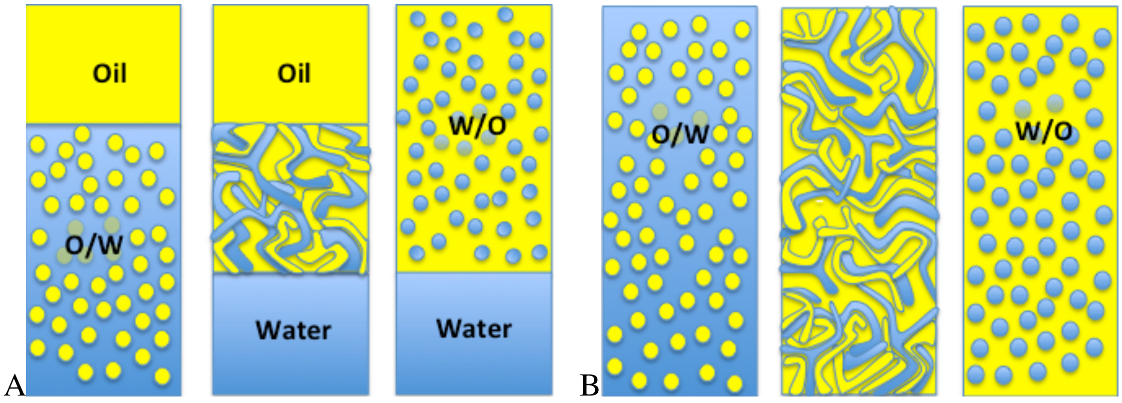

Figure 1.4.1: A: Winsor I, III, II Microemulsions and B: Possible Structures of Winsor Type IV Microemulsions

They are commonly referred to by their Winsor classification[45]: Winsor I (oil-in-water, O/W), Winsor II (water-in-oil, W/O), Winsor III (bicontinuous/middle phase), or Winsor

IV (single-phase). Winsor type I and II microemulsions are a two-phase system; the microemulsion phase exists in equilibrium with an excess dispersed phase of either oil or water. Winsor type III microemulsions are a three-phase system wherein a surfactant-rich middle phase co-exists with an upper phase of excess oil and a lower phase of excess water.[46,47] Winsor type IV microemulsions exist as a single-phase and can be of droplet or bicontinuous structure type. Winsor type IV microemulsions are formed with high total surfactant concentrations, whereas Winsor I, II, and III microemulsions require less total surfactant concentration.[48] The domain sizes within these microemulsion structures are typically well below 50nm, thus resulting in optically transparent solutions.

1.4.2. Phase Behaviour

Phase diagrams can be used to help establish microemulsion phase behaviour. A Gibbs phase triangle is used for ternary systems to evaluate all possible combinations of oil, water, and surfactant. Each corner of the phase diagram represents 100% of the individual component. Some microemulsions introduce a fourth component in the form of a short chain alcohol (co-surfactant). In this case, one corner of the phase diagram generally consists of the surfactant/alcohol mixture and forms a “pseudo” phase diagram.[49] Phase prisms can be constructed from phase diagrams if multiple phase diagrams are constructed at varying temperatures.[50]

Temperature variations can be very important to microemulsion stability, depending on the type of surfactant used. The spontaneous curvature of non-ionic surfactant films is affected by temperature changes, resulting in phase transitions from one structure type to another.[51] Essentially, temperature can change the hydrophilic-lipophilic balance (HLB) of an ethylene oxide surfactant owing to decrease hydrogen bonding between EO units and water molecules.[52]

Low temperature favours O/W type structure and increasing the temperature can lead to the formation of a bicontinuous phase, while high temperature favours W/O structure. However, microemulsion structure is determined from a number of different parameters, aside from temperature, which can lead to other outcomes. For example, a microemulsion system ($C_{12}E_5$/water/tetradecane) with a high content of water at high temperature exhibits a bicontinuous structure, while a low water content microemulsion and low temperature also exhibits bicontinuous structuring.[50] Although there can be similarities and generalities regarding the phase behaviour of microemulsion systems, each one can exhibit unique phase behaviour dependent on its specific set of conditions, such as surfactant type, temperature, and composition.

Microemulsion structure is determined by multiple parameters. The hydrophilic-lipophilic balance (HLB) of the surfactant affects the curvature of the film and is, therefore, a determining factor for microemulsion structure. Surfactants with HLB<10 tend to form W/O structures, while O/W structures are formed when HLB>10. When the HLB≈10, bicontinuous structures tend to form.[53] In addition to surfactant HLB, the amount of water or oil present in the system also affects microemulsion structure type. When a low content of water relative to oil is present, water is more likely to form an internal droplet phase, while when large quantity of water relative to oil is present; the water is likely to form the continuous, external phase. Equal amounts of water and oil are more likely to form microemulsions where both water and oil are co-continuous phases (bicontinuous structure).

1.4.3. Microemulsion Stability

Microemulsions are thermodynamically stable oil/water dispersions that form spontaneously in the presence of surfactant. They are complex systems and as a result, there are multiple explanations and theories to explain the origin of their stability. Ultimately, microemulsion stability arises from having a negative free energy for the system. A simplified thermodynamic equation for microemulsion formation is described below (Equation 1).

$$\Delta G_{form} = \Delta A \gamma_{12} - T\Delta S_{config} \qquad (1)$$

In the thermodynamic theory of microemulsion stability, ΔG_{form} represents the total free energy associated in the formation of one cm^3 of microemulsion. ΔA is the change in interfacial area, assuming spherical droplets, γ_{12} is the interfacial tension between two phases at temperature (T), and ΔS_{config} is the change in entropy associated with droplet dispersion. The entropy upon droplet dispersion is always a positive term, which is favourable towards decreasing the free energy of the system, however, decreasing the size (and increasing the number) of droplets results in the creation of greater interfacial area. As a result, the interfacial tension must be significantly reduced so that $\Delta A\gamma_{12} \leq T\Delta S_{config}$, allowing for an overall negative free energy value and thus spontaneous microemulsion formation.[53]

The change in interfacial area (ΔA) upon microemulsion formation can be determined if the total number of surfactant molecules (N_A), the moles of surfactant (n_s and n_{co}), and area per surfactant molecule (A_s and A_{co}) are known (Equation 2).[54]

$$A = \frac{(n_S N_A A_S + n_{co} N_A A_{co})}{\phi} \qquad (2)$$

During microemulsion formation, the change in interfacial area (ΔA) is usually on the order of 10^4 to 10^5, which means an interfacial tension of approximately 0.01 mNm^{-1} is required in order to achieve a small enough value for $\Delta A\gamma_{12}$ to result in negative free energy. In order to achieve the desired interfacial values, often a combination of surfactants or the addition of a co-surfactant is required.

This thermodynamic explanation for microemulsion formation is overly simplistic and ignores other factors that contribute to stability or instability.[55] The dilution effect contributes significantly to microemulsion stability. Upon microemulsion formation, surfactant and co-surfactant monomers migrate to the oil/water interface, which both decreases interfacial tension and decreases their concentration in the bulk solution. A decrease in monomer concentration in the bulk solution results in a decrease in chemical potential. A decrease in chemical potential in the bulk solution contributes to an overall decrease in free energy of formation.[56]

Microemulsion formation and stability can be described using a combination of factors: an increase in entropy upon microemulsion formation, the adsorption of surfactant/co-surfactant at the interface leading to a decrease in interfacial tension, and a decrease in chemical potential in the bulk solution as surfactant preferentially adsorbs onto the interface.

Unlike normal emulsions that are kinetically unstable, microemulsions are simple to make and are prepared by titrating water into a starting mixture of oil and surfactant. If the composition is predetermined, changing the order of addition should not affect microemulsion formation. When a co-surfactant is required to reach a microemulsion state, a common method for establishing microemulsion formulations is first to prepare a course emulsion consisting of oil, water, and primary surfactant. A co-surfactant (commonly a short-chain alcohol) is then titrated into the course emulsion until a microemulsion is formed and optical transparency is achieved. In theory, all surfactants are capable of forming microemulsions, given the appropriate concentration, an effective co-surfactant, and the right set of conditions.[57] Aside from short-chain alcohol, other additives and ingredients have the potential to affect the interfacial properties of a microemulsion. The addition of ingredients that are soluble in one particular phase or that are susceptible to hydrolysis can alter the oil/water interface through selective interactions with either the hydrophilic or hydrophobic portion of the surfactant molecule.[58]

1.4.4. Silicone Microemulsions

Silicone microemulsions are a relatively new development when compared to their hydrocarbon counterparts. In 1998, a patent by Randal Hill described microemulsion compositions containing water, a volatile linear or cyclic silicone, and low molecular weight silicone polyether surfactant. Little to no mechanical energy was required in order to form transparent and stable microemulsions. Additionally, the order of addition in the preparation of these microemulsions could be changed without consequence to their properties, however, the microemulsions required a significant amount of surfactant (between 15-30 wt% by weight).[59] Since the initial patent describing the formation of silicone microemulsions, further developments by Feng et al. have disclosed the formation of silicone microemulsions using high molecular weight silicone polyethers, in contrast to the previous patent, which claimed the preparation of silicone microemulsions with short-chain silicone polyethers. In addition, later developments showed that non-essential ingredients could be formulated into a silicone microemulsion without compromising microemulsion stability.[60] Feng et al. also showed that mixtures of volatile and non-volatile silicones could be incorporated into microemulsion formulations in the presence of a significant amount of silicone polyether surfactant (30-50wt%).[60]

Since the initial development of silicone microemulsions, other surfactants (aside from silicone polyethers) have been used to stabilize volatile silicone microemulsions. Water in-oil (W/O) silicone microemulsions containing hexamethyldisiloxane and diphenyltetramethyldisloxane were stabilized by the surfactant dioctyl sodium sulfosuccinate (Aerosol-OT). The solubility of water in this microemulsion system was shown to improve upon the addition of an alcohol co-surfactant. [61]

Silicones have unique solubility parameters that differ from hydrocarbons, and the silicone portion of a siloxane surfactant is hydrophobic, but not lipophilic.[62] Because of these differences, the hydrophilic-lipophilic balance (HLB system) that is used to predict the emulsifying properties of hydrocarbon surfactants cannot be directly applied to silicone surfactants.[63] Silicone surfactants contain a silicone soluble portion, an oil soluble portion, and a water-soluble portion, which has led to the development of the 3D HLB system. The 3D HLB system takes into account the silicone solubility, oil solubility, and water solubility of silicone surfactants, whereas the original HLB system only accounts for the oil soluble and water-soluble portions of hydrocarbon surfactants. The 3D HLB scale is represented on triangular coordinates, whereas the original (2D) HLB scale is linear. The 3D HLB has three parameters (x, y, z) that represent the silicone portion, oil portion, and water portion of the surfactant.[62] The 3D HLB system predicts six different structure types: W/O, O/W, silicone-in-water, water-in-silicone, silicone-in-oil, and oil-in-silicone.[63] Unfortunately, we were unable to find any published work that relates the 3D HLB system to predicting bicontinuous microemulsion structures. In the original HLB system, balanced surfactants, resulting in zero net curvature, have an HLB of ~10 and resulted in the formation of bicontinuous structures.[64]

Further understanding of the behavior of silicone microemulsions has been reported by investigating potential parallels between silicone and well-studied hydrocarbon microemulsions. The effect of *n*-alkyl polyglycol ether surfactant type on the phase composition of D_4 microemulsions was investigated and the results were found to be similar for octane and n-hexyl methacrylate microemulsions. The addition of didodecyldimethylammonium bromide (DDAB) to D_4/water/n-alkyl polyglycol ether microemulsions was also investigated and found to increase surfactant efficiency and expand the single-phase microemulsion region.[65]

Most studies on silicone microemulsions are based on volatile short-chain or cyclic PDMS.[66,67] However, there have been a few more recent reports of microemulsions prepared with high molecular weight silicones. Sharma et al. prepared microemulsions containing a non-volatile (~23000 g/mol) dimethicone of PDMS and polyethylene/polypropylene oxide. The microemulsion was reported to transition from bicontinuous to oil-in-water structure type upon titration with water.[68] Other reports of silicone microemulsions comprised of A-B type silicone surfactants (dimethicone), high molecular weight aminosilicone fluid, and non-volatile linear silicone oil have been disclosed,[68,69] however, there is still a lack of insight into these systems in comparison to well-studied hydrocarbon microemulsions.

1.5. Microemulsion Polymerization

Microemulsion polymerization began to develop in the 1980's,[70] primarily as a template for the polymerization of monomers, such as acrylamide, styrene, methyl methacrylate, acrylic acid, etc. The kinetics of microemulsion polymerization is distinct from the emulsion polymerization process, allowing for the formation of small particles that cannot be achieved by traditional emulsion polymerization routes. In an O/W emulsion polymerization, monomer is dispersed and stabilized by surfactant as large monomer droplets (oil phase) and monomer-swollen micelles within the continuous (water) phase. Initiator is solubilized within the continuous (water) phase and diffuses into monomer-swollen micelles to initiate nucleation and polymerization. As monomer is depleted in the micelles, more monomer diffuses into the micelle to continue the polymerization.[71] In microemulsion polymerization the process is quite different in that the formation of the microemulsion upon addition of monomer is spontaneous and no large droplets are formed in the dispersed phase. In contrast to macroemulsions, all monomers exist within monomer-swollen micelles, meaning the reaction terminates once polymerization within each micelle is complete, limiting the particle size that can be achieved. The polymerization of microemulsions reported in literature can be categorized by two main outcomes: the polymerization of microemulsions to form latexes and the polymerization of microemulsions to form nanostructured polymers. We are primarily interested in the polymerization of microemulsions to form nanoporous materials, but we discuss both outcomes as the polymerization of monomers into particles has led to developments of "locking in" interfacial structure using acrylate-functionalized monomers and surfactants.

1.5.1. Microemulsion Polymerization to form Latex Particles

Microemulsions are advantageous for the preparation of latex particles owing to their small domain sizes, which can act as nanoreactors in controlled particle synthesis. Latexes formed from emulsion polymerization often have problems with stability whereas preparation of latexes from microemulsions can help circumvent this issue.[72] In addition, smaller latex particles (<50nm) with high surface area can be formed when compared to traditional emulsion polymerization methods. Reducing particle size is of particular interest in the development of novel materials with unique morphologies and properties.[73] Microemulsion templates commonly used for this purpose are of the W/O (inverse) or O/W structure types, where monomer is incorporated into oil or water phase, depending on its solubility.[74] Common surfactants that have been traditionally used in microemulsion polymerization include sodium dodecyl sulfate (SDS), poly(ethylene glycol) sorbitol hexaoleate, cetyltrimethylammonium bromide (CTAB), dodecyltrimethylammonium bromide (DTAB), and Aerosol-OT (AOT), to name a few. They are often used in conjunction with a short-chain alcohol (as a co-surfactant), which has shown to have important implications on the polymerization kinetics of the system due to the differences in equilibrium partitioning between the oil/water phases, which changes depending on alcohol type.[75]

The latex particles produced during microemulsion polymerizations generally have a narrow size distribution and domain sizes of less than 100 nm.[75] Each individual particle typically consists of only a few high molecular weight polymer chains.[76] Some degree of control can be achieved using microemulsions as templates for polymerization. For example, varying the initiator, chain-transfer agent, or surfactant concentration can control molecular weight and particle size.

A less common template for microemulsion polymerization is the bicontinuous structure type. Low monomer loading levels are generally a limiting factor of O/W or W/O microemulsion polymerization, since industrial applications often require high solid latex content. Candau et al. investigated regions of the phase diagram (bicontinuous structure type) that can sustain high monomer concentration. Although the bicontinuous structure was not retained upon monomer polymerization, uniform spherical latex particles with high solid content were produced.[77]

1.5.2. Nanoporous Solids from Microemulsion Polymerization

Although microemulsion polymerization is commonly used for the purpose of synthesizing latex, the polymerization of microemulsions to produce porous solids has also been investigated.[78] The first case of synthesizing porous polymers using microemulsion polymerization techniques was achieved by Qutubuddin and Haque.[79] They polymerized microemulsions of all structure types and investigated the use of anionic and nonionic surfactants to yield solid materials and their effect on polymer structure. The materials produced were of a porous nature, but on length scales far larger (micron and sub-micron) than the parent microemulsion. Other microemulsion systems have since been polymerized into porous materials.[80] Raj et al. polymerized single-phase Winsor IV microemulsions containing methyl methacrylate, acrylic acid, ethylene glycol dimethacrylate (crosslinker), water, and surfactant sodium dodecyl sulfate. Scanning electron microscopy revealed the formation of a highly porous solid.[81,82] Raj et al. have found that the morphology of the porous polymer is influenced by the structure of the parent microemulsion; however, the length scales of the polymer product were of a greater magnitude than the original template.[78]

Common methods for polymerization within a microemulsion are either thermal or photochemical, based on a free radical polymerization process.[74] Thermal polymerization techniques use persulfate initiators or azobisisobutyronitrile (AIBN) at reaction temperatures between 45-70 °C. Photopolymerization can be advantageous because light intensity and exposure time can be used to control molecular weight of the polymer product.[74] Some common photoinitiators are dibenzyl ketone (DBK) and 2,2-dimethyoxy-2-phenylacetophenone (DMPA). Microemulsions that are photopolymerized retained their transparency throughout the process, while thermally polymerized microemulsions tend to become opaque.[74] The resulting particle sizes in microemulsions that turn opaque are often larger than the initial dispersed microemulsion droplets. Reaction speed has been shown to be an important factor in obtaining polymer particles that are on the same size scale as the template and UV methods of cure have been shown to be effective in retaining droplet diameter of original template.

In the formation of porous solids from microemulsion templates, the use of polymerizable surfactants has also been shown to be beneficial towards retaining the structure of micelles, bilayers, and microemulsions. Kline showed that the morphology of rod-like micelles could be preserved upon polymerization using reactive surfactant cetyltrimethylammonium 4-vinylbenzoate (CTVB) to lock-in structure.[83] O'Brien et al. polymerized lyotropic liquid crystals and lipid bilayers by thermally initiated radical chemistry with AIBN and UV irradiation.[84] These studies have shown the ability to "lock-in" structures by reaction of the polymerizable moieties on surfactant molecules, which can also be applied to retaining structure upon microemulsion polymerization. Chew et al. synthesized transparent nanostructured materials by polymerizing bicontinuous microemulsions using polymerizable surfactants ((acryloyloxy)undecyl) dimethylammonium acetate (AUDMAA) and ((acryloyloxy)undecyl)trimethylammonium bromide (AUTMAB). The effect of water and monomer, HEMA, content on polymer morphology was investigated, revealing that higher water content resulted in more intertwined and larger water channels, while increasing the content of HEMA resulted in narrowing and shortening of water channels.[85] Gan et al. have also demonstrated the polymerization of bicontinuous microemulsions using a polymerizable nonionic PEO-based surfactant into transparent materials with pore sizes between 1-10nm.[86]

1.5.3. Polymerization in Silicone Microemulsions

Silicone microemulsion polymerization is a more recent development. Halloran et al. patented a process in 2002 in which silicone latexes with diameters greater than 20 nm were formed by a hydrosilylation reaction. The silicone microemulsion consists of a silicone polyether surfactant, water, and reactive siloxane oligomers. Catalyst was then added after the initial microemulsion preparation to initiate the polymerization of siloxane oligomers into latex particles.[87]

Even more recent is the polymerization of silicone microemulsions to create nanoporous silicone elastomers, an idea that has only begun to surface within the last five years: little is known about these systems and materials. Very few reports have been published on silicone microemulsions or the polymerization of silicone microemulsions with the intent of forming structure materials.[61,66,88,89,90] We discuss the limited publications that have been made in this particular area.

Castellino et al. formed porous silicone materials by independently polymerizing methacrylate monomers and volatile silicone oligomers. Peroxide-initiated radical polymerization was used for the polymerization of methacrylate monomers and platinum-catalyzed hydrosilylation chemistry was used to crosslink silicone oligomers of the oil phase. Despite the use of a polymerizable silicone macromonomer, the polymeric product was opaque and domain sizes of the resulting elastomers were on the order of microns.[91]

Peng et al. investigated the bulk polymerization of a silicone microemulsion and monitored the process using small angle X-ray scattering (SAXS). In this system, a methacrylate-terminated silicone macromonomer (MTSM) was prepared and polymerized in-situ synchrotron SAXS a silicone microemulsion consisting of MTSM and water, stabilized by Teric G_9A_8 surfactant.[92] Optically transparent materials were only obtained for formulations containing 5wt% and 10wt% water and the presence of nanomorphology was not confirmed. Transparent materials were not obtained when 15wt% and 20wt%

water was present in the precursor microemulsions. Peng et al. examined the effects of precursor microemulsion water content on the rate of polymerization and mechanical properties of the porous silicone elastomer.[93] Again, only compositions containing 5wt% and 10wt% water resulted in transparent materials and observed morphology was micrometer in size, although SAXS measurements indicate nanophase separation.

1.6. Microemulsion Characterization

The characterization of microemulsions can be challenging due to small domain sizes and the presence of an aqueous phase. Traditional techniques used in the characterization of macroemulsions are not always applicable to microemulsions; however, there are alternative and suitable methodology and instruments that have been developed. Three techniques that are commonly used in literature in the characterization of these materials will be discussed.

1.6.1. Electron Microscopy & Preparation Techniques

Microemulsions can be difficult to characterize due to domain sizes on the nanometer scale and the presence of aqueous media. The nanometer size scale of microemulsion structures requires imaging techniques with high enough resolution power and is, therefore, limited to electron-based imaging techniques. Transmission electron microscopy (TEM) and scanning electron microscopy (SEM) are commonly used for imaging microemulsions, however, both of these techniques require the sample to be placed in a vacuum.[94] This can be problematic for sample preparation of microemulsions, which contain a volatile aqueous component and possibly volatile oil component as well. TEM is used to image internal mesophase nanostructures as an electron beam passes through the sample.[95] The image is formed from contrast differences that arise in the sample as electrons pass through the material being imaged. Electrons will absorb and scatter differently if there are changes in the material composition on a chemical level.[96] SEM images surface mesophase nanostructures by scanning an electron beam over the surface of the sample. Similar to TEM, the image is created based on how the electrons interact with different areas of the sample.[94]

Imaging microemulsions using electron microcopy techniques can be especially challenging due to their aqueous content. Some techniques have been developed to circumvent this issue, such as cryogenic preparation (cryo-TEM) or freeze fracture (FF-TEM). These techniques are useful for preserving initial structures and preventing artifacts that can occur as a result of sample dehydration. In cryo-TEM, a sample is rapidly frozen in liquid ethane and maintained at liquid nitrogen temperatures throughout the imaging process.[94] The rapid freezing of the sample ideally results in vitrifying any aqueous components of the microemulsion. Unfortunately, cryo-TEM is not a trivial technique, requiring that samples always be kept at cryogenic temperatures in order to avoid conversion of aqueous components to crystalline ice, which can cause defects within the sample making a representative image hard to acquire. In addition cryo-TEM requires specialized holders and cannot be used on viscous samples. These limitations can result in cryo-TEM being a time consuming and expensive task in order to obtain a representative image. There remains a lot of 'art' in the technique.

Freeze fracture TEM (FF-TEM) is a complementary technique to cryo-TEM where samples are fractured under vacuum at cryogenic temperatures with a microtome after being cryogenically frozen. After fracturing, the sample is coated with carbon and platinum to create a replica coating. After creating the replica coating, the sample is removed and the replica is imaged under TEM. This is advantageous for samples that are susceptible to damage by the electron beam and have poor inherent contrast, however, replicas are fragile, difficult to prepare, and require specialized equipment.

1.6.2. Electrical Conductivity

Electrical conductivity is a simple technique for determining structural transitions and regions of microemulsions and is often used a complementary technique to other characterization methods. Electrical conductivity is measured along a dilution line as a mixture of surfactant/oil is titrated with water and the resulting conductivity of the sample is measured as a function of water addition. Oil continuous structures exhibit low conductance, due to isolated water droplets, while conductance increases as more water is titrated into the microemulsion, resulting in a transition to the bicontinuous structure (Figure 1.6.1). The bicontinuous structure has increased conductivity due to the formation of interconnected water channels. The conductivity continues to clime with the addition of water due to greater channel formation, until the structure collapses into water continuous O/W structure type.[97]

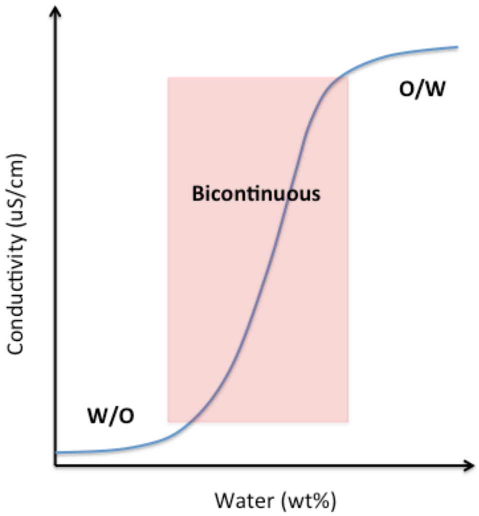

Figure 1.6.1: A representative conductivity curve for the structural transitions between w/o-bicontinuous-o/w in a microemulsion.

1.6.3. Small Angle X-ray Scattering (SAXS)

Scattering techniques are common characterization methods for microemulsion systems. They probe the shape, size, and morphology of microemulsion domains using X-rays or neutrons depending on the specific scattering technique chosen. In neutron scattering, the sample is irradiated with a neutron beam, which scatters depending on atomic interactions within the samples. X-ray scattering has a similar principle, except the radiation source is an X-ray beam. Interactions between the radiation source and the sample are based upon the difference in average electron density between interfaces within a sample.[98] The scattered beam is recorded and analyzed by a detector; the intensity (I) relates to the vector of the scattering amplitude (q) by Equation 3. Equation 4 and Equation 5 relate information regarding distances between interfaces to the scattering vector.

$$I(\vec{q}) = \left|A(\overrightarrow{q})\right|^2 \qquad (3)$$

$$q \equiv 4\pi sin\frac{\theta}{\lambda} \qquad (4)$$

$$d = \frac{\lambda}{2sin\theta} = \frac{2\pi}{Q} \qquad (5)$$

Each characterization technique has both advantages and limitations in the characterization of nanoscale morphologies. Transmission electron microscopy can be prone to misinterpretation due to artifacts or defects within the sample, while SAXS results in a loss of phase information and only provides data based on averages within the material. Electrical conductivity can provide information based on predicted microemulsion structure behavior, but definitive conclusions cannot be drawn based on these results alone. Therefore, a combination of characterization techniques is ideal for the deducing microemulsion structure and morphology information with confidence.

1.7. Applications of Microemulsions

Microemulsions have a broad range of applications such as drug delivery, nanofiltration, cosmetic, and nanoparticle synthesis.[99] Microemulsions are an attractive vehicle for drug delivery owning to their thermodynamic stability, leading to long shelf life, and their ability to solubilize lipophilic and hydrophilic drugs.[100] Drug delivery can be through topical administration or by oral ingestion, however, both methods of drug delivery pose significant challenges. Drugs delivered orally must first be absorbed by the digestive system, which can greatly reduce the concentration of the drug reaching the blood stream, while drugs delivered topically must contend with the skin barrier to function.[101] Microemulsions have been suggested as a suitable vehicle that can help circumvent both of these challenges.

Both drug delivery methods require the drug to be sufficiently soluble in the administering vehicle. Methods currently used to improve drug solubility require one to create salt forms of the drug (hydrochlorides, sulfates, nitrates, etc.) or to reduce particle size of the drug to improve dissolution.[102] Encapsulating drugs into carrier vesicles is an alternative method for improving solubilization and, also, for targeting drug delivery. Microemulsions have been shown to improve drug permeation rates when compared to topical emulsion formulations and, with respect to oral drug delivery, droplet size is correlated with absorption in the intestinal track.[99,102] The drug flux through human skin was compared between drugs (indomethacin and diclofenac) formulated into microemulsions and in an oil vehicle of isopropyl palmitate. Higher drug loadings were attainable in the microemulsion system compared to the neat oil system, leading to increased transdermal delivery.[103] Topical penetration of drugs from microemulsion systems is correlated with high surfactant concentration, which can lead to skin irritation, however, single surfactant systems of n-alkyl polyoxyethylene type can be used to minimize skin irritation.[101] In addition to benefits associated with enhanced permeation of drugs, microemulsions can also act as a protective barrier from the environment and chemical transformations such as hydrolysis, degradation, and oxidation.

A popular microemulsion application is the synthesis of nanoparticles.[99,104] Synthesis of polymeric nanoparticles from monomers such as acrylamide, styrene, methacrylic acid, etc. has been previously discussed within the context of microemulsion polymerization.

Metal nanoparticles can also be synthesized via the microemulsion method where microemulsions are used as nanoreactors to control particle size, surface area, morphology, etc.[105] Particles of Fe_3O_2, TiO_2, and Al_2O_3 have been formed using microemulsion methodology.[106]

Dispersed water droplets in reverse microemulsions can be used as sites for nucleation and growth to form multiple nanoreactor sites. After the initial nucleation phase, particles being to grow and as they form they retain the surfactant layer of the initial micelle, which can lead to sterically stabilized particles (Figure 1.7.1). Particles that do not have sufficient stabilization will begin to form larger aggregates.

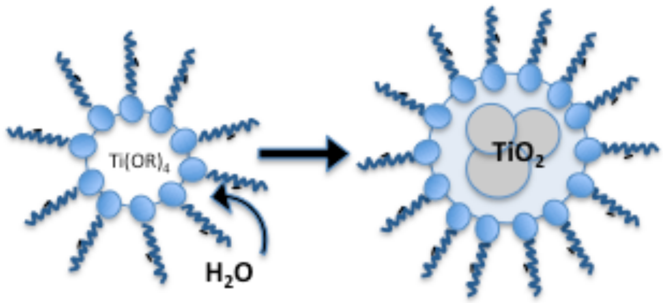

Figure 1.7.1: Micellization of titanium alkoxide and subsequent nucleation and formation of primary titania particles

The two common methods of metal oxide nanoparticle synthesis are the "two-microemulsion" method and the "microemulsion-plus-reactant" method.[105] In the "microemulsion-plus-reactant method" a microemulsion containing a nanoparticle precursor is first prepared. The reaction is initiated when a second reactant required for the reaction is added to the microemulsion.[105] The "microemulsion-plus-reactant" method is a diffusion-mediated process where the diffusion of a second reactant into microemulsion droplets containing the initial reactant initiates particle formation. In the hydrolysis of a metal alkoxide into a metal oxide nanoparticle, the initiating reactant is water, which forms the microemulsion upon its addition.[107]

In the “two-microemulsion” method, two reactants are each solubilized in their own microemulsion. The two individual microemulsions containing reactants are then mixed together in order to initiate the reaction. The mechanism of action in this system involves the fusion and fission of droplets of the “two-microemulsion” systems.[108]

Metal oxide nanoparticles are formed via hydrolysis where the metal alkoxide (particle precursor) reacts with the water droplets of reverse microemulsions. An example of metal oxide formation is the hydrolysis of titanium tetrabutoxide (TTB) in a reverse micelle microemulsion of AOT and isooctane.[109] The microemulsion was first prepared and then injected into a TTB/1-butanol solution to initiate the reaction. The formation of particles within the microemulsion was monitored using UV-Vis spectroscopy**.** It was found that increasing the amount of TTB and water, while decreasing surfactant content, facilitates particle formation and that the number of micelles formed was correlated to the rate of particle growth.[109]

Another approach to the formation of TiO_2 nanoparticles within a microemulsion has been to synthesize a functionalized surfactant containing a Ti^{4+} core by the exchange of Na^+ ion in surfactant sodium bis(2-ethylhexyl) sulfosuccinate (Na-DEHSS) (commonly known as Aerosol-OT). The functionalized surfactant Ti-$(DEHSS)_4$ stabilized the W/O microemulsion and provided the source of titanium in the synthesis of titanium dioxide. Particles were formed within the aqueous core of the Ti-$(DEHSS)_4$ micelle, as water was titrated into the system. Smaller particles were obtained when the water/surfactant ratio was decreased.[107]

There has only been one silicone-based microemulsion system, to my knowledge, that has reported the synthesis of metal oxide nanoparticles. Amorphous aluminum oxide-hydroxide nanoparticles were formed from microemulsions containing water, octanol, and acetylacetone, stabilized by trisiloxane silicone PEG surfactant Silwet L-7607. Particles were synthesized by adding surfactant and water to a solution of aluminum isopropoxide in acetylacetone and octanol.[110] Aluminum isopropyl acetylacetonate was formed upon the interaction of aluminum isopropoxide with acetylacetone. Aluminum isopropyl acetylacetonate hydrolyzed upon contact with water. All particles formed were under 3 nm in diameter; an increase in surfactant concentration resulted in an increase in particle size from ~1nm to ~2.4nm. These aluminum oxide compositions exhibited long-term stability (~1 week) with respect to their transparency and low viscosity, as determined by estimated amounts of aluminum precursor from FTIR measurements taken over time.[110]

1.8. Thesis Focus

There are very few reports of silicone microemulsions containing non-volatile silicone oil and there are even fewer reports of the polymerization of non-volatile silicone microemulsions with the intent of making nanoporous materials. Although there are some reports of crosslinking the oil phase of a silicone microemulsion, which were published after the work disclosed in Chapter 2, there have been none that have resulted in transparent, bicontinuous materials. The goal of Chapter 2 was to polymerize a bicontinuous silicone microemulsion while retaining optical transparency to form nanoporous silicone elastomers that are permeable to aqueous solutions. These materials could find potential uses in drug delivery, biomaterials, or in cosmetic applications. We believe that the polymerization of non-volatile silicone microemulsions can be achieved by using a polymerizable surfactant. The use of polymerization of surfactants to form transparent materials has been investigated in hydrocarbon-based microemulsions, but not been reported, to our knowledge, in the polymerization of silicone microemulsions.

Characterizing the polymerization of silicone microemulsions is an important step in determining the factors that influence morphology and stability during the polymerization process. There are a few reports that attempt to characterize the transition from liquid to solid in the polymerization of a silicone microemulsion in order to better understand the retention and control of morphology. In addition, aside from free radical polymerization processes, there is limited information regarding other types of chemical processes. In Chapter 3, we aim to better understand how the liquid template changes upon polymerization by characterizing microemulsions before and after polymerization using small angle X-ray scattering and transmission electron microscopy. We also focus on exploring the use of room temperature vulcanization (RTV) cure to rigidify silicone microemulsions. RTV is an important commercial process in silicone chemistry and it would be advantageous if RTV could be used to create nanoporous elastomers.

Hydrocarbon-based microemulsions have been previously used to form metal oxide nanoparticles, however, there have been no reports that use silicone microemulsions in the synthesis of TiO_2. Understanding the hydrolysis and condensation of a titanium alkoxide within a silicone microemulsion is an important step towards the development of transparent UV absorbent silicone elastomers. The focus of Chapter 4 is to understand how microemulsion structure affects the formation of TiO_2 particles from the hydrolysis of a titanium alkoxide. We aim to understand how water content (and thus microemulsion structure) affects the rate at which visible TiO_2 is formed and whether particle size can be correlated with rate of formation and microemulsion structure type.

1.9. References

1. Stevens, M. P., *Polymer Chemistry An Introduction* 3rd ed.; Oxford University Press, Inc.: New York, New York, 1999.

2. Brook, M. A., *Silicon in Organic, Organometallic, and Polymer Chemistry*. John Wiley & Sons, Inc.: New York, New York 2000.

3. Rochow, E., *An Introduction Chemistry of The Silicones*. 2 ed.; John Wiley & Sons Inc. : United States, 1947.

4. Palaprat, G.; Ganachaud, F., Synthesis of polydimethylsiloxane microemulsions by self-catalyzed hydrolysis/condensation of dichlorodimethylsilane. *Chimie* **2003,** *6*, 1385-1392.

5. Housecroft, C. E.; Constable, E. C., *Chemistry* Pearson Education Limited Essex, England 2006.

6. Owen, M. J., Surface-Activity of Silicones - Short Review. *Ind Eng Chem Prod Rd* **1980,** *19* (1), 97-103.

7. Hill, R. M., *Silicone Surfactants* Marcel Dekker, Inc.: New York, New York 1999; Vol. 86, p 2-4.

8. He, M.; Hill, R. M.; Lin, Z.; Scriven, L. E.; Davis, H. T., Phase-Behavior and Microstructure of Polyoxyethylene Trisiloxane Surfactants in Aqueous-Solution. *J Phys Chem-Us* **1993,** *97* (34), 8820-8834.

9. O'lenick, A. J., Silicone emulsions and surfactants. *J Surfactants Deterg* **2000,** *3* (3), 387-393.

10. Tiberg, F.; Cazabat, A. M., Self-Assembly and Spreading of Nonionic Trisiloxane Surfactants. *Europhys Lett* **1994,** *25* (3), 205-210.

11. Rosen, M. J.; Song, L. D., Superspreading, skein wetting, and dynamic surface tension. *Langmuir* **1996,** *12* (20), 4945-4949.

12. Radulovic, J.; Sefiane, K.; Shanahan, M. E. R., Spreading and Wetting Behaviour of Trisiloxanes. *J Bionic Eng* **2009,** *6* (4), 341-349.

13. Walderhaug, H.; Knudsen, K. D., Microstructures in aqueous solutions of a polyoxyethylene trisiloxane surfactant and a cosurfactant studied by SANS and NMR self-diffusion. *Langmuir* **2008,** *24* (19), 10637-10645.

14. Svitova, T. F.; Hill, R. M.; Radke, C. J., Spreading of aqueous trisiloxane surfactant solutions over liquid hydrophobic substrates. *Langmuir* **2001,** *17* (2), 335-348.

15. Hill, R. M., Silicone surfactants - new developments. *Curr Opin Colloid In* **2002,** *7* (5-6), 255-261.

16. Dong, J. P.; Mao, G. Z.; Hill, R. M., Nanoscale aggregate structures of trisiloxane surfactants at the solid-liquid interface. *Langmuir* **2004,** *20* (7), 2695-2700.

17. Kunieda, H.; Taoka, H.; Iwanaga, T.; Harashima, A., Phase behavior of polyoxyethylene trisiloxane surfactant in water and water-oil. *Langmuir* **1998,** *14* (18), 5113-5120.

18. Hill, R. M.; He, M. T.; Davis, H. T.; Scriven, L. E., Comparison of the Liquid-Crystal Phase-Behavior of 4 Trisiloxane Superwetter Surfactants. *Langmuir* **1994,** *10* (6), 1724-1734.

19. Li, X.; Washenberger, R. M.; Scriven, L. E.; Davis, H. T.; Hill, R. M., Phase behavior and microstructure of water/trisiloxane E-6 and E-10 polyoxyethylene surfactant/silicone oil systems. *Langmuir* **1999,** *15* (7), 2278-2289.

20. Kunieda, H.; Uddin, H.; Horii, M.; Furukawa, H.; Harashima, A., Effect of Hydrophilic- and Hydrophobic-Chain Lengths on the Phase Behaviour of A-B-type Silicone Surfactants in Water. *J Phys Chem B* **2001,** *105*, 5419-5426.

21. Hollis, S.; Rader, J.; Casey, M. Silicone surfactant-based agricultural formulations and methods for the use thereof. US 8,734,821 2014.

22. Esteves, A. C. C.; Brokken-Zijp, J.; Laven, J.; Huinink, H. P.; Reuvers, N. J. W.; Van, M. P.; de With, G., Influence of cross-linker concentration on the cross-linking of PDMS and the network structures formed. *Polymer* **2009,** *50*, 3955-3966.

23. Lambert, J. M., The Nature of Platinum in Silicones for Biomedical and Healthcare Use. *Journal of Biomedical Materials Research Part B: Applied Biomaterials* **2006,** *78B* (1), 167-180.

24. Sommer, L. H.; Pietrusza, E. W.; Whitmore, F. C., Peroxide-catalyzed addition of trichlorosilane to 1-octene. *Journal of the American Chemical Society* **1947,** *69*, 188.

25. RTV moisture cure systems for silicone polymers. http://www.dowcorning.com/content/discover/discoverchem/rtv-moisture-cure.aspx (accessed November 17).

26. Colas, A.; Curtis, J., Silicone biomaterials: history and chemistry. In *Biomedical Engineering Desk Reference* Academic Press/Elsevier Jordan Hill, Oxford, UK

San Diego, California, USA, 2009; pp 167-171.

27. Comaills-Autin, L.; Cassagnau, P.; Seggio, A.; Mondiere, A.; Spitz, R.; Monteil, V., Investigations on interactions between titanium alkoxides and α,ω-dihydroxy PDMS by a combination of rheology and spectroscopy. *European Polymer Journal* **2014,** *57*, 37-46.

28. Cantor, M. O., Silicone Rubber T Tubes for Common Duct Drainage *The American Journal of Surgery* **1964,** *107*, 666-668.

29. http://www.dowcorning.com/content/discover/discovershowcase/healthcare.aspx (accessed November 7, 2015).

30. Ghanbari, H.; Cousins, B. G.; Seifalian, A. M., A Nanocage for Nanomedicine: Polyhedral Oligomeric Silsesquioxane (POSS). *Macromol Rapid Comm* **2011,** *32* (14), 1032-1046.

31. Ghanbari, H.; de Mel, A.; Seifalian, A. M., Cardiovascular application of polyhedral oligomeric silsesquioxane nanomaterials: a glimpse into prospective horizons. *Int J Nanomed* **2011,** *6*, 775-786.

32. Li, Y.; Tao, P.; Viswanath, A.; Benicewicz, B. C.; Schadler, L. S., Bimodal Surface Ligand Engineering: The Key to Tunable Nanocomposites. *Langmuir* **2013,** *29* (4), 1211-1220.

33. Crick, C. R.; Bear, J. C.; Southern, P.; Parkin, I. P., A general method for the incorporation of nanoparticles into superhydrophobic films by aerosol assisted chemical vapour deposition. *J Mater Chem A* **2013,** *1* (13), 4336-4344.

34. Lei, L., Xishan, W., Dengke, C., Corona Ageing Tests of RTV and RTV nanocomposite Materials. In *2004 International Conference on Solid Dielectrics* Toulouse, France, 2004.

35. Dhoke, S. K.; Bhandari, R.; Khanna, A. S., Effect of nano-ZnO addition on the silicone-modified alkyd-based waterborne coatings on its mechanical and heat-resistance properties. *Prog Org Coat* **2009,** *64* (1), 39-46.

36. Sun, F.; Hu, Y.; Du, H. G., Synthesis and Characterization of MQ Silicone Resins. *J Appl Polym Sci* **2012,** *125*, 3532-3536.

37. Xiang, H.; Ge, J.; Cheng, S.; Han, H.; Cui, S., Synthesis and characterization of titania/MQ silicone resin hybrid nanocomposite via sol-gel process. *J Sol-Gel Sci Techn* **2011,** *59*, 635-639.

38. Huang, W.; Huang, Y.; Yu, Y., Synthesis of MQ silicone resins through hydrolytic condensation of ethyl polysilicate and hexamethyldisiloxane. *J Appl Polym Sci* **1998,** *70* (9), 1753-1757.

39. Yoshii, K.; Yamashita, T.; Machida, S.; Horie, K.; Itoh, M.; Nishida, F.; Morino, S., Photo-probe study of siloxane polymers. I. Local free volume of an MQ-type silicone

resin containing crosslinked nanoparticles probed by photoisomerization of azobenzene. *J Non-Cryst Solids* **1999,** *246*, 90-103.

40. Han, Y.; Zhao, Y. M.; Xie, C.; Powers, J. M.; Kiat-Amnuay, S., Color stability of pigmented maxillofacial silicone elastomer: Effects of nano-oxides as opacifiers. *J Dent* **2010,** *38*, E100-E105.

41. Hoar, T. P.; Schulman, J. H., Transparent Water-in-Oil Dispersions: the Oleopathic Hydro-Micelle. *Nature* **1943,** *152* (3847), 102-103.

42. Schulman, J. H.; Stoeckenius, W.; Prince, L. M., Mechanism of Formation and Structure of Micro Emulsions by Electron Microscopy *J Phys Chem-Us* **1959,** *63* (10), 1677-1680.

43. Schulman, J. H.; Montagne, J. B., Formation of Microemulsions by Amino Alkyl Alcohols. *Annals New York Academy of Sciences* **1961,** *92* (2), 366-371.

44. Rosano, H. L., Clausse, M., *Microemulsion Systems* Marcel Dekker, INC.: New York, New York, 1987.

45. Winsor, P. A., Hydrotropy, solubilisation, and related emulsification processes. Part 1. *Transactions of the Faraday Society* **1948,** *44*, 376-398.

46. Kahlweit, M., Strey, R., Busse, G., Microemulsions: A Qualitative Thermodynamic Approach *The Journal of Physical Chemistry* **1990,** *94* (10), 3381-3894.

47. Ruckenstein, E., Microemulsions, Macroemulsions, and the Bancroft Rule. *Langmuir* **1996,** *12*, 6351-6353.

48. Oldfield, C., Enzymes in Water-in-oil Microemulsions ('Reversed Micelles'): Principles and Applications. *Biotechnology and Genetic Engineering Reviews* **1994,** *12*, 255-327.

49. Komura, S., Mesoscale structures in microemulsions. *Journal of PHysics: Condensed Matter* **2007,** *19*.

50. Wennerstrom, H.; Soderman, O.; Olsson, U.; Lindman, B., Macroemulsions versus microemulsions. *Colloids and Surfaces A: Physiochemical and Engineering Aspects* **1997,** *123-124*, 13-26.

51. Ning, H.; Kita, R.; Kriegs, H.; Luettmer-Strathmann, J.; Wiegand, S., Thermal diffusion behavior of nonionic surfactants in water. *J Phys Chem B* **2006,** *110* (22), 10746-10756.

52. Ruckenstein, E., Phase inversion temperatures of macro- and microemulsions. *Langmuir* **1997,** *13* (9), 2494-2497.

53. Cosgrove, T., *Colloid Science Principles, Methods and Applications*. Second ed.; John Wiley & Sons Ltd: West Sussex, United Kingdom 2010; p 91-105.

54. Tadros, T. F., *An Introduction to Surfactants*. Walter de Gruyter GmbH: Berlin, Germany 2014.

55. Ruckenstein, E.; Chi, J. C., Stability of microemulsions *Journal of the Chemical Society-Faraday Transactions 2* **1975,** *71*, 1690-1707.

56. Ruckenstein, E., Origin of Thermodynamic Stability of Microemulsions. *Chem Phys Lett* **1978,** *57* (4), 517-521.

57. Kronberg, B.; Holmberg, K.; Lindman, B., *Surface Chemistry of Surfactants and Polymers* John Wiley & Sons, Ltd.: West Sussex, United Kingdom, 2014; p 330-333.

58. Stokes, R. J.; Evans, D. F., Amphiphilic Systems-Liquid-Liquid Interfaces. In *Fundamentals of Interfacial Engineering*, Wiley-VCH, Inc.: New York, New York, 1997; pp 235-243.

59. Hill, R. M. Spontaneously formed clear silicone microemulsions. US 5705562, 1998.

60. Feng, Q. J.; Lin, Z.; Hill, R. M. Clear silicone microemulsions formed spontaneously. 2006.

61. Steytler, D. C., Dowding, P. J., Robinson, B. H., Characterization of Water-in-Oil Microemulsions Formed in Silicone Oils. *Langmuir* **1998,** *14*, 3517-3523.

62. Somasundaran, P.; Mehta, S. C.; Purohit, P., Silicone emulsions. *Advances in Colloid and Interface Science* **2006,** *128*, 103-109.

63. O'Lenick, A. J.; Parkinson, J. K., Three-Dimensional HLB. *Cosmetics & Toiletries Magazine* 1996, pp 37-43.

64. Shah, D. O., *Micelles, Microemulsions, Monolayers*. Marcel Dekker, Inc.: New York, New York, 1998; p 197-198.

65. Silas, J. A., Kaler, E. W., Hill, R. M., Effect of Didodecyldimethylammonium Bromide on the Phase Behaviour of Nonion Surfactant-Silicone Oil Microemulsions *Langmuir* **2001,** *17*, 4534-4539.

66. Castellino, V.; Cheng, Y. L.; Acosta, E., The Hydrophobicity of silicone-based oils and surfactants and their use in reactive microemulsions. *J Colloid Interf Sci* **2011,** *353*, 196-205.

67. Li, X.; Washenberger, R. M.; Scriven, L. E.; Davis, H. T.; Hill, R. M., Phase Behaviour and Microstructure of Water/Trisiloxane E12 Polyoxyethylene Surfactant/Silicone Oil Systems *Langmuir* **1999,** *15*, 2267-2277.

68. Sharma, S. C., Tsuchiya, K., Sakai, K., Sakai, H., Abe, M., Komura, S., Sakamoto, K., Miyahara, R., Formation and Characterization of Microemulsion Containing Polymeric Silicone. *Langmuir* **2008,** *24*, 7658-7662.

69. Gee, R. P., Oil-in-water microemulsions from association structures of surfactant, water and aminosilicone polymer oil. *Colloids and Surfaces A: Physiochemical and Engineering Aspects* **1998,** *137*, 91-101.

70. Yan, F.; Texter, J., Capturing nanoscopic length scales and structures by polymerization in microemulsions. *Soft Matter* **2006,** *2* (2), 109-118.

71. Texter, J., *Reactions and Synthesis in Surfactant Systems* Marcel Dekker, Inc.: New York, New York, 2001; Vol. 100, p 455-457.

72. Candau, F.; Zekhnini, Z.; Heatley, F.; Franta, E., Characterization of Poly(Acrylamide-Co-Acrylates) Obtained by Inverse Microemulsion Polymerization. *Colloid Polym Sci* **1986,** *264* (8), 676-682.

73. Pavel, F. M., Microemulsion Polymerization. *J Disper Sci Technol* **2004,** *25* (1), 1-16.

74. Gupta, B.; Singh, H., Polymerization in Microemulsion Systems. *Polym-Plast Technol* **1992,** *31* (7-8), 635-658.

75. Hentze, H. P.; Kaler, E. W., Polymerization of and within self-organized media. *Curr Opin Colloid In* **2003,** *8* (2), 164-178.

76. Gan, L. M.; Chew, C. H.; Lye, I.; Imae, T., Microemulsion Polymerization of Styrene. *Polymer Bulletin* **1991,** *25* (2), 193-198.

77. Candau, F.; Zekhnini, Z.; Durand, J. P., Copolymerization of Water-Soluble Monomers in Nonionic Bicontinuous Microemulsions. *J Colloid Interf Sci* **1986,** *114* (2), 398-408.

78. Raj, W. R. P.; Sasthav, M.; Cheung, H. M., Polymerization of Single-Phase Microemulsions - Dependence of Polymer Morphology on Microemulsion Structure. *Polymer* **1995,** *36* (13), 2637-2646.

79. Qutubuddin, S.; Lin, C. S.; Tajuddin, Y., Novel Polymeric Composites from Microemulsions. *Polymer* **1994,** *35* (21), 4606-4610.

80. Raj, W. R. P.; Sasthav, M.; Cheung, H. M., Microcellular Polymeric Materials from Microemulsions - Control of Microstructure and Morphology. *J Appl Polym Sci* **1993,** *47* (3), 499-511.

81. Raj, W. R. P.; Sasthav, M.; Cheung, H. M., Formation of Porous Polymeric Structures by the Polymerization of Single-Phase Microemulsions Formulated with Methyl-Methacrylate and Acrylic-Acid. *Langmuir* **1991,** *7* (11), 2586-2591.

82. Raj, W. R. P.; Sasthav, M.; Cheung, H. M., Polymerization of Microstructured Aqueous Systems Formed Using Methyl-Methacrylate and Potassium Undecenoate. *Langmuir* **1992,** *8* (8), 1931-1936.

83. (a) Kline, S., Structural evolution during micelle polymerization. *J Appl Crystallogr* **2000,** *33* (1), 618-622; (b) Kline, S. R., Polymerization of rodlike micelles. *Langmuir* **1999,** *15* (8), 2726-2732.

84. O'Brien, D. F.; Armitage, B.; Benedicto, A.; Bennett, D. E.; Lamparski, H. G.; Lee, Y.; Srisiri, W.; Sisson, T. M., Polymerization of Preformed Self-Organized Assemblies *Accounts of Chemical Research* **1998,** *31* (12), 861-868.

85. Chew, C. H.; Li, T. D.; Gan, L. H.; Quek, C. H.; Gan, L. M., Bicontinuous-nanostructured polymeric materials from microemulsion polymerization. *Langmuir* **1998,** *14* (21), 6068-6076.

86. Gan, L. M.; Liu, J.; Poon, L. P.; Chew, C. H.; Gan, L. H., Microporous polymeric composites from bicontinuous microemulsion polymerization using a polymerizable nonionic surfactant. *Polymer* **1997,** *38* (21), 5339-5345.

87. Halloran, D. J.; Hill, R. M.; Wrolson, B. M.; Zimmerman, B. L. Polymerization of Silicone Microemulsions. 2002.

88. Peng, S., Hartley, P. G., Hughes, T. C., Guo, Q., Controlling morphology and porosity of porous siloxane membranes through water content of precursor microemulsion. *Soft Matter* **2012,** *8*, 10493-10501.

89. Wolf, L.; Hoffmann, H.; Watanabe, K.; Okamoto, T., Microemulsions from silicone oil with an anionic/nonionic surfactant mixture. *Physical Chemistry Chemical Physics* **2011,** *13*, 3248-3256.

90. Brook, M. A.; Whinton, M.; Gonzaga, F.; Li, N., Elastomeric hydrogels by polymerizing silicone microemulsions. *Chem Commun* **2011,** *47* (31), 8874-8876.

91. Castellino, V., Acosta, E., Cheng, Y., Interpenetrating polymer networks templated on bicontinuous microemulsions containing silicone oil, methacrylic acid, and hydroxyethyl methacrylate *Colloid Polymer Science* **2013,** *291*, 527-539.

92. Peng, S.; Guo, Q.; Hughes, T. C.; Hartley, P. G., In Situ Synchrotron SAXS Study of Polymerizable Microemulsions. *Macromolecules* **2011,** *44*, 3007-3015.

93. Peng, S.; Hartley, P. G.; Hughes, T. C.; Guo, Q., Controlling morphology and porosity of porous siloxane membranes through water content of precursor microemulsion. *Soft Matter* **2012,** *8*, 10493-10501.

94. Acharya, D. P.; Hartley, P. G., Progress in microemulsion characterization. *Curr Opin Colloid In* **2012,** *17* (5), 274-280.

95. Von Heimendahl, M., *Electron Microscopy of Materials An Introduction*. Academic Press, Inc.: New York, New York, 1980; p 1-6.

96. Milne, J. L. S.; Borgina, M. J.; Bartesaghi, A.; Tran, E. E. H.; Earl, L. A.; Schauder, D. M.; Lengyel, J.; Pierson, J.; Patwardhan, A.; Subramaniam, S., Cryo-electron microscopy- a primer for the non-microscopist. *Federation of European Biochemical Societies Journal* **2013,** *280*, 28-45.

97. Kogan, A.; Shalev, D. E.; Raviv, U.; Aserin, A.; Garti, N., Formation and Characterization of Ordered Bicontinuous Microemulsions. *J Phys Chem B* **2009,** *113* (31), 10669-10678.

98. Chu, B.; Hsiao, B. S., Small-Angle X-ray Scattering of Polymers. *Chem Rev* **2001,** *101*, 1727-1761.

99. Solans, C.; Izquierdo, P.; Nolla, J.; Azemar, N.; Garcia-Celma, M. J., Nano-emulsions. *Curr Opin Colloid In* **2005,** *10* (3-4), 102-110.

100. Lawrence, M. J.; Rees, G. D., Microemulsion-based media as novel drug delivery systems. *Adv Drug Deliver Rev* **2012,** *64*, 175-193.

101. Kreilgaard, M., Influence of microemulsions on cutaneous drug delivery. *Adv Drug Deliver Rev* **2002,** *54*, S77-S98.

102. Kogan, A.; Garti, N., Microemulsions as transdermal drug delivery vehicles. *Advances in Colloid and Interface Science* **2006,** *123*, 369-385.

103. Dreher, F.; Walde, P.; Walther, P.; Wehrli, E., Interaction of a lecithin microemulsion gel with human stratum corneum and its effect on transdermal transport. *Journal of Controlled Release* **1997,** *45*, 131-140.

104. Rao, J. P.; Geckeler, K. E., Polymer nanoparticles: Preparation techniques and size-control parameters. *Prog Polym Sci* **2011,** *36* (7), 887-913.

105. Malik, M. A.; Wani, M. Y.; Hashim, M. A., Microemulsion method: A novel route to synthesize organic and inorganic nanomaterials. *Arab J Chem* **2012,** *5* (4), 397-417.

106. Eastoe, J.; Warne, B., Nanoparticle and polymer synthesis in microemulsions. *Curr Opin Colloid In* **1996,** *1* (6), 800-805.

107. Lal, M.; Chhabra, V.; Ayyub, P.; Maitra, A., Preparation and characterization of ultrafine TiO2 particles in reverse micelles by hydrolysis of titanium di-ethylhexyl sulfosuccinate. *J Mater Res* **1998,** *13* (5), 1249-1254.

108. Kumar, P.; Mittal, K. L., *Handbook of Microemulsion Science and Technology*. Marcel Dekker, Inc: New York, New York, 1999; p 556-558.

109. Hirai, T.; Sato, H.; Komasawa, I., Mechanism of Formation of Titanium-Dioxide Ultrafine Particles in Reverse Micelles by Hydrolysis of Titanium Tetrabutoxide. *Ind Eng Chem Res* **1993,** *32* (12), 3014-3019.

110. Berkovich, Y.; Aserin, A.; Wachtel, E.; Garti, N., Preparation of amorphous aluminum oxide-hydroxide nanoparticles in amphiphilic silicone-based copolymer microemulsions. *J Colloid Interf Sci* **2002,** *245* (1), 58-67.

2. Chapter 2: Elastomeric Hydrogels by Polymerization Silicone Microemulsions[1]

2.1. Abstract

Robust, transparent elastomeric hydrogels encoded with a bicontinuous structure result from the sequential photopolymerization of the aqueous hydroxyethyl methacrylate phase and crosslinking of the silicone phase of a silicone microemulsion stabilized with an acrylate-functional silicone-poly(ethylene glycol) surfactant.

2.2. Introduction

Silicones possess many properties that make them of interest for biomaterials applications, including low foreign body and inflammatory responses, ease of preparation of complex shapes, high oxygen permeability, etc.[1] However, their hydrophobicity, which is only surpassed by fluorocarbon polymer[2], can be problematic at biological interfaces. For example, current contact lenses are based on hydrophilically-modified silicone hydrogels because pure silicone contact lenses adhere strongly to corneal tissues.[3]

Microemulsions (μE) are thermodynamically stable, optically transparent mixtures derived from water, oil and a high loading of surfactants. In addition to water-in-oil (W/O) and oil-in-water (O/W) dispersions, bicontinuous structures are accessible with appropriate formulations.[4,5]

---

[1] This chapter was adapted from M. A. Brook, M. Whinton, F. Gonzaga, and N. Li, *Chemical Communications*, **2011**, 47, 8874-8876 and has been reproduced with permissions. Whinton & Li developed and polymerized microemulsion formulations. Whinton constructed phase diagrams and performed conductivity experiments. Brook & Whinton wrote the manuscript.

Silicone μE are well known.[6] Although they have been prepared using block silicone-oligoEO (ethylene oxide) non-ionic surfactants, most are based, optionally with co-surfactants[7], on so-called superwetter surfactants comprised of a short trisiloxane chain 2with a pendant EO chain **1** (typically n = 6-8, Figure 2.3.1): different manufacturers sell variations with different EO chain lengths and/or OMe, or OAc in place of the alcohol end groups. Microemulsions are relatively easy to prepare with these surfactants using low molecular weight silicone oils[8], but the use of higher molecular weight materials has been reported only in rare instances.[9]

Bicontinuous, optically transparent silicone μE should possess a very useful combination of properties for use as biomaterials if both phases could be polymerized to give robust hydrogels: water and ion permeability and enhanced surface hydrophilicity would result from the water-rich phase, while oxygen permeability would result from the silicone phase. Dow Corning has described the crosslinking of the silicone phase within a microemulsion.[10] One report of acrylate polymerization in the aqueous phase with a silane co-monomer has also appeared[11], and Acosta and Chen have noted that silicone oils may be crosslinked in oil phases of μE that contain acrylate monomers in the water phase.[12] We are unaware of any reports of the preparation of transparent, bicontinuous hydrogels derived from silicone microemulsions by polymerizing both phases.

The key challenge to preparing polymerizable silicone microemulsions is control of the internal interfaces such that the bicontinuous structure, encoded during the initial microemulsion formation, is maintained during polymerization of both the aqueous and

---

silicone phases. Frequently, changes in surfactancy during polymerization are destabilizing to the water/oil interface and lead to morphological changes in the microemulsion. We describe below a strategy to achieve such dual polymerization leading to optically transparent, bicontinuous silicone elastomeric hydrogels.

2.3. Results & Discussion

Hill provided a practical recipe for the preparation of silicone microemulsions, which included low molecular weight silicones MM ($Me_3SiOSiMe_3$)[13] or D_4 ($(Me_2SiO)_4$)[14,15] as the oil phase, water, and large quantities of non-ionic silicone surfactant **1**. This was used as the starting point for polymerizable microemulsion formulations. Systematic variation of the surfactant concentrations permitted the preparation of μE with somewhat higher (15–35 cSt, ~400-700 g mol^{-1}) and much higher molecular weight hydroxy-terminated silicone oils (45-85 cSt, ~2500-3500 g mol^{-1}). In both cases, only high concentrations of surfactant **1** or **2** led to stable microemulsions (Table 2.3.1); **1** was more effective than **2** (Figure 2.3.1).

The phase diagram, determined using conductivity measurements, showed a relatively narrow μE zone that was, however, considerably broader when acrylic monomers were included in the aqueous phase (Supporting Information), as has been previously noted:[16] the bicontinuous μE region of the phase diagram was also larger. Formulations prepared with surfactant **2** (Figure 2.3.2) had broader microemulsion regions than those formulated with **1**.

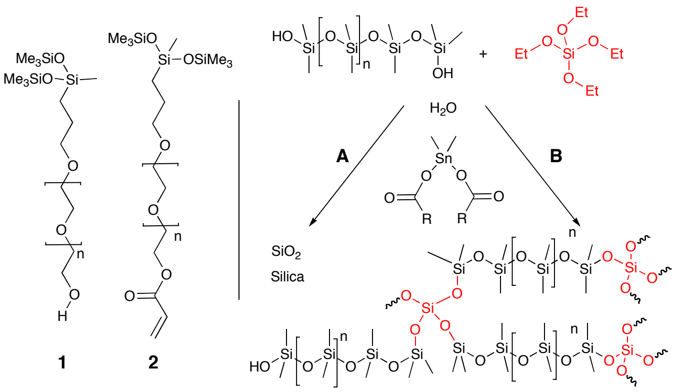

Figure 2.3.1: Silsurf A008-UP, **2**: Silmer ACR A008-UP (n~8), A: formation of silica under the same reaction conditions, B: condensation cure of silicones

Either or both the silicone and aqueous phases could be polymerized with the addition of appropriate additives. The polymerization/crosslinking reactions were specifically chosen to be orthogonal, so it was possible to independently cure/crosslink either phase in either order. The silicone portion of the μE was thermally crosslinked using condensation cure of hydroxy-terminated silicones with TEOS ($Si(OEt)_4$) crosslinker at room temperature (Figure 2.3.1 B). Excess TEOS was utilized such that reinforcing silica (Figure 2.3.1 A) could simultaneously be produced during cure.[17,18] Microemulsion formulations based on this system become more rigid after about 48 hours at room temperature or more rapidly at 50 °C. The ultimate hardness of the resulting silicone elastomer depended on the crosslink density, which correlated with the amount of TEOS added. However, the polymerized silicone-based hydrogels were not of practical utility as biomaterials, as they were too soft and barely self-supporting: they could not be removed from the vessel in which they were prepared.

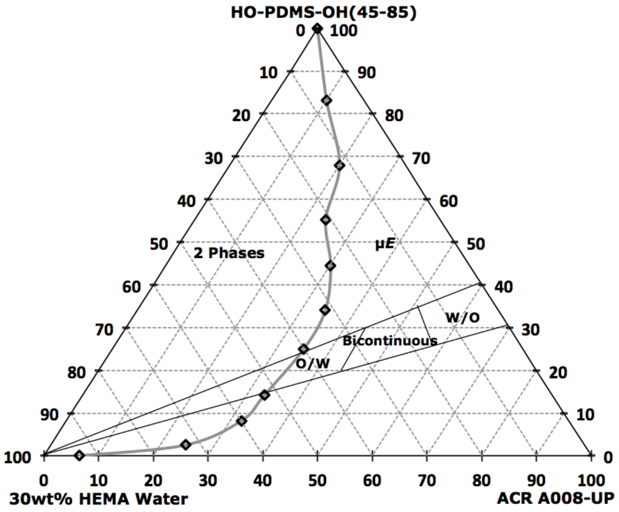

Figure 2.3.2: Phase diagrams according to entry 6, Table 2.3.1.

More robust elastomeric materials were prepared by also polymerizing an acrylic monomer (hydroxyethyl methacrylate, HEMA) in the aqueous phase water at concentrations ranging from 10-50wt% (Table 2.3.1) either before or after silicone cure. Radical cure of the HEMA monomer was facilitated by the incorporation of either the photoinitiator 2-hydroxy-2-methylpropiophenone (HMP) or 2,2´-dimethoxy-2-phenylacetophenone (DMPA) into the uncured microemulsion at 0.5wt%, a concentration that did not appear to affect stability of the microemulsion. Photoinduced polymerization at 254 nm was complete after 15 minutes. After silicone cure, optically clear, flexible elastomeric hydrogels resulted. They were also surprisingly stable to dehydration/rehydration cycles. As shown in Figure 2.3.3 most, but not all, cracks that formed during the dehydration process under vacuum at 50 °C for 24 hour reheated after rehydration in water for 24 hours.

The product elastomer was comprised of domains of approximately 10 nm as shown by SEM measurements (Figure 6.1.3, Supporting Information) as confirmed by EDX measurements (data not shown). The water domains were permeable, as shown by the ability of an aqueous solution of the pH indicator phenol red to be absorbed into the water channels (Figure 2.3.4). After subsequently soaking the dyed elastomers in water, the elastomer released about 75% of the absorbed phenol red over 3 days (Supporting Information).

The mechanical strength of the optically clear hydrogels resulting from polymerizing/crosslinking both the aqueous and silicone phases of mE depended strongly on the constituents. The concentrations of HEMA, TEOS and the respective catalysts in the silicone and aqueous phases played minor roles, while the molecular weight of the silicones and the specific surfactants highly influenced hydrogel properties.

We compare four different materials, those prepared with low and high molecular weight silicones, respectively, and stabilized with surfactant **1** or surfactant **2**, respectively (Table 2.3.1, entries 6, 9, 12, 13). With either surfactant, the hydrogels were more rigid when prepared with lower molecular weight silicones. However, the hydrogel prepared from surfactant **1** (Table 2.3.1, entry 9), which was initially rigid, became brittle on storage for a day or two, consistent with increased crosslinking of TEOS and/or loss of water. It was not stable. The hydrogels prepared from high molecular weight silicones and surfactant **1** (Table 2.3.1, entry 12) were soft gels with little cohesive strength.

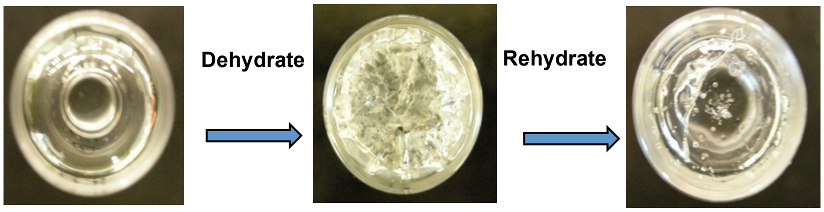

Figure 2.3.3: Top view of polymerized microemulsion after a de/rehydration cycle (vial diameter ~ 1 cm).

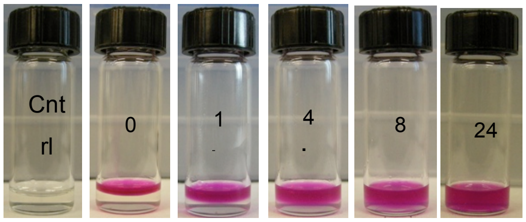

Figure 2.3.4: Polymerized microemulsion absorption of phenol red over time (hours) (vial diameter ~ 1.5 cm).

The hydrogels derived from **2** and either lower or higher molecular weight silicones (Table 2.3.1, entry 6, 13) were, by contrast, self-supporting, mechanically robust and flexible: the hydrogel derived from the lower molecular weight silicone was the more rigid of the two and almost tack free. Both hydrogels were (barely) too soft to characterize using a Shore A Hardness instrument before extraction, although they became harder after extraction (which led to 48% weight loss of water, silicone and ungrafted surfactant; the Shore A Hardness of the extracted product (Table 2.3.1, entry 13) was 10.

Frequently, microemulsions are destabilized by processes that lead to changes in surfactancy: structural conversions from bicontinuous to W/O or O/W or complete phase separation are well known, particularly during the enormous changes that occur during polymerization. The silicone-based formulations described above are very forgiving in this regard, although some subtleties could be seen by comparing the effect of lower and higher molecular weight silicones on the ability to prepare bicontinuous microemulsions. With the lower molecular weight silicone, much more surfactant was necessary to make bicontinuous microemulsions than with the higher molecular weight silicone. This is ascribed to a need for more surfactant to anchor the interface of a highly mobile silicone phase (Figure 2.3.5 A). Provided that relatively large fractions of surfactant were present (>40%) in the microemulsion formulation, however, it was possible to form bicontinuous structures with water contents ranging from about 17 to 35 % and silicone ranging from about 21 to 38 % (Table 2.3.1).

Table 2.3.1: Microemulsion Formulations

Entry	Surfactant	Wt%	Water Phase (wt%)	H_2O	HEMA	Silicone Phase (wt%)	PDMS
1	**1**	45.0	25.0	25.0	0	30.0	30.0 L
2	**1**	23.9	37.9	33.0	3.7	38.2	38.2 H
3	**2**	50.0	20.0	18.0	2.0	30.0	30.0 L
4	**2**	38.0	30.0	15.0	15.0	32.0	32.0 L
5	**2**	42.0	33.0	23.1	9.9	25.0	25.0 L
6*	**2**	42.0	26.5	18.2	7.8	31.5	28.0 H
7	**2**	43.4	26.9	23.8	2.6	28.6	25.6 H
8	**2**	46.1	28.6	24.8[b]	3.0	25.6	22.5 H
9*	**1**	38.8	29.8	20.2	8.6	30.9	16.2 L
10	**1**	40.0	30.0	-	-	30.0[c]	18.0 L
11	**2**	45.4	27.1	24.4	2.7	27.5	25.2 H
12*	**1**	39.3	29.3	25.4	2.8	31.4	27.1 H
13*	**2**	45.6	26.8	18.4	7.9	27.6	15.1 L
14	**2**	44.4	29.4	25.1	3.3	26.2	22.6 H
15	**2**	46.6	27.8	24	2.9	25.6	22.1 H

[a]For complete formulations, including catalyst concentrations, see Table 6.1.1 in supporting information. L = 15-35 cSt PDMS, H = 45-85 cSt PDMS. [b]No photoinitiator in the formulation. [c]Benzylamine was the catalyst for this recipe only, otherwise dibutyltin dilaurate was used.[*] Practical, doubly polymerized/crosslinked microemulsions.

The microemulsions were readily converted to transparent elastomeric hydrogels provided sufficient surfactant was present and that both phases were polymerized.

Crosslink density in the silicone phase can be manipulated by changes in the crosslinker concentration and average chain length of the silicone oil. The solids content of the aqueous phase is variable over a relatively low range, in the case of HEMA from about 10 to 50wt%. For practical purposes, only when reactive surfactant **2** was used did stable, elastomeric hydrogels result. This is ascribed to the stabilization of the interface that occurs when the surfactant becomes tethered there by a radical polymerization process (Figure 2.3.5 B).

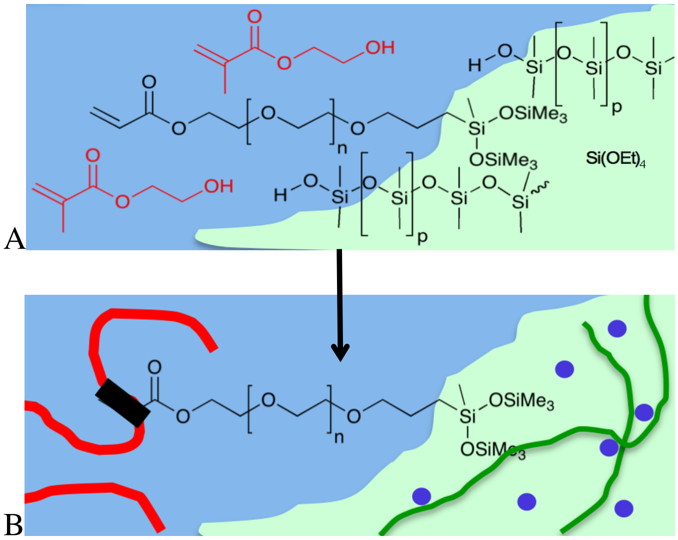

Figure 2.3.5: Model of the internal water/silicone oil interface during crosslinking/photopolymerization.

Biomaterials face challenges both with respect to achieving acceptable properties and with respect to regulatory requirements. With silicone biomaterials, there are concerns about low molecular weight silicones (<1500 MW) leaching from devices in vivo.[19] The latter concern is partly mitigated by moving to higher molecular weight silicones. Future work will examine strategies that reduce further any biological and environmental burden posed by extractables from the device while maintaining the structural integrity of the polymerized silicone microemulsion.

2.4. Conclusion & Acknowledgements

Transparent, robust silicone elastomeric hydrogels can be created by polymerizing both the aqueous phase and oil phase of appropriate functionalized silicone microemulsions using polymerizable surfactants. The authors acknowledge with gratitude the financial support of 20/20: NSERC Ophthalmic Materials Network and Rick Vrckovnik (Siltech Corp.) for providing samples of 2.

2.5. Experimental

2.5.1. Materials

Hydroxy-terminated polydimethylsiloxane (PDMS, 15–35 cSt, ~400-700 g mol^{-1}) "lower molecular weight silicones" and aminopropyl-terminated PDMS ($H_2N(CH_2)_3(SiMe_2O)_nSiMe_2(CH_2)_3NH_2$, n~11, 10–15 cSt, ~875 g mol^{-1}) both from Gelest, phenol red (Fisher), hydroxy-terminated PDMS (45-85 cSt, ~2500-3500 g mol^{-1}) "higher molecular weight silicones", tetraethoxysilane ($Si(OEt)_4$, TEOS, 99.999%), benzylamine (99%), dibutyltin dilaurate (95%), 2-hydroxy-2-methylpropiophenone (97%, HMP), and 2,2-dimethoxy-2-phenylacetophenone (99%, DMPA) all from Aldrich, and Silsurf A008-UP **1** and Silmer ACR A008-UP **2** from Siltech, Toronto were used as received. The hydrophilic monomer, hydroxyethyl methacrylate (HEMA, 98%) was obtained from Sigma and the inhibitor MEHQ was removed by passing the chemicals through a commercial column (Aldrich) designed for this purpose prior to formulation into a microemulsion.

2.5.2. Formation of Microemulsions

2.5.2.1. Non Polymerizable

Initial microemulsion formulations consisted of hydroxy-terminated PDMS, **1** and water. The phase diagram of the **1**/PDMS/H_2O ternary system (Figure 6.1.2 A, Supporting Information) was constructed by titration with water as follows. First, the required masses of surfactant and PDMS were mixed. For each titration, the PDMS/A008 weight ratio (I) was fixed. The phase boundaries were determined by observing the transition from turbidity to transparency or from transparency to turbidity. The region marked "μE" was transparent and the region marked ''two phases'' was turbid, i.e., a microemulsion in equilibrium with an excess of PDMS or water phase, respectively. The phase diagram was established by repeating the experiment for a series of I values. The transition of the microemulsion into a bimodal, continuous structure was identified by conductivity measurements at room temperature and 1 atm.

2.5.2.2. Polymerizable μE

Phase diagrams were determined as described in the previous paragraph. However, additional materials were present in the polymerizable formulations: *surfactant* non-polymerizable **1** or polymerizable **2**; *water phase* water + HEMA and photoinitiator; *silicone phase* PDMS + TEOS and catalyst. In all cases, the aqueous phase was titrated into the silicone/surfactant mixture to create the phase diagram.

2.5.2.3. Silicone Cure

Silicone cure was induced using three different types of moisture cure room temperature vulcanization (RTV) catalysts: benzylamine, aminopropyl-terminated silicone and dibutyltin dilaurate. The former amine catalysts are less efficient but facilitate both crosslinking and large particle silica formation from TEOS, which was used in the crosslinker. Large particle silica formation was always more problematic with amine-based catalysts than dibutyltin dilaurate. Therefore, the silicone phases of the polymerized μE reported (Table 6.1.1, Supporting Information) were generally cured using the tin catalyst at lower TEOS loadings (<3%), which produced much smaller silica particles and higher levels of transparency in the crosslinked product. Tin-catalyzed crosslinking was complete within 24-48h at room temperature and 30 min at 50 °C; benzylamine-catalyzed processes usually required many weeks to cure.

2.5.2.4. Acrylate-containing Microemulsions: Pre Cure

Test microemulsion formulations consisted of hydroxy-terminated PDMS, surfactant A008 UP **1**, or ACR A008 UP **2** and different concentrations of HEMA in water. Each component was added by weight and the solution mechanically stirred until it became clear and homogeneous. As can be seen from the phase diagrams, the microemulsion region becomes larger with increasing HEMA concentration.

2.5.2.5. Acrylate-containing Microemulsions: Curing into Transparent Elastomers

Microemulsions were prepared in 5 mL glass vials according to the weight ratios in Table 2.3.1 (Table 6.1.1, Supporting Information). After combining the ingredients –

except water and catalysts – the reaction mixtures were stirred, water was added, and then they were stirred again to give transparent, water white microemulsions. The microemulsions were purged with nitrogen before adding the photo-initiator and tin catalyst. The emulsion was again mixed, transferred into a 5mm Petri dish and then cured in a UV reactor at 254 nm (low pressure mercury lamp, 220W) for 15 min. After acrylate polymerization, the microemulsion system was heated 50 °C for 30 min to complete crosslinking of the silicone oil phase. Note that transparent hydrogels also result if the order of polymerization is reversed.

2.6. References & Notes

Appendix 6.1: Conductivity plot of microemulsion titration, phase diagrams of microemulsions containing 0% and 10% HEMA, SEM of polymerized microemulsion, plot of release of phenol red from a polymerized microemulsion, and tables of additional formulations leading to polymerizable microemulsions.

1. Brook, M. A., *Silicon in Organic, Organometallic, and Polymer Chemistry*. John Wiley & Sons, Inc.: New York, New York. Published simultaneously in Canada., 2000.

2. Owen, M. J., Surface Chemistry and Applications. In *Siloxane Polymers*, Prentice Hall Englewood Cliffs, New Jersey, USA, 1993.

3. Jones, L.; Dumbleton, K., Silicone hydrogels part 1: Technological developments. 2005; pp 23-29.

4. Yan, F.; Texter, J., Capturing nanoscopic length scales and structures by polymerization in microemulsions. *Soft Matter* **2006,** *2* (2), 109-118.

5. Yaghmur, A.; Glatter, O., Characterization and potential applications of nanostructured aqueous dispersions. *Advances in Colloid and Interface Science* **2009,** *147-48*, 333-342.

6. Hill, R. M., *Silicone Surfactants* Marcel Dekker, Inc.: New York, New York 1999; Vol. 86, p 2-4.

7. Feng, Q. J.; Lin, Z.; Hill, R. M. Clear Silicone Microemulsions Formed Spontaneously. US 6,998,424, 2006.

8. Silas, J. A.; Kaler, E. W.; Hill, R. M., Effect of didodecyldimethylammonium bromide on the phase behavior of nonionic surfactant-silicone oil microemulsions. *Langmuir* **2001,** *17* (15), 4534-4539.

9. Sharma, S. C.; Tsuchiya, K.; Sakai, K.; Sakai, H.; Abe, M.; Miyahara, R., A Narrow Bicontinuous Microemulsion Domain in Mixed Polymeric Silicone Systems. *J Oleo Sci* **2008,** *57* (12), 669-673.

10. Halloran, D. J.; Hill, R. M.; Wrolson, B. M.; Zimmerman, B. L. Polymerization of Silicone Microemulsions. 2002.

11. Zhang, L.; Zhang, C.; Li, G. M., Synthesis and properties of copolymer microemulsions of siloxane and acrylate with a high solid content. *J Appl Polym Sci* **2007,** *104* (2), 851-857.

12. Castellino, V.; Cheng, Y. L.; Acosta, E., The hydrophobicity of silicone-based oils and surfactants and their use in reactive microemulsions. *J Colloid Interf Sci* **2011,** *353* (1), 196-205.

13. Steytler, D. C.; Dowding, P. J.; Robinson, B. H.; Hague, J. D.; Rennie, J. H. S.; Leng, C. A.; Eastoe, J.; Heenan, R. K., Characterization of water-in-oil microemulsions formed in silicone oils. *Langmuir* **1998,** *14* (13), 3517-3523.

14. Hill, R. M. Spontaneously formed clear silicone microemulsions. US 5705562, 1998.

15. Li, X.; Washenberger, R. M.; Scriven, L. E.; Davis, H. T.; Hill, R. M., Phase behavior and microstructure of water/trisiloxane E-6 and E-10 polyoxyethylene surfactant/silicone oil systems. *Langmuir* **1999,** *15* (7), 2278-2289.

16. Chow, P. Y.; Gan, L. M., Microemulsion polymerizations and reactions. *Adv Polym Sci* **2005,** *175*, 257-298.

17. Patwardhan, S. V.; Taori, V. P.; Hassan, M.; Agashe, N. R.; Franklin, J. E.; Beaucage, G.; Mark, J. E.; Clarson, S. J., An investigation of the properties of poly(dimethylsiloxane)-bioinspired silica hybrids. *Eur Polym J* **2006,** *42* (1), 167-178.

18. Clarson, S. J.; Mark, J. E.; Semlyen, J. A., Studies of Cyclic and Linear Poly(Dimethylsiloxanes) .24. Topological Trapping of Cyclic Polymers into Unimodal and Bimodal Model Network Structures. *Polym Commun* **1987,** *28* (5), 151-153.

19. *Safety of Silicone Breast Implants*; Institute of Medicine Committee Washington, DC, USA, 2000.

3. Chapter 3: Silicone Microemulsion Structures are maintained during Polymerization using Reactive Surfactants[§]

3.1. Abstract

Bicontinuous silicone microemulsions exhibit domain structures on the nanoscale (<20 nm). It would be of interest to maintain such fine details during the conversion to solid elastomeric materials via polymerization of either the silicone oil phase, or of olefins in the aqueous phase. Generally, loss of structure is observed when polymerization of microemulsions is attempted, as a consequence of interface destabilization. Very little is known about the polymerization of silicone microemulsions and the morphological changes that occur upon transition from a nanostructured liquid to solid template. Microemulsions polymerized by free radical (aqueous phase) and condensation (silicone phase) processes, respectively, were characterized by small angle X-ray scattering (SAXS) and transmission electron microscopy (TEM). It was determined that polymerization of the silicone phase alone led, over time, to the loss of microemulsion domain nanostructure. By contrast, photo-induced polymerization of a reactive surfactant and acrylic monomers in the aqueous phase was most effective at retaining bicontinuous nanomorphology irrespective of the degree of crosslinking of the silicone phase.

[§] Whinton designed all experiments with guidance from Dr. Timothy Hughes and Dr. Michael Brook. Dr. Timothy Hughes ran the microemulsion samples on the Australian Synchrotron and Whinton analyzed the scattering data. Whinton wrote the manuscript with edits and guidance from Dr. Michael Brook. Manuscript is in preparation for journal submission

3.2. Introduction

Nanostructured materials are used in biomedical, cosmetic, membrane filtration membranes and for drug delivery, to name a few applications.[1,2,3] Microemulsions would be an ideal template for creating nanostructured materials if their initial morphology could be retained in an elastomeric material.

Microemulsions are nanostructured dispersions consisting primarily of surfactant (with optional co-surfactant), oil and water. They consist of three main structure types: oil-in-water, water-in-oil, and bicontinuous.[4,5,6] Domain sizes are well below the scattering of visible light (<100nm), resulting in optically transparent dispersions.[7,8,9] Of particular interest is the bicontinuous structure type, containing both continuous oil and water phases, which should be highly permeable to either or both hydrophobic and hydrophilic solutes.

Microemulsions containing hydrocarbon-based oils have been well documented.[10,11] Structure type depends on multiple parameters that can influence the amphiphilic film curvature, such as the HLB of the surfactant, temperature and/or salinity of the system, and the ratio of oil:water within the microemulsion.[12] Water-rich microemulsions tend to form O/W structures, while oil-rich microemulsions favour the formation of W/O structures. The bicontinuous microemulsion structure is favoured when there are roughly equal amounts of water and oil present and both water and oil exist as the continuous phase.[13] Microemulsions commonly exist in equilibrium with an excess oil and/or water phase (Winsor type I, II, III), however, at a sufficiently high surfactant concentration, a single-phase (Winsor IV) microemulsion can form.

Although the phase behaviour of hydrocarbon microemulsions has been well reported, little is known about the phase behaviour of microemulsions containing volatile or non-volatile silicone oils.[14,15] Silicones are an ideal oil to incorporate into microemulsions because of their prevalent use in biomedical and pharmaceutical applications owing to their desirable properties, such as high thermal stability and biocompatibility.[16,17]

The polymerization of hydrocarbon microemulsions into nanostructured materials has been previously reported. Reactive surfactants that can be physically tethered at the interface have been shown to be particularly effective at stabilizing hydrocarbon microemulsions during polymerization, resulting in transparent materials.[9,11] For example, Chew et al. were able to create transparent elastomeric materials exhibiting nanomorphologies by polymerizing bicontinuous microemulsions containing hydrophilic monomers and cationic, polymerizable surfactants. Increasing the amount of monomer (HEMA) in the formulation was also shown to drastically reduce domain sizes within the polymerized material.[11] Typical microemulsions domain sizes are below 50 nm[9], however, Chew et al. showed that increasing water or salt content could alter bicontinuous domain sizes from 20 to 100 nm in polymerized materials. The incorporation of 4.2 wt% HEMA decreased domain sizes in polymerized materials from 40 nm to 20 nm, while the incorporation of 12 wt% HEMA in the precursor microemulsion further decreased domain size to 2 nm in width.[18]

There are very few reports on the polymerization of silicone microemulsions[19,20] and none (to our knowledge) that have investigated morphological retention and one-to-one templating using room temperature vulcanization (RTV) chemistry. Studies that have investigated the polymerization of silicone microemulsions have focused on the UV polymerization of acrylic modified silicone phase or hydrosilylation chemistry within the silicone phase. The application of hydrosilylation chemistry to polymerize silicone microemulsions did not result in defined nanostructuring, while the UV polymerization of an acrylic modified silicone phase was limited in the total water content (<10wt%) required to obtain transparency and nanostructuring in the final materials.[21,22] The polymerization of microemulsions is challenging due to lack of interfacial stabilization during the polymerization process, leading to phase separation and/or opaque materials with micron-scale structures.[8]

Castellino et al. reported on the polymerization of silicone microemulsions using hydrosilylation chemistry within the oil phase, however, the TEM/SEM micrographs of their polymerized formulations showed bicontinuous morphologies, but with micron rather than nanometer domain sizes[21], indicative of interfacial destabilization during polymerization. The effect of polymerizing each phase (oil and water) independently was not studied and so it is not clear which polymerization process contributed more to phase separation and opacity. In addition, despite the use of reactive surfactants, it was not possible to obtain transparent, stable materials.

Aside from radical polymerization methods, other processes have been seldom explored with respect to microemulsion polymerization. Here we examine the tolerance of silicone microemulsions to alternative types of polymerizing chemistries. Room temperature vulcanization (RTV) is a commonly used industrial process in the formation of silicone elastomers from silicone pre-polymers. The additives required for RTV cure, and the process itself were examined to see if RTV could be used on its own or in conjunction with a radical polymerization process to rigidify the microemulsion and create nano-structured elastomers. We previously reported the polymerization of bicontinuous silicone microemulsions[19] and have aimed to better understand the structural transitions associated with this process by characterizing the initial and final morphologies with SAXS and TEM. In particular, the extent to which the polymerization process is key to retaining structure was investigated.

3.3. Experimental

3.3.1. Materials

Hydroxy-terminated PDMS (PDMS-OH 25cSt, ~550 g mol^{-1}) was obtained from Gelest, while tetraethoxysilane ($Si(OEt)_4$, TEOS, 99.999%) and dibutyltin dilaurate (95%, DBTDL) were purchased from Sigma Aldrich. The photoinitiator (Irgacure 184) was obtained from BASF chemicals. These reagents were used as received. The hydrophilic monomer, hydroxyethyl methacrylate (HEMA, 98%) was obtained from Sigma and the inhibitor MEHQ was removed by passing the chemicals through a commercial column (Aldrich). The surfactant, Silmer ACR A008-UP, was obtained from Siltech, Toronto and the inhibitor MEHQ was removed in the same manner as previously described. Borosilicate glass capillary tubes with an outside diameter of 1 mm were obtained from Capillary Tube Supplies Ltd. (Cornwall, United Kingdom).

3.3.2. Microemulsion Formulation

Initial microemulsion formulations consisted of hydroxy-terminated PDMS, a silicone surfactant ACR A008-UP, and water. The phase diagram of the ACR A008-UP/PDMS/H_2O ternary system (Figure 3.3.2.1) was constructed by titrating water into surfactant/oil mixtures of varying weight ratios. The phase boundary and regions designated as 2 phase or microemulsion (μE) were determined by observing the transition from turbidity to transparency or vice versa. The region marked "μE" was transparent and the region marked ‘‘two phases’’ was turbid, i.e., a microemulsion in equilibrium with an excess of PDMS or water phase, respectively. The phase diagram was established by titrating water into different weight ratios of surfactant:oil.

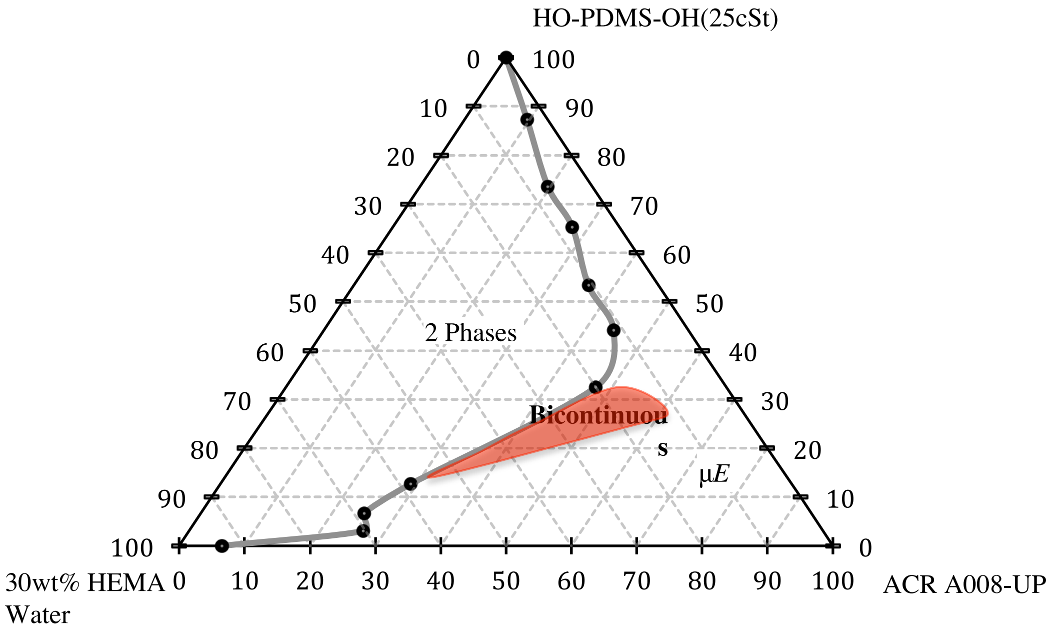

Figure 3.3.2.1: Phase diagram for ACR A008-UP/OH-PDMS/30wt% HEMA-water. The bicontinuous zone is shown in red.

3.3.3. Conductivity Measurements

Electrical conductivity measurements were performed within the single-phase region of the pseudo phase diagram. The dilution line along which the electrical conductivity was measured is indicated on the phase diagram in Figure 3.3.2.1. Conductivities were measured using a CDM 83 conductivity meter (Radiometer Copenhagen). Measurements were taken by inserting a probe (cell constant 1 cm^{-1}) into an oil/surfactant mixture and monitoring the conductivity while titrating water into the solution.

3.3.4. Microemulsion Formulations Prepared for Polymerization

Microemulsion formulations (Table 3.3.1) were prepared by mixing the surfactant, oil, and water in the indicated weight ratios. These formulations reside within the bicontinuous area of the phase diagram and were individually prepared according to their required ingredients. If present within the formulation the crosslinker, TEOS, was added to the surfactant/oil/water mixture. For microemulsion formulations containing catalyst, the photocatalyst (Irgacure 184) and/or tin catalyst (dibutyltin dilaurate) were added just prior to the polymerization step, which was performed at CSIRO in Melbourne, Australia. The polymerization processes are described in detail below.

3.3.5. RTV Silicone Cure

Silicone cure was induced using a type of moisture cure, room temperature vulcanization (RTV), catalyzed by dibutyltin dilaurate (Figure 3.3.5.1). Formulations 3 and 8 under go the RTV process for silicone elastomer formation. Polymerization was initiated upon addition of dibutyltin dilaurate, according to the weight percent indicated in

Table 3.3.1 to formulations 3 and 8, which contained all other required ingredients. Tin-catalyzed crosslinking was complete within 24-48 h at room temperature.

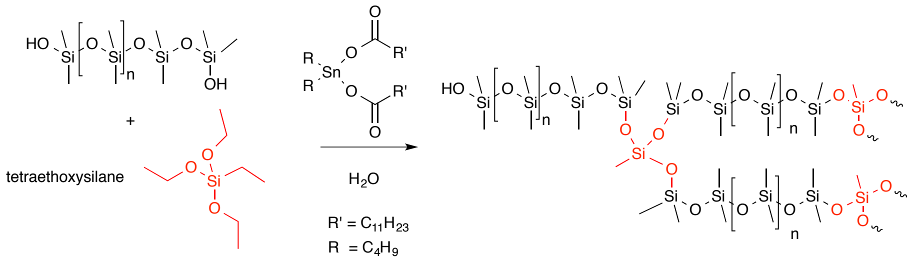

Figure 3.3.5.1: RTV crosslinking of the silicone phase in silicone microemulsion cure.

3.3.6. Photopolymerization

Microemulsion formulations 5 to 8 undergo a photopolymerization process (Figure 3.3.6.1) and were prepared in 5 mL glass vials according to the weight percentages in Table 3.3.1. Surfactant (ACR A008-UP) and silicone oil (DMS S12) were mixed together, followed by the addition of water under mixing to give transparent, water clear microemulsions. The remaining ingredients (if required) were added to the microemulsion while stirring. Photo-initiator and tin catalyst (if required) were then added at CSIRO in Melbourne, Australia just prior to being transferred into 1mm glass capillaries. Formulations 5 to 8 were UV polymerized (Spectroline 365nm, 10mW/cm^2, 20 minutes) and formulation 8 also underwent RTV cure at room temperature for 24-48 h to complete crosslinking of the silicone oil phase.

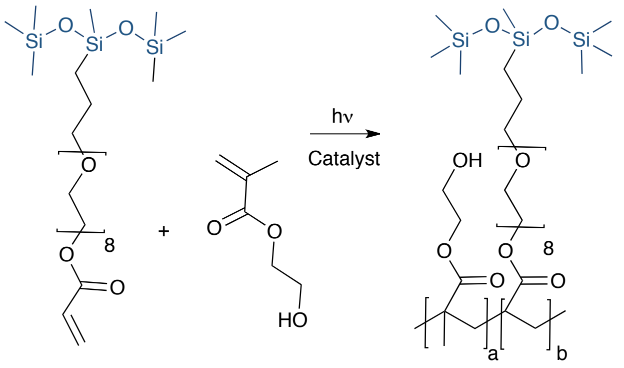

Figure 3.3.6.1: Photopolymerization of surfactant with hydrophilic monomer, HEMA.

Table 3.3.1: Formulations leading to polymerized microemulsions[a]

Formulation	ACR A008-UP (wt%)	OH-PDMS-OH (DMS S12) (wt%)	30wt% HEMA-in-H_2O Solution (wt%)	TEOS (wt%)	IRGACURE 184 (wt%)	DBTDL (wt%)
1	46.96	21.74	31.30			
2	46.84	21.68	31.23			0.25
3	45.00	20.81	30.00	3.94		0.25
4	45.00	21.02	30.00	3.98		
5	44.55	21.02	29.70	3.98	0.75	
6	46.49	21.74	30.99		0.78	
7	46.49	21.52	30.99		0.75	0.25
8	44.55	20.81	29.70	3.94	0.75	0.25

[a] See also Supporting Information.

3.3.7. Structural Determination by Small Angle X-ray Scattering (SAXS)

SAXS experiments at the Australian Synchrotron following previously reported procedures.[22]

Scattering from the samples was measured within the q-range of 0.01 Å to 0.6 Å $^{-1}$, where q is the magnitude of the scattering vector. The scattering vector is dependent on the X-ray wavelength (λ) and the angle (θ) at which scattering occurs, as shown in Equation 1.

$$q = \frac{4\pi}{\lambda}\sin\left(\frac{\theta}{2}\right)$$

(1)

The microemulsions were exposed to X-rays with a wavelength of 0.062 nm at an energy of E=20 keV for one second. One-second exposure time provides a snapshot into the morphology of the microemulsion precursor and also of the polymerized microemulsions. Exposure times were kept short to prevent in situ polymerization of the microemulsion (particularly of acrylics in the water phase), as has been previously reported.[23]

The collected data was analyzed using the program SaSView developed by the SANS Group at the University of Tennessee.[24] The acquired data was fitted to the Teubner-Strey model.[25] Data was fitted in the q-range of 0.01 Å to 0.25 Å, which is the range over which scattering from samples was observed.

The Teubner-Strey model describes the broad scattering observed from microemulsions using three parameters (A, B, and C) in the functional form of the scattering intensity distribution (Equation 2).[26]

$$I(q) = \frac{1}{A + Bq^2 + Cq^4}$$

(2)

The parameters obtained from the Teubner-Strey model can be used to obtain the domain size and correlation length from their respective function forms (Equations 3 & 4).

$$d = 2\pi \left[\frac{1}{2} \left(\left[\frac{A}{C} \right]^{\frac{1}{2}} - \frac{B}{2C} \right) \right]^{-\frac{1}{2}} \tag{3}$$

$$\xi = \left[\frac{1}{2} \left(\left[\frac{A}{C} \right]^{\frac{1}{2}} + \frac{B}{2C} \right) \right]^{-\frac{1}{2}} \tag{4}$$

The Teubner-Strey model has been extended to describe the order/disorder within a structured fluid. This is described by the amphiphilicity factor (Equation 5).[27]

$$f_a = \frac{B}{\sqrt{4AC}} \tag{5}$$

Values arising from this parameter range from -1 to +1 with strongly structured microemulsions falling in the range below 0 and values above 0 indicating poorly structured microemulsions.

3.3.8. Transmission Electron Microscopy

Microemulsions formulations were prepared for TEM by embedding the samples with a hydrophilic resin (Nanoplast FB101, a melamine resin) or cryogenically frozen in liquid nitrogen before being sectioned with a Diatom Diamond knife and placed on a formvar coated copper grid. Liquid microemulsions could not be imaged by TEM. Micrographs of polymerized materials were obtained with a JEOL JEM 1200 EX TEMSCAN scanning transmission electron microscope (JEOL, Peabody, MA, USA), operated in transmission mode at 80 kV.

3.4. Results

Microemulsions of the bicontinuous structure type were prepared by mixing silicone oil, water, surfactant, and additives (Table 3.3.1). The effects of microemulsion structure as a result of water phase, silicone phase, or dual phase polymerization was investigated by SAXS experiments.

3.4.1. Effect of RTV Additives on Microemulsion Morphology

Silicone room temperature vulcanization (RTV) cure requires the presence of silicone oil, crosslinker, and catalyst. In order to understand if the bicontinuous morphology could be retained during the RTV process, it was first necessary to evaluate the individual structural effects of catalyst and crosslinker on the initial microemulsion morphology.

Microemulsions containing DTBDL (RTV catalyst) or the TEOS (crosslinker) were evaluated by SAXS and compared to the original "parent" silicone microemulsion, which contained none of these additional microemulsion ingredients. The RTV cure process only occurs if both catalyst and crosslinker are present in a formulation. We investigated the individual effects of these additives on microemulsion formulations (Table 3.3.1, Formulations 2 and 4). The acquired scattering data was fitted to the Teubner-Strey Model for bicontinuous microemulsions, allowing for the determination of domain size, correlation length, and amphiphilicity factor in the different microemulsion formulations (Table 3.4.1, Chart 3.4.1).

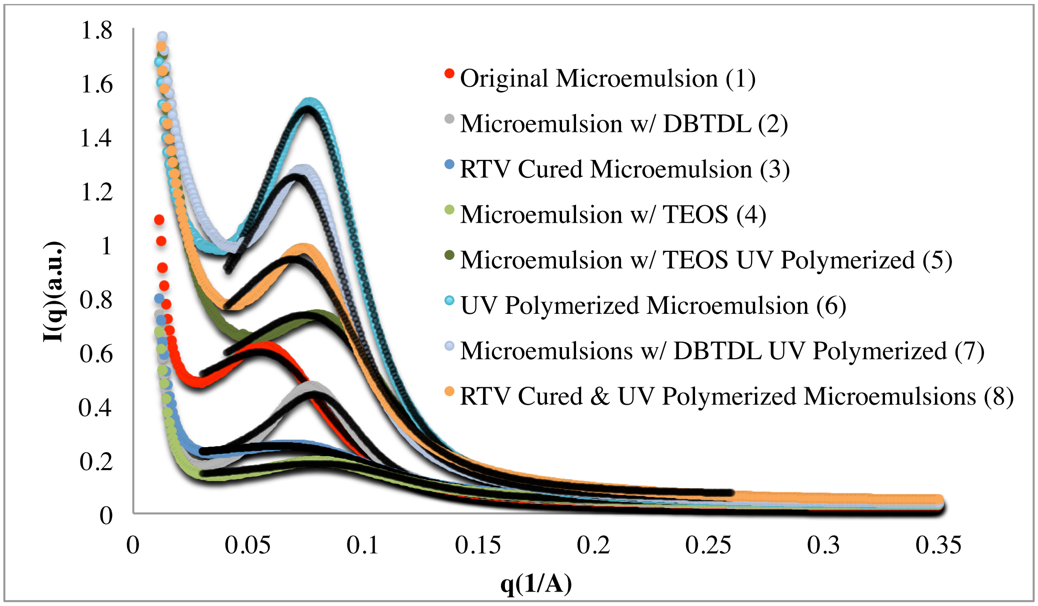

Chart 3.4.1: Acquired SAXS curve and fitted Teubner-Strey model (black curve) for microemulsion formulations

The addition of TEOS resulted in significant decrease in scattering intensity and poorly resolved q-peak, while, the addition of DBTDL resulted in a slight decrease in scattering intensity while still retaining a well-resolved q-peak. The chi^2 parameter for both cases increased when compared to the parent microemulsion.

Table 3.4.1: Structural parameters determined from the Teubner-Strey model

Description (Formulation #)	Domain Spacing (nm)	Correlation Length (nm)	Amphiphilicity Factor	Chi^2 Value
Original Microemulsion (1)	8.14	2.62	-0.51	81.632
Microemulsion with DBTDL (2)	6.26	3.61	-0.80	433.45
RTV Cured Microemulsion (3)	6.60	1.80	-0.39	68.905

Microemulsion with TEOS (4)	5.72	2.02	-0.57	126.96
Microemulsion with TEOS Photopolymerized (5)	6.18	2.25	-0.58	133.75
Photopolymerized Microemulsion (6)	6.44	3.27	-0.75	46.031
Microemulsion Photopolymerized with DBTDL (7)	6.91	3.10	-0.70	203.47
RTV Cured & Photopolymerized Microemulsion (8)	6.72	2.53	-0.61	360.77

[a] See also Supporting Information.

3.4.2. RTV (Condensation) Polymerization of Silicone Microemulsions

The incorporation of both DBTDL and TEOS into the microemulsion (Table 3.3.1, Formulation 3) results in the RTV cure of the silicone phase over the course of 48 hours. We explored the ability of this type of chemistry to create nanoporous silicone elastomers and investigated the resulting elastomer morphology by SAXS and fitting analysis to the Teubner-Strey model.

RTV cure of the silicone phase of the microemulsion resulted in a poorly resolved q-peak and a decrease in scattering intensity when compared to the parent microemulsion. Fitting to the Teubner-Strey model indicates a decrease in correlation length and increase in amphiphilicity factor when compared to the parent microemulsion. Microemulsions in which only the silicone phase was cured using RTV chemistry were initially transparent, but turned opaque over the course of one week, which is consistent with ongoing structural reorganization within the material.

3.4.3. Photopolymerization of Silicone Microemulsions

Although previous studies have examined the radical polymerization of hydrocarbon-based microemulsions, little is known about morphological changes that result when silicone microemulsions are polymerized, in comparison to the initial template. In addition, there are no reports that use reactive siloxane surfactants in silicone microemulsions to produce optically transparent materials with defined nanomorphology. The proposal that copolymerization of an acrylic trisiloxane surfactant with a methacrylate monomer (co-surfactant) within the aqueous phase of a silicone microemulsion would "lock-in" the bicontinuous structure was investigated using SAXS (Chart 3.4.1). A microemulsion formulation (Table 3.3.1, Formulation 6) in which the water phase was photopolymerized was compared to the parent microemulsion.

Photopolymerization of the acrylic monomers – both surfactant and simple monomers – within the aqueous domains of the silicone microemulsion resulted in a decrease in domain size, increase in correlation length, and decrease in amphiphilicity factor. The increase in scattering intensity and improved fit to the Teubner-Strey model suggests that the bicontinuous morphology had become more structured upon polymerization in comparison to the unpolymerized microemulsion. The bicontinuous structure was not identical in physical parameters to the original microemulsion, but the bicontinuous structure type was still conserved, as indicated by the shape of the SAXS curve and fitting to the Teubner-Strey model.

In order to better understand the effect of photopolymerization on microemulsion structure, microemulsions that also contained TEOS and DBTDL (Table 3.3.1, Formulations 5 & 7) were photopolymerized and the elastomer products were evaluated using SAXS.

A surprising outcome of the photopolymerization of microemulsions, formed from mixtures also containing TEOS and DBTDL (Table 3.3.1, Formulations 5 & 7), was that materials with a more defined q-peak resulted, indicating greater interfacial contrast and, therefore, a greater extent of nanophase morphology in comparison to unpolymerized microemulsions containing either TEOS or DBTDL (Table 3.3.1, Formulation 2 & 4). The photopolymerization of microemulsions containing either TEOS or DBTDL alone resulted in a decrease in domain size, however, the two additives influenced correlation length and amphiphilicity factor to different extents. The polymerized microemulsion containing TEOS resulted in a correlation length and amphiphilicity factor that was more similar to the original microemulsion when compared to the photopolymerized microemulsion containing DBTDL, which resulted in an elastomer with a significantly increased correlation length and decreased amphiphilicity factor.

3.4.4. Dual Polymerization of Silicone Microemulsions: RTV Cure & Photopolymerization

The RTV process does not appear to be sufficient on its own to retain the templating of the initial microemulsion structure. However, we wanted to determine if the RTV process would have deleterious effects when used in conjunction an initial photopolymerization step of monomers in the aqueous phase. Therefore, a microemulsion was photopolymerized, subsequently allowed to undergo RTV cure, and then analyzed for morphology changes from the template.

RTV curing of the silicone after photopolymerization of the acrylic in the aqueous phase does not appear to significantly impact the structural parameters of the system. The correlation length and amphiphilicity factor decreased only slightly, consistent with retention of the original morphology. Microemulsions in which both phases were polymerized has structural parameters most similar to the original microemulsion, whereas microemulsions in which only one of the phases were polymerized had parameters that were either significantly lower or higher in value than the original microemulsion.

3.4.5. Transmission Electron Microscopy of Polymerized Materials

Polymerized microemulsions were imaged with transmission electron microscopy in order to further validate the analysis performed using SAXS. The dark areas of the micrographs (Figure 3.4.5.1 A & B) represent electron dense regions and, therefore, correlate with a silicone rich phase. Photopolymerization alone of the microemulsion results in a bicontinuous structure with domains that appear to be less intertwined than the microemulsion that has undergone both photopolymerization and RTV cure. This correlates with the parameters determined using the Teubner-Strey model, in which the photopolymerized microemulsion sample was shown to have the greatest correlation length.

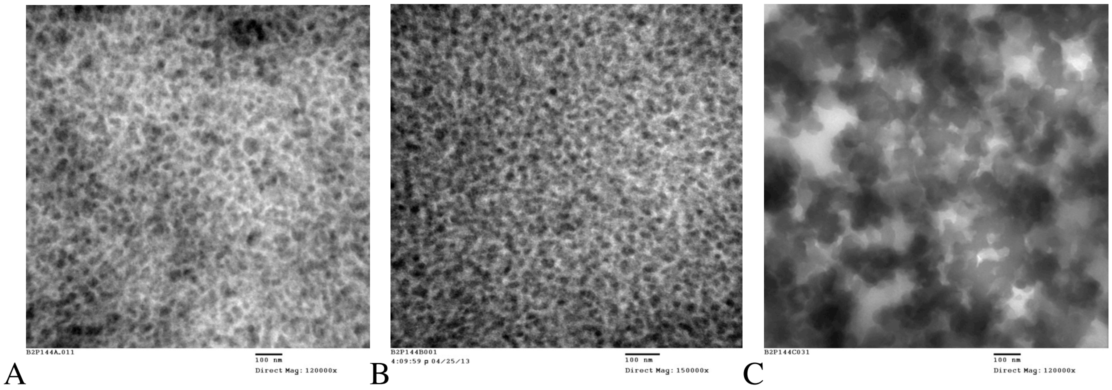

Figure 3.4.5.1: TEM micrographs of selected cured microemulsions A: Photopolymerized Microemulsion (Table 3.3.1, Formulation 6); B: Photopolymerized & RTV Microemulsion (Table 3.3.1, Formulation 8); C: RTV Cure Microemulsion (Table 3.3.1, Formulation 3).

Micrographs of the microemulsion sample that only underwent an RTV cure process (e.g., Figure 3.4.5.1 C) reveal a nanoporous elastomer in which bicontinuous structuring was not retained. This silicone was cured in the presence of water, creating a porous material, however, the interface stabilizing the bicontinuous structure was destroyed during polymerization.

3.5. Discussion

Microemulsion polymerization often leads to phase separation and, consequently, conversion of transparent to opaque materials due to temperature and compositional changes that occur during the physical process of polymerization: the interface becomes destabilized (note that temperature can also destabilize interfaces, but these reactions were performed at room temperature).[28] There have been a few reports of silicone microemulsion polymerization, with micrographs of polymerized materials revealing micron rather than nano scale morphologies.[21]

Previous methods for polymerization of the oil phase in silicone microemulsions have used hydrosilylation[21] and radical methods.[22] When hydrosilylation was used to cure the oil phase, stable transparent materials were not obtained. The radical polymerization of the oil phase only resulted in transparent materials when the precursor water content was kept below 10wt%. Thus, it is particularly difficult to polymerized bicontinuous microemulsions based on silicones while maintaining nanoscale domains.

Microemulsion formulation 3 underwent RTV silicone cure and exhibited a decrease in domain size and a significant decrease in correlation length. In addition, the amphiphilicity factor increased, indicating that microemulsion has lost structure from the initial template. Although nanoporosity was observed from TEM, there is a distinct lack of bicontinuous morphology. These observations lead us to believe that either the RTV process on its own is too disruptive to the interface during the polymerization process or the additives required for polymerization drastically affects morphology. Nevertheless, a higher fraction of nanoscale features were retained using only this silicone cure when compared to alternative methods.

In order to determine whether the polymerization itself or the additives required for RTV cure alone were responsible for this loss of morphology, individual microemulsions containing only TEOS or DBTDL were evaluated. The addition of tin catalyst (DBTDL) or TEOS to a microemulsion resulted in a reorganization of structure from the template. TEOS and DBTDL are both only soluble in the oil phase, which could result in preferential interactions with the hydrophobic trisiloxane portion of the surfactant, leading to changes in interfacial curvature, and therefore, microemulsion structure. The scattering intensity decreases significantly upon the addition of TEOS, indicating poor contrast between water/oil domains, which is consistent with a lack of nanophase separation or the presence of a disordered micellar/polymeric solution.[29] That is, the additives alone compromised the nanoscale bicontinuous structure, which is reflected in a microemulsion that has undergone only the silicone RTV cure.

The second part of this study examined the effect of a radical polymerization process within the water phase (surfactant and monomer) on microemulsion structure. Radical polymerization in hydrocarbon microemulsions using reactive surfactants has been well studied and shown to be effective at "locking-in" structure.[8,11,30] However, there are no published reports showing the successful retention of morphology of nanostructured bicontinuous structures in the polymerization of silicone microemulsions.

Peng et al. reported on the polymerization of silicone microemulsions by the UV polymerization of the silicone oil phase. A reactive surfactant was not used in this system to retain structure, although similar changes in parameters (domain size, correlation length, and amphiphilicity factor) were observed during the conversion from liquid to solid.[22] However, polymeric products from the polymerization of silicone microemulsions studied in this system were only transparent when the precursor microemulsion contained <10wt% water.[20] Although morphology on the nanoscale is indicated via SAXS measurements, domains on this length scale were imaged as polymerized materials were characterized by SEM.[20,22] This differs significantly from the silicone microemulsion we studied, which contained a reactive surfactant and resulted in optically transparent materials even at high (≥20wt%) water content. We also observed distinct nanometer sized bicontinuous channels by transmission electron microscopy, something that has not previously been observed with silicone microemulsions.

We have shown that, provided a polymerizable (reactive surfactant) and a methacrylic monomer (HEMA) were present in the microemulsion, transparent elastomeric hydrogels could be produced that retained the bicontinuous microemulsion nanoscale morphology. Castellino et al. also examined the polymerization of microemulsions using reactive surfactants[21] after our initial publication, but where unable to obtain transparent materials.

Analysis of our formulations by SAXS and fitting to the Teubner-Strey model for bicontinuous microemulsions showed a decrease in domain size (d) upon transition from liquid to solid. Physical parameters such as correlation length (ξ) and amphiphilicity factor (f_a) varied depending on whether the water phase, or both oil and water phases were polymerized.

A decrease in domain size and increase in correlation length would be expected due to the physical constraints and volume changes associated with a liquid-to-solid transition.[31] Additionally, most liquids lack structure and long-range order, whereas even amorphous solids exhibit some degree of long-range order.[32]

Initially, the microemulsion we studied has an amphiphilicity factor of -0.51, indicating a strongly structured liquid. However, upon photopolymerization this value decreased to -0.75, indicating a better-structured microemulsion. The increase in structuring is consistent with the observable increase in q-peak intensity, implying improved nanophase contrast and an increase in rigidity at the interface upon polymerization of the surfactant with monomer consistent with “locking-in” of the nanomorphology.

An interesting outcome was observed when microemulsions containing either TEOS or DBTDL were photopolymerized. Even though the presence of TEOS and DBTDL caused significant structural changes from the initial template, photopolymerization of these materials mitigated these effects and showed more pronounced q-peaks and improved microemulsion structure suggesting that RTV cure may be used in conjunction with photopolymerization with minimal consequence on structure.

In fact, SAXS results of a microemulsion that underwent both a photopolymerization and RTV cure (Formulations 8) indicated that aside from a decrease in domain size, all other structural parameters (correlation length and amphiphilicity factor) are similar to the original microemulsion. This is quite different from the case in which the microemulsion only undergoes RTV cure or photopolymerization (Formulations 3 and 6, respectively). If either polymerization technique (photopolymerization or RTV) is applied independently to the microemulsion, the physical parameters of the resulting polymer are quite different from the initial template. The transmission electron micrographs of materials that underwent both photopolymerization and RTV cure reveals retention of bicontinuous morphology, similar to what was observed with the microemulsion that underwent photopolymerization only.

Despite not retaining the one-to-one template of the original microemulsion when performing RTV cure, this type of chemistry can be used in conjunction with a photopolymerization technique to create one-to-one templated materials with defined nanomorphology. This suggests that the RTV process could be used to polymerize microemulsions if the surfactant could be anchored more effectively within the silicone phase.

3.6. Conclusion

The tolerance of silicone microemulsions to RTV and photocure was investigated. Elastomers formed from the RTV process alone did not possess sufficient interfacial stabilization to retain morphology of the original microemulsion template. By contrast, microemulsions containing a polymerizable surfactant that underwent a radical polymerization process were effective at retaining morphology irrespective of whether the oil phase is polymerized using an RTV process to "lock-in" structure. Using these methods, microemulsions with precursor water content in excess of 20wt% were successfully polymerized into transparent nanostructured materials by polymerization of either the water phase or both water and oil phase

3.7. Acknowledgments

We thank the Natural Sciences and Engineering Research Council of Canada and 20/20: NSERC Ophthalmic Materials Network for financial support of this research. We would also like to express our gratitude to Marcia Reid for assistance in obtaining TEM data. SAXS experiments were undertaken at the Australian Synchrotron, Victoria, Australia.

3.8. References

1. Goldberg, M.; Langer, R.; Jia, X., Nanostructured materials for applications in drug delivery and tissue engineering. *Journal of biomaterials science. Polymer edition* **2007,** *18* (3), 241-68.

2. Antonietti, M., Self-organization of functional polymers. *Nat Mater* **2003,** *2* (1), 9-10.

3. Tang, Z., Wang, Y., Podsiadlo, P., Kotov, N. A., Biomedical Applications of Layer-by-Layer Assembly: From Biomimetics to Tissue Engineering. *Advanced Materials* **2006,** *18*, 3203-3224.

4. Spernath, A., Aserin, A., Microemulsons as carriers for drugs and nutraceauticals *Advances in Colloid and Interface Science* **2006,** *128-130*, 47-64.

5. Ruckenstein, E., Microemulsions, Macroemulsions, and the Bancroft Rule. *Langmuir* **1996,** *12*, 6351-6353.

6. Nagarajan, R., Ruckenstein, E., Molecular Theory of Microemulsions. *Langmuir* **2000,** *16*, 6400-6415.

7. Komura, S., Mesoscale structures in microemulsions. *Journal of PHysics: Condensed Matter* **2007,** *19* (46), 463101.

8. Yan, F., Texter, J., Capturing nanoscopic length scales and structures by polymerization in microemulsions. *Soft Matter* **2006,** *2*, 109-118.

9. Chow, P. Y., Gan, L. M., Microemulsion Polymerizations and Reactions. *Advances in Polymer Science* **2005,** *175*, 257-298.

10. Candau, F., Pabon, M., Anquetil, J. Y., Polymerizable microemulsions: some criteria to achieve an optimal formulation. *Colloids and Surfaces A: Physiochemical and Engineering Aspects* **1999,** *153*, 47-59.

11. Chew, C. H., Li, T. D., Gan, L. H., Quek, C. H., Gan, L. M., Bicontinuous-Nanostructured Polymeric Materials from Microemulsion Polymerization *Langmuir* **1998,** *14*, 6068-6076.

12. Strey, R., Microemulsion Microstructure and Interfacial Curvature. *Colloid Polym Sci* **1994,** *272* (8), 1005-1019.

13. Schwuger, M. J.; Stickdorn, K.; Schomacker, R., Microemulsions in Technical Processes. *Chem Rev* **1995,** *95* (4), 849-864.

14. Sharma, S. C., Tsuchiya, K., Sakai, K., Sakai, H., Abe, M., Miyahara, R., A Narrow Bicontinuous Microemulsion Domain in Mixed Polymeric Silicone Systems. *Journal of Oleo Science* **2008,** *57* (12), 669-673.

15. Silas, J. A., Kaler, E. W., Effect of Didodecyldimethylammonium Bromide on the Phase Behavior of Nonionic Surfactant-Silicone Oil Microemulsions. *Langmuir* **2001,** *17*, 4534-4539.

16. Wang, J. J., Liu, F., UV-curing of simultaneous interpenetrating network silicone hydrogels with hydrophilic surface. *Polymer Bulletin* **2012,** *69*, 685-697.

17. Cifkova, I., Lopour, P., Vondracek, P., Jelinek, F., Silicone rubber-hydrogel composites as polymeric biomaterials *Biomaterials* **1990,** *11* (6), 393-396.

18. Chew, C. H.; Li, T. D.; Gan, L. H.; Quek, C. H.; Gan, L. M., Bicontinuous-nanostructured polymeric materials from microemulsion polymerization. *Langmuir* **1998,** *14* (21), 6068-6076.

19. Brook, M. A., Whinton, M., Gonzaga, F., Li, N., Elastomeric hydrogels by polymerizing silicone microemulsions *Chem Commun* **2011,** *47*, 8874-8876.

20. Peng, S., Hartley, P. G., Hughes, T. C., Guo, Q., Controlling morphology and porosity of porous siloxane membranes through water content of precursor microemulsion. *Soft Matter* **2012,** *8*, 10493-10501.

21. Castellino, V., Acosta, E., Cheng, Y., Interpenetrating polymer networks templated on bicontinuous microemulsions containing silicone oil, methacrylic acid, and hydroxyethyl methacrylate *Colloid Polymer Science* **2013,** *291*, 527-539.

22. Peng, S., Guo, Q., Hughes, T. C., Hartley, P. G., In Situ Synchrotron SAXS Study of Polymerizable Microemulsions. *Macromolecules* **2011,** *44*, 3007-3015.

23. Peng, S.; Guo, Q.; Hughes, T. C.; Hartley, P. G., In Situ Synchrotron SAXS Study of Polymerizable Micremulsions. *Macromolecules* **2011,** *44*, 3007-3015.

24. Butler, P. DANSE Small Angle Neutron Scattering Project. http://danse.chem.utk.edu/intro.html.

25. Tuebner, M., Strey, R., Origin of the scattering peak in microemulsions. *The Journal of Chemical Physics* **1987,** *87* (5), 3195-3200.

26. Strey, R.; Teubner, M., Origin of the scattering peak in microemulsions. *The JOurnal of chemical Physics* **1987,** *87* (5), 3195-3200.

27. Morkved, T. L.; Stepanek, P.; Krishnan, K.; Bates, F. S.; Lodge, T. P., Static and dynamic scattering from ternary polymer blends: Bicontinuous microemulsions, Lifshitz lines, and amphiphilicity. *Journal of Chemical Physics* **2001,** *114* (16), 7247-7259.

28. Summers, M., Eastoe, J., Applications of polymerizable surfactants. *Advances in Colloid and Interface Science* **2003,** *100-102*, 137-152.

29. Baldenegro-Perez, L. A.; Navarro-Rodriguez, D.; Medellin-Rodriguez, F. J.; Hsiao, B.; Avila-Orta, C. A.; Sics, I., Molecular Weight and Crystallization Temperature Effects on Poly(ethylene terephthalate) (PET) Homopolymers, an Isothermal Crystallization Analysis *Polymers* **2014,** *6* (2), 583-600.

30. Stubenrauch, C., Tessendorf, R., Salvati, A., Topgaard, D., Sottmann, T., Strey, R., Lynch, I., Gelled Polymerizable Microemulsions. 2. Microstructure. *Langmuir* **2008,** *24*, 8873-8482.

31. Hillert, M., *Phase Equilibria, Phase Diagrams and Phase Transformations Their Thermodynamic Basics*. Cambridge University Press: Cambridge, UK, 1998.

32. Seitz, F., Turnbull, D., *Solid State Physics Advances in Research and Applications*. Academic Press Inc.: New York, NY, 1955; Vol. 1, p 199-209.

4. Chapter 4: Very slow formation of TiO_2 nanoparticles by hydrolysis of an alkoxytitanate within a bicontinuous silicone/water microemulsion[†]

4.1. Abstract

Particles of TiO_2 are used in a variety of applications because of their high refractive index and, more importantly, photocatalytic behaviour. The sol-gel process normally used to create titanium dioxide particles from $Ti(O\text{-}i\mathrm{Pr})_4$ or related alkoxides is difficult to control because hydrolysis and condensation of titanium alkoxides occur concurrently and is incredibly rapid, except at low pH. Aggregation of TiO_2 particles is also an extremely facile process that occurs concomitantly with condensation. We report that the templating provided by a microemulsion and interactions between the surfactant and titanium alkoxide delay the formation of visible TiO_2 by retarding the previously mentioned processes. Small TiO_2 nanoparticles (< 40 nm) can be prepared under mild and neutral conditions in water-in-oil and bicontinuous silicone microemulsions: particles aggregate only slowly, as shown by transmission electron microscopy and UV absorption spectroscopy. Retarded particle growth is ascribed to the enhanced rigidity of the water/surfactant/silicone interface, which must reorganize before aggregation can occur.

4.2. Introduction

Titanium dioxide is extensively used in coatings, water treatment, cosmetics, and as a pigment in paint because of its photocatalytic properties and UV blocking capabilities.[1]

[†] Whinton designed and performed all experiments in this chapter. Whinton wrote the manuscript with additions, edits, and guidance from Brook (Submitted 2015).

Many applications, including sunscreens, thin films, transparent coatings, and photovoltaics use titania in the form of nanosized particles because they can reflect UVA/UVB radiation while being transparent to visible light, have high surface areas and, depending on structure, can have enhanced photocatalytic properties.[2] Amorphous nano-titania, in particular, is desirable for cosmetic and coating applications owing to its optical transparency while exhibiting decreased photocatalytic properties when compared to crystalline TiO_2.[3]

A common process used to create TiO_2 is the sol-gel method, where a titanium alkoxide precursor, typically titanium tetraethoxide or titanium tetraisopropoxide (or titanium tetrachloride), is dissolved in an organic solvent and then hydrolysed with water under a variety of conditions.[4] The hydrolysis of titanium alkoxides is extremely rapid (typically <1 second), followed by extremely fast condensation and then particle formation and aggregation/growth, which is difficult to control. This high reactivity can make titanium alkoxide solutions difficult to store and often leads to highly polydisperse and inhomogeneous precipitates, which can be undesirable, particularly when used in coatings or films.[5]

Decreasing the rates of hydrolysis and condensation of titania precursors, in order to prepare transparent TiO_2 particles, can be achieved, to a degree, by altering the structure of the starting titanium alkoxide.[4] For example, the use of acetylacetone as a chelating agent under acidic conditions leads to transparent solutions containing 1-10 nm titania particles. The dispersions remained transparent for up to a year owing to the stability of surface hydroxyl groups against further condensation.[4] An alternative method to retard the hydrolysis of titanium esters at neutral pH involves the use of glycerol as a chelating agent around the titanium centre in lieu of simple alcohols. Once transesterified with glycerol to give diglyceryltitanium, hydrolysis and condensation of the titanium alkoxide was delayed, but not to the degree found using acetylacetone as a chelating agent at low pH. The latter strategy also allows for kinetic control over the gelation process by altering glycerol and/or water concentrations.[6]

In addition to the rapid rate of hydrolysis and condensation of alkoxytitanium compounds, TiO_2 particle growth and aggregation is also typically very fast and hard to control. Titania particles tend to aggregate at neutral pH, an effect that can be undesirable in many applications. Steric or electrostatic stabilization can be used to stabilize the particles: the stability of particles at low pH[4, 7] is a consequence of electrostatic stabilization caused by cationic species on the particle surface.[8]

Rather than changing the reaction conditions, the growth of TiO_2 particles can be limited by using constricting domains of a physical template. Szymanski et al. gelled a polymerizable microemulsion to form a monolithic titania structure comprised of aggregated particles.[9] Exchanging water into the porous template triggered the hydrolysis of the precursor leading to the formation of titania particles ranging from 200-250 nm. The template did not delay hydrolysis or condensation processes, but restricted the dimensions that the particles could ultimately achieve.

During our exploration of the use of titanium dioxide as a reinforcing agent in a previously reported silicone microemulsion system[10], we were surprised to learn that the formation of visible titania particles was very slow at neutral pH within the microemulsion. In this report, we examine the factors that affect the rates of hydrolysis and condensation of alkoxytitanium species, and TiO_2 particle formation within the microemulsion as a function of microemulsion structure.

4.3. Experimental Section

4.3.1. Materials

The surfactant Silsurf A008-UP (632 g/mol, Figure 4.3.1) was donated by Siltech Corporation (Toronto, Canada). Titanium tetraisopropoxide (TTIP) (284.22 g/mol) was purchased from Sigma Aldrich (Oakville, ON) and silanol-terminated polydimethylsiloxane DMS-S14 (35-45 cSt, 700-1500 g/mol) was obtained from Gelest (Morrisville, Pennsylvania).

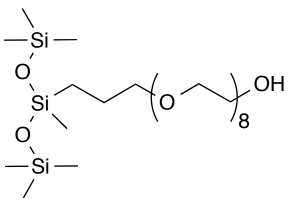

Figure 4.3.1: Silsurf A008-UP.

4.3.2. Methods

4.3.2.1. UV Absorption Spectroscopy

UV absorption measurements were taken at different time points after the reaction was initiated (see below) using a Cary 50 UV spectrophotometer at a scan rate of 300 nm/min. A baseline was obtained using an analogous microemulsion differing only in that it did not contain a titanium alkoxide (Table 4.3.2.1). Formulations were directly measured by depositing ~50 mg of microemulsion between two quartz slides.

4.3.2.2. Transmission Electron Microscopy

Titania particles were isolated by centrifugation (Eppendorf Centrifuge 5424) at 15000 rpm for ~1.5 h after diluting the microemulsion (~0.25 g) with isopropanol (IPA) (1 mL). The supernatant (a mixture of microemulsion and IPA) was removed using a pipette and the isolated titania was then dispersed in a fresh aliquot of 1 mL isopropanol. The titania dispersion was deposited onto a formvar-coated copper grid. The solvent was evaporated from the grid and images were immediately obtained with a JEOL JEM 1200 EX TEMSCAN scanning transmission electron microscope (JEOL, Peabody, MA, USA) operated in transmission mode. Images were obtained after 4, 24, and 48 h, respectively, of initial microemulsion preparation and subsequent in situ particle formation (no particles could be isolated before 4 h).

4.3.2.3. Microemulsion Formulations

Microemulsions were prepared using the formulations shown in Table 4.3.2.1. The order of addition was important to obtain transparent microemulsions (otherwise rapid formation of opaque dispersions of TiO_2 occurred). The surfactant Silsurf A008-UP was first placed in a 2-dram (~7 mL) vial, followed by the slow addition of titanium isopropoxide while mixing using a magnetic stir plate. Silanol-terminated polydimethylsiloxane (PDMS-OH, DMS-S14, Gelest) was added to the surfactant/TTIP solution while mixing, and led to a transparent, yellow mixture. Water (in a large molar excess) was then slowly added into the formulation (drop-wise) to form a pale yellow, transparent microemulsion.

Table 4.3.2.1: Microemulsion Formulations using Trisiloxane-PEG Surfactant Silsurf A008-UP with and without TTIP[a].

Formulation	Titanium Isopropoxide (wt%)	Silsurf A008-UP (wt%)	PDMS-OH (DMS S14) (wt%)	Water (wt%)
1	3.51	49.18	39.64	7.67
2		51.12	41.57	7.31
3	3.31	46.32	37.44	12.93
4		47.80	38.84	13.36
5	3.04	43.36	35.35	18.25
6		44.69	36.50	18.81
7	2.47	34.60	28.20	34.73
8		35.55	28.91	35.54

[a]All data on the table represents weight%. For formulations in grams, see Supporting Information.

4.4. Results

The formation of visible titania particles is usually quite rapid – essentially instantaneous – when titanium alkoxides are exposed to even small quantities of water at neutral pH. Control experiments in which microemulsions were prepared with the following the order of addition A008-UP → TTIP → Water → PDMS resulted in the immediate formation of large, visible titania particles (Figure 4.4.1). To avoid this, it was necessary to prepare formulations by first mixing Silsurf A008-UP with TTIP, followed by the addition of silicone oil (hydroxy-terminated polydimethylsiloxane, PDMS). Water must be added last in order to obtain optically transparent materials in which TiO_2

formation and aggregation was delayed. Note that if either the silicone oil or surfactant were missing from in the formulation, the mixtures also immediately became opaque upon the addition of water due to the instantaneous formation of TiO_2.

The preparation of microemulsions containing titanium isopropoxide led to initially transparent microemulsions (no visible titania formation) despite a large molar excess of water to titanium in each formulation. The UV absorption spectra of TTIP in isopropanol and the surfactant/TTIP mixture in isopropanol were measured to determine changes associated with interactions between TTIP and Silsurf A008-UP (Figure 6.3.2, Supporting Information). The decrease in absorbance and slight change in absorbance curve is consistent with a change in optical properties due to different ligand attachments to the titanium centre, but not to the formation of TiO_2.

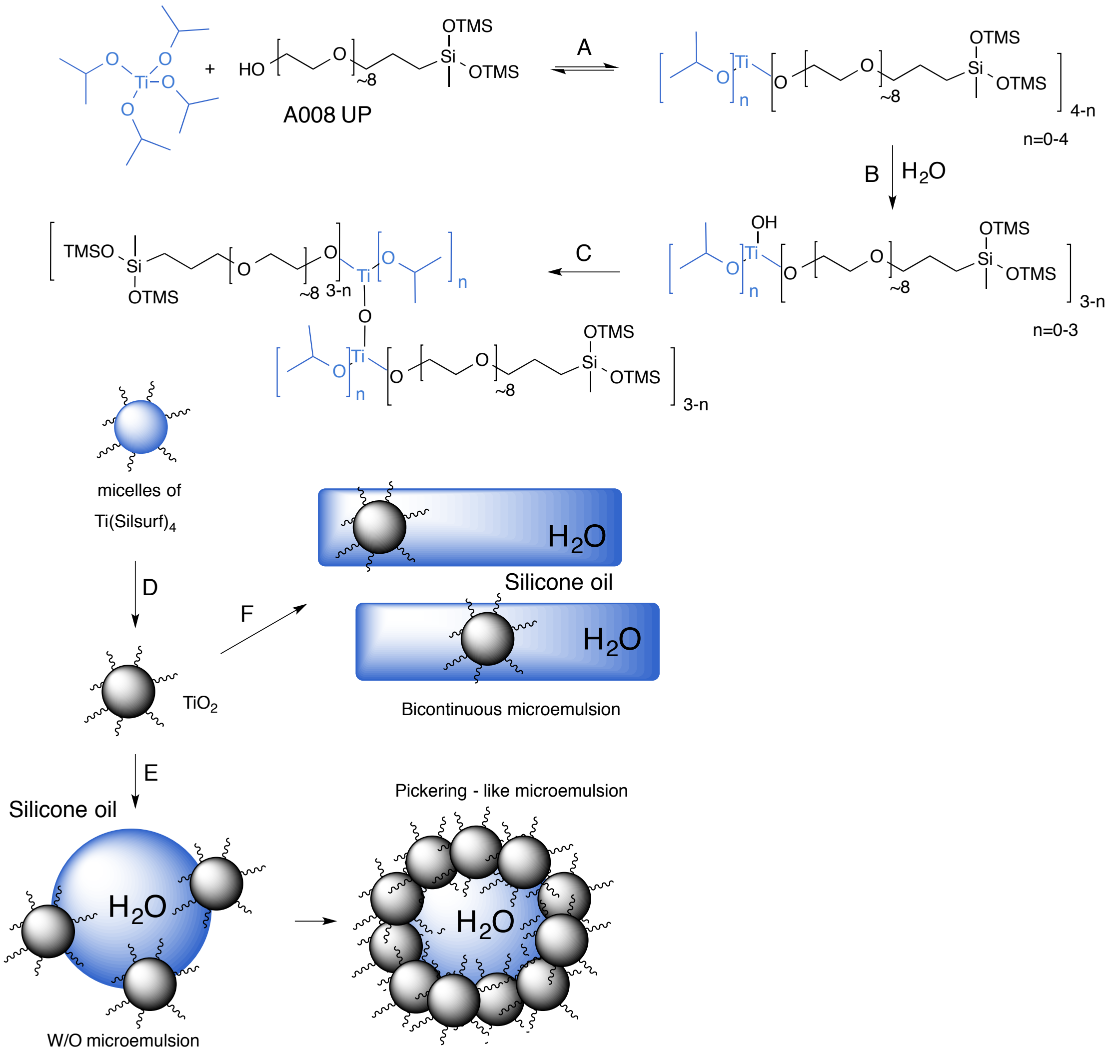

Figure 4.4.1: Formation of TiO_2 particles in microemulsion: A: transetherification of TTIP with the surfactant Silsurf A008 UP. B: hydrolysis and C: condensation/micellization D: formation of TiO_2 particles that adsorb onto the surface of a E: W/O or F: bicontinuous microemulsion

Four microemulsions containing different concentrations of water were prepared, which represented examples from all three different microemulsion structure types: oil/water (Chart 4.4.1: A); bicontinuous (Chart 4.4.1: B,C); and water/oil (Chart 4.4.1: D). The formulations contained a large molar excess of water when compared to the molar quantity of Ti-OR groups present. In spite of this, all of the microemulsions, except oil/water, remained transparent for at least 1 day: the microemulsion structure was affiliated with transparency and the suppression of TiO_2 large particle formation over an extended period of time: in the absence of such structuring, visible particles formed within < 1 second.

An examination of the microemulsions prepared with the four different water concentrations showed different kinetics for the TiO_2 particle formation process within the mobile structures, all of which were very different – typically much slower – than the process in solution. The microemulsion formulation containing a large excess of water (224:1 mole ratio $[H_2O]$:[TTIP) represents an oil-in-water structure. Immediately after addition of water to form the microemulsion there was, unsurprisingly, the immediate formation of visible titania – the dispersion became opaque – which resulted in low initial absorbance readings due to decrease in ligand-metal charge transfer absorbance of the isolated Ti^{4+} tetrahedrally coordinated precursor (Chart 4.4.1: A).

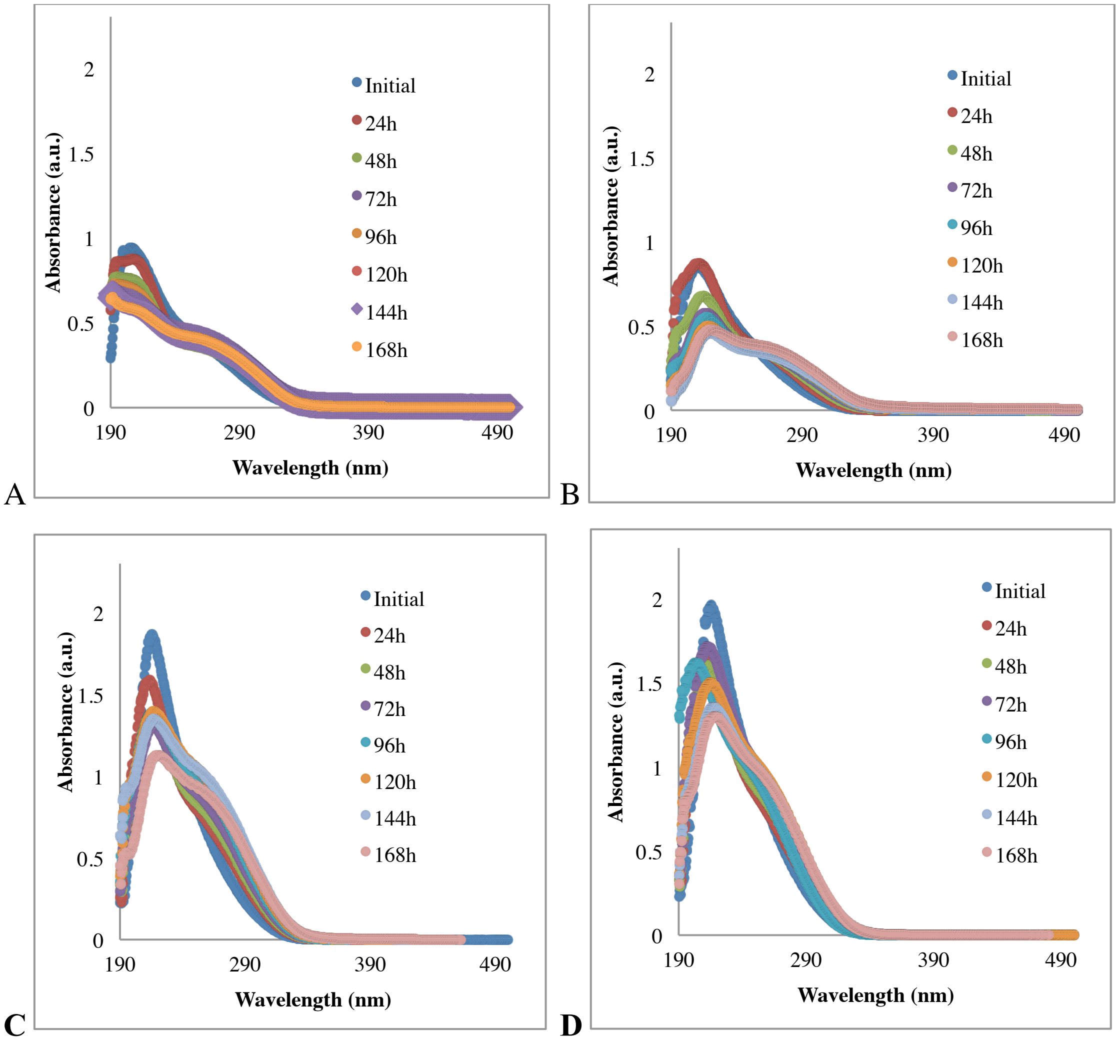

Chart 4.4.1: TTIP microemulsions. A: Oil-in-water with a total water content 34.73wt% (224:1 mole ratio [H_2O]:[Ti(Silsurf)$_4$). B-C: Bicontinuous with a total water content 18.25wt% (94:1 mole ratio [H_2O]:[Ti(Silsurf)$_4$) and 13.37wt% (66:1 mole ratio [H_2O]:[Ti(Silsurf)$_4$]), respectively. D: Water-in-oil with a total water content of 7.67wt% (35:1 mole ratio [H_2O]:[Ti(Silsurf)$_4$]).

The outcomes with bicontinuous microemulsions were quite different. Two water-loading levels were examined within the bicontinuous region; both lower than the previously described O/W microemulsion system. At water concentration levels, ~18wt% and ~13wt%, respectively, visible titania formation could be observed only after 24 hours; the materials became translucent and then increasingly opaque slowly over time. A decrease in UV absorbance at 215 nm was observed after 24 hours and continual decrease in UV absorbance thereafter was observed over the course of 166 hours (Chart 4.4.1: B,C). This decrease was accompanied by the growth over time of a small shoulder between 280-310 nm.

At low concentrations of water (7.67wt%), representing a water-in-oil microemulsion structure that still contains a huge molar excess when compared to TTIP (35:1 molar ratio [H_2O]:[TTIP]), no change in transparency was observed after 4 days. The UV absorbance for this low water content microemulsion decreased very gradually after the first 24 hours (Chart 4.4.1: D)

4.4.1 Particle Size Distribution

Titania particle sizes and distribution were determined by the analysis of TEM images using Image J software (see Supporting Information) for the formulation containing ~13wt% water at 4, 24 and 48 hours, respectively.

Particle analysis at 4 hours revealed a number of smaller particles (<40 nm) compared to later time points. After 24 hours a few particles between 900-2000 nm could be observed, which were not observed at the initial time point. The average particle sizes were 45, 48, and 72 nm for the time points 4, 24 and 48 hours, respectively. TEM images of the particles do not show well-defined structures, likely due to high silicone content as shown by EDX of the particles formed in situ (Figure 6.3.9, Supporting Information). After 24 hours, fewer small particles (<20nm) were observed, and more of the particles were found as compact aggregates. That is, the major activity over time within the microemulsion was particle aggregation, although particle growth did continue. This trend continued with time: after 48 hours a greater number of particles were found in larger and denser aggregates, with aggregates as large at 1800 nm observed, although some small particles were still present (Figure 4.4.1.1).

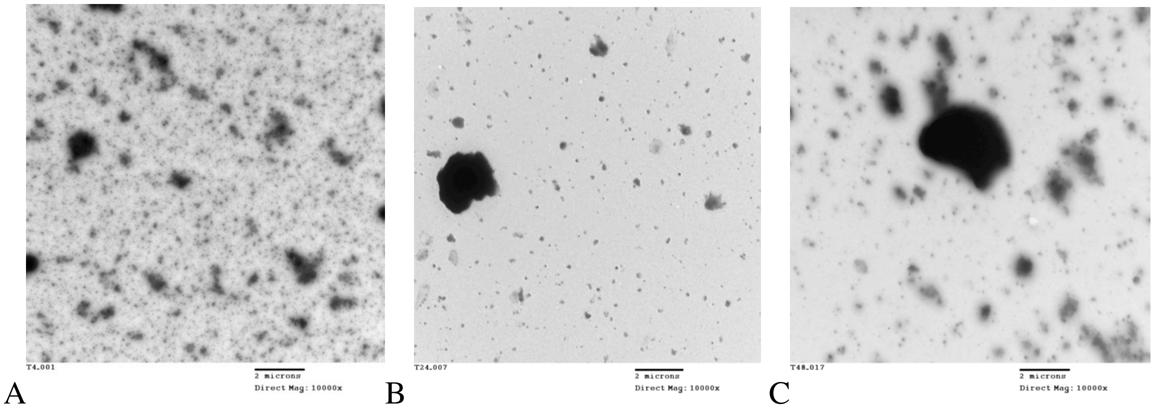

Figure 4.4.1.1: TEM analysis of particles formed within a silicone microemulsion containing 13.37wt% water at A: 4hr, B: 24hr and C: 48hr.

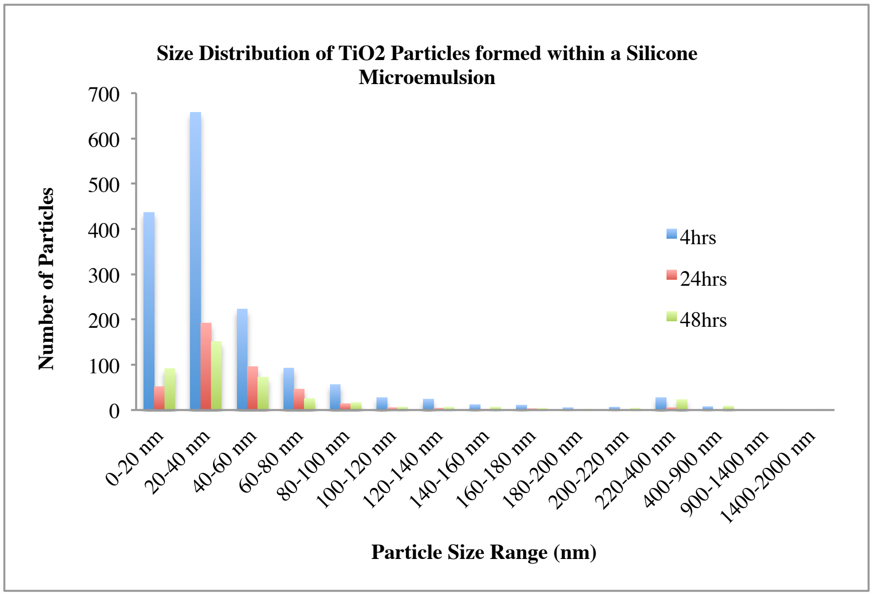

Chart 4.4.1.1: Particle distribution of titania formed overtime in a silicone microemulsion with ~13wt% water.

4.5. Discussion

Titanium dioxide has a refractive index ranging between 2.5-2.8 depending on its structure, amorphous vs crystalline and, in the latter case, the rutile/anatase ratio.[11] However, titania particles under 25 nm do not scatter visible light and are ideal for formulations and applications requiring UV absorption with high optical transparency in the visible region[12]: such particles are used as UV absorbers in commercial sunscreens.[13] Thus, changes in transparency of the microemulsions in the visible region provide guidance about the titania particles contained within.

Controlling titania particle size (and therefore optical transparency), using a sol-gel process with alkoxytitanium derivatives, is difficult to achieve under neutral conditions in part due to the high reactivity of the metal centre towards nucleophilic attack, which leads to rapid rates of hydrolysis.[14] In addition, the rate of titanol condensation is of the same order of magnitude as alkoxytitanium hydrolysis, resulting in both steps occurring simultaneously[15], which typically leads to rapid and uncontrollable particle formation. The rate of hydrolysis has been shown to be dependent on a number of different factors: the nature of the alkoxide ligand, the concentration of TiOR, and concentration of water in the sol-gel system are a few of the parameters that have been shown to affect hydrolysis and gel times.[14]

The chain length of the alkoxide has also been shown to influence the rate of hydrolysis, with higher alkyl chain lengths resulting in decreased rates.[16] Partial or complete transetherification of the OiPr groups of TTIP with the surfactant Silsurf A008-UP occurred when the two materials were mixed (Figure 6.3.1, Supporting Information).

The attachment of this longer chain, with its terminal hydrophobic trisiloxane residue was initially expected to be partly responsible for the much slower rate of titania formation: the hydrolysis steps should be retarded. However, rapid hydrolysis and condensation of Ti-Silsurf conjugates occurred when the mixture was exposed to water in the absence of a microemulsion structure.

The concentration of water in each microemulsion system was in large excess compared to the titanium alkoxide, indicating that any observed decrease with respect to induction times for visible titania formation must be attributed to microemulsion nanostructuring. The formation of particles within three different microemulsion structures was therefore examined as a function of water content: the microemulsion structures evaluated were water-in-oil, bicontinuous, and oil-in-water types.

The high water content TTIP O/W microemulsions (224:1 molar ratio [H_2O]:[TTIP]) resulted in the immediate formation of visible titania once enough water was added to the initial surfactant/TTIP/oil mixture to create the O/W structure. UV showed the presence of titania (Chart 4.4.1: A) as the absorbance peak between 260-340 nm was present upon initial measurement and remained consistent (showing no additional growth) over the course of a week. With water as the continuous phase, once there is sufficient interfacial area, delivery of water to the titanium center is facile leading to rapid hydrolysis/condensation: particle growth was not restricted within a given domain (droplet) of the microemulsions (see below). Thus, in the O/W microemulsion structure, the hydrolysis, condensation and TiO_2 particle formation were very efficient, comparable to the situation where a microemulsion was not present. Unsurprisingly, the surfactant molecules and microemulsion structure could not act to retard particle formation.

The one W/O and two bicontinuous microemulsions containing TTIP were initially transparent, but a slow increase in opacity was observed over the course of 72 hours at a rate that depended on the water content and microemulsion structure type: all formulations contained a huge excess of water relative to TTIP. We propose that it is the reinforcement of interfaces by Silsurf A008-UP at domain intersections within the microemulsion that retards the rate of particle formation and growth once particle sizes approach the domain sizes.

Water-in-oil microemulsions (reverse micelles) have previously been used to control the size of inorganic nanoparticles, by isolating two reacting species in separate microemulsion solutions and mixing the solutions together under controlled conditions.[17] For example, microemulsions containing different types of oils were used in the formation of CdS particles and the rate of particle formation was found to be dependent on temperature and nature of the continuous phase, which is turn was dependent on oil type and concentration. The size of CdS particles was found to be dependent on the R value (mole ratio of water to surfactant) within the microemulsion, which is directly related to hydrodynamic radius of the droplets. The formation of CdS particles was shown to be a complex mechanism governed by multiple variables including droplet size and rate of formation, which are influenced by concentration and nature of the oil phase, and the concentration of water within a microemulsion. This system is quite different from the one under consideration.

Water-in-oil microemulsions can also serve as a template for titanium dioxide particle synthesis from titanium chloride.[18] However, for the reasons noted above, acidic conditions were required to form titania particles that did not aggregate and the reactants (aqueous ammonia solution and titanium chloride in HCl) were incorporated into separate microemulsions, which were then mixed together to initiate particle formation. The system we've described in this publication is quite different in that bulk water at neutral pH is added to the alkoxytitanium reagent that is dispersed in oil. The microemulsion method previously described resulted in the formation of visible titania within three hours[18], whereas, the system described using Silsurf A008-UP avoids visible particle formation for up to three days (depending on the formulation). Again, these are quite different outcomes.

The low water content TTIP microemulsion (35:1 molar ratio [H_2O]:[TTIP]) has a water-in-oil structure. Both the surface area of the water droplet and droplet diffusion should limit the growth of titanium dioxide particles. The process begins with hydrolysis that can take place at the droplet interface, but the possibility of swollen micellar structures of partly hydrolyzed TTIP/Silsurf A008-UP and of sterically stabilized TiO_2 particles cannot be excluded (Figure 4.4.1). The UV spectra obtained for the TTIP microemulsion with low water content (~8wt%) showed an absorption peak at ~210 nm, which indicates ligand-to-metal charge transfer from an isolated Ti(IV) species. This implies that initially the initial titanium alkoxide species present is resistant to hydrolysis and/or that the condensation process is delayed (Chart 4.4.1 D). Both swollen micelles of TTIP and sterically stabilized TiO_2 particles could interact with the water droplet to form a sort of Pickering emulsion. While neither of these structures will be ultimately stable, they each could provide barriers to the delivery of water to the Ti-OR bond and, more importantly, to the formation of large titania aggregates.

Unlike previous microemulsion studies that focused specifically on water-in-oil microemulsions, we were able to evaluate particle synthesis in the bicontinuous structure type microemulsion by changing water content in the microemulsion. Titania monoliths comprised of aggregated particles have been reported[9], but we have been unable to find precedent for the preparation of discrete titanium oxide particles within bicontinuous silicone microemulsions. It is likely that both the continuous and internal phases are important in the design of nanoparticle synthesis within microemulsion systems.

At higher water content, ~18% or ~13% water, respectively (94:1 or 66:1 molar ratio [H_2O]:[TTIP), the microemulsions were bicontinuous with domain sizes between 5-10 nm[19]. Hydrolysis should normally be very efficient because the titanium alkoxide species in the bicontinuous microemulsion would be exposed to water more readily than in the W/O microemulsion due to very high interfacial area. UV spectra show, however, that hydrolysis is not particularly efficient (Chart 4.4.1). The $Ti(OR)_4$ absorption peak (~210 nm) was initially observed with TTIP microemulsions, as with the W/O microemulsion (Chart 4.4.1 B, C). As time progressed, however, the absorption of alkoxysilanes medium and high water content microemulsions slowly decreased and additional absorption bands could been seen between 280-310 nm, indicating the presence of octahedrally coordinated titanium dioxide.[20]

Titania nanoparticles can be characterized using UV-Vis absorption spectroscopy. UV absorption bands are attributed to ligand-metal charge transfer from the oxygen to titanium(IV) centre. The position of the absorption band is affected by the geometry of the titanium centre and the size of titanium dioxide particle. Particle sizes below 5nm will exhibit absorption between 280-300 nm, while particles larger than 5nm will absorb between 350-400 nm.[21] Absorptions within this latter range were not observed until 48 and 24 hours, respectively, for the two microemulsions (Chart 4.4.1 C, D) and the intensity of the peak continued to grow over the course of a week, indicating the very slow and continual formation of larger TiO_2 aggregates.

TEM micrographs obtained of TiO_2 formed within the bicontinuous structure type, and ImageJ analysis, revealed that at the four-hour time point there is a greater number of small particles (20 nm) when compared to later time points. Only after 24 hours did the smaller particles begin to aggregate to form a fewer number of larger aggregates (Figure 4.4.1.1, B). That is, there is significantly more resistance to particle aggregation in a bicontinuous microemulsion than in solution, due to the presence of the interface.

These observations support the contention that both hydrolysis/condensation and particle aggregation are retarded within a bicontinuous microemulsion. We attribute the difference in the rate of formation of large TiO_2 particles to reinforcement of the domain walls by the surfactant. The first formed particles (< 20 nm) would be optically transparent (Figure 4.5.1 $A \rightarrow B$), as was initially observed, but further growth would be inhibited once the particles have filled the available space within the domain, that is, once they reach the domain walls/interface. Particles are free to grow and aggregate until they become surrounded by the highly viscoelastic interface. For further particle growth or aggregation the interface needs to distort and/or reform to facilitate interparticle clustering and then aggregation (Figure 4.5.1 B→C). It took over a day before this occurred to a significant degree.

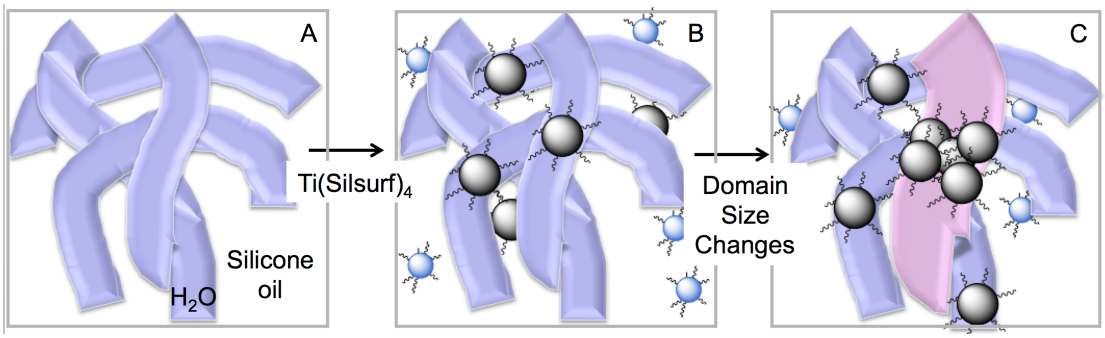

Figure 4.5.1: Model showing bicontinuous microemulsion domains constraining TiO_2 particle aggregation initially to the size of the aqueous domains. A: hydrolysis and condensation leading to micelles and TiO_2 particles. B: Expansion of domains over time, which requires reorganization of the domains, allows particle aggregation.

The interactions between TTIP and Silsurf A008-UP slows the rate at which TiO_2 particles form by hydrolysis and condensation. More importantly, although the formation of visible titania particles is not arrested completely following the hydrolysis of a tetraalkoxysilane, it is significantly retarded in a W/O or bicontinuous microemulsion. Despite the fluidity of the microemulsion ingredients, and neutral pH, it appears that surfactant structuring at the water/oil interface particularly in bicontinuous microemulsions is able to resist TiO_2 particle growth and aggregation.

4.6 Conclusion

The formation of titanium dioxide in a microemulsion is highly dependent on the structure of the microemulsion. The rate of TiO_2 particle formation can be controlled by microemulsion structure, which in turn depends on water content. Oil-in-water microemulsions did not significantly retard titania formation. By contrast, water-in-oil type microemulsions exhibited the slowest titania formation, while the bicontinuous structure type resulted in an increased, but still very slow, rate of titania formation compared to the reaction with neutral water in the absence of a microemulsion structure. In the latter tow cases, even though the silicone fluids used in the microemulsion were of low viscosity, the nanostructuring provided by water-in-oil and bicontinuous type microemulsions dramatically retarded the growth and aggregation of titanium dioxide nanoparticles. This is ascribed to reinforcement of the nanodomains by the surfactant at the oil/surfactant/water interface, movement of which is needed for particle aggregation to occur.

4.7 Supporting Information

Appendix 6.3: General procedure for the synthesis of titanium-siloxane complexes $(i\mathrm{PrO})_n\mathrm{Ti}(\mathrm{Silsurf})_{4-n}$, ^{1}H NMR spectra, UV-Vis absorption spectra of $\mathrm{Ti}(\mathrm{O}\text{-}i\mathrm{Pr})_4$ and TTIP/A008-UP complex, Table giving formulations in grams, TEM micrographs and EDX spectra for particles derived from a microemulsion containing 13% water at 4, 24 and 48 hours, ImageJ analysis of the micrographs, microemulsion formulation used in titania sol-gel process analyzed for domain size via SAXS and structural information obtained from Teubner-Strey Model fitting to acquired scattering data.

4.8 Acknowledgements

We thank the Natural Sciences and Engineering Research Council of Canada and 20/20: NSERC Ophthalmic Materials Network for financial support of this research. We would also like to express our gratitude to Marcia Reid for assistance in obtaining TEM data.

4.9 References

1. Macwan, D. P.; Dave, P. N.; Chaturvedi, S., A review on nano-TiO2 sol-gel type syntheses and its applications. *J Mater Sci* 2011, *46* (11), 3669-3686.

2. Ohtani, B.; Ogawa, Y.; Nishimoto, S., Photocatalytic activity of amorphous-anatase mixture of titanium(IV) oxide particles suspended in aqueous solutions. *J Phys Chem B* 1997, *101* (19), 3746-3752.

3. Carlotti, M. E.; Ugazio, E.; Sapino, S.; Fenoglio, I.; Greco, G.; Fubini, B., Role of particle coating in controlling skin damage photoinduced by titania nanoparticles. *Free Radical Res* 2009, *43* (3), 312-322.

4. Okunaka, S.; Tokudome, H.; Hitomi, Y.; Abe, R., Facile preparation of stable aqueous titania sols for fabrication of highly active TiO2 photocatalyst films. *J. Mater. Chem. A* 2015, *3* (4), 1688-1695.

5. Dunuwila, D. D.; Gagliardi, C. D.; Berglund, K. A., Application of Controlled Hydrolysis of Titanium(Iv) Isopropoxide to Produce Sol Gel-Derived Thin-Films. *Chem Mater* 1994, *6* (9), 1556-1562.

6. Chen, Y.; Yi, Y. Y.; Brennan, J. D.; Brook, M. A., Development of macroporous Titania monoliths using a biocompatible method. Part 1: Material fabrication and characterization. *Chem Mater* 2006, *18* (22), 5326-5335.

7. (a) Sugimoto, T.; Zhou, X. P.; Muramatsu, A., Synthesis of uniform anatase TiO2 nanoparticles by gel-sol method - 1. Solution chemistry of Ti(OH)(n)((4-n)+) complexes. *J Colloid Interf Sci* 2002, *252* (2), 339-346; (b) Sugimoto, T.; Zhou, X. P.; Muramatsu, A., Synthesis of uniform anatase TiO2 nanoparticles by gel-sol method 3. Formation process and size control. *J Colloid Interf Sci* 2003, *259* (1), 43-52; (c) Mahshid, S.; Askari, M.; Ghamsari, M. S., Synthesis of TiO2 nanoparticles by hydrolysis and peptization of titanium isopropoxide solution. *J Mater Process Tech* 2007, *189* (1-3), 296-300.

8. Pacia, M.; Warszynski, P.; Macyk, W., UV and visible light active aqueous titanium dioxide colloids stabilized by surfactants. *Dalton T* 2014, *43* (33), 12480-12485.

9. Szymanski, L.; Surolia, P.; Byrne, O.; Thampi, K. R.; Stubenrauch, C., Porous “sponge-like” anatase TiO2 via polymer templates: synthesis, characterization, and performance as a light-scattering material. *Colloid Polym. Sci.* 2013, *291*, 805–815.

10. Brook, M. A.; Whinton, M.; Gonzaga, F.; Li, N., Elastomeric hydrogels by polymerizing silicone microemulsions. *Chem. Commun.* 2011, *47* (31), 8874-8876.

11. Pelaez, M.; Nolan, N. T.; Pillai, S. C.; Seery, M. K.; Falaras, P.; Kontos, A. G.; Dunlop, P. S. M.; Hamilton, J. W. J.; Byrne, J. A.; O'Shea, K.; Entezari, M. H.; Dionysiou, D. D., A review on the visible light active titanium dioxide photocatalysts for environmental applications. *Appl. Catal., B* 2012, *125*, 331-349.

12. (a) Chau, J. L. H.; Tung, C. T.; Lin, Y. M.; Li, A. K., Preparation and optical properties of titania/epoxy nanocomposite coatings. *Mater. Lett.* 2008, *62* (19), 3416-3418; (b) Kockler, J.; Oelgemoller, M.; Robertson, S.; Glass, B. D., Photostability of sunscreens. *J Photoch Photobio C* 2012, *13* (1), 91-110.

13. Lewicka, Z. A.; Yu, W. W.; Oliva, B. L.; Contreras, E. Q.; Colvin, V. L., Photochemical behavior of nanoscale TiO2 and ZnO sunscreen ingredients. *J. Photochem. Photobio. A: Chem.* 2013, *263*, 24-33.

14. Sanchez, C.; Livage, J.; Henry, M.; Babonneau, F., Chemical Modification of Alkoxide Precursors. *J. Non-Cryst. Solids* 1988, *100* (1-3), 65-76.

15. Golubko, N. V.; Yanovskaya, M. I.; Romm, I. P.; Ozerin, A. N., Hydrolysis of titanium alkoxides: Thermochemical, electron microscopy, SAXS studies. *J. Sol-Gel Sci. Technol.* 2001, *20* (3), 245-262.

16. Brinker, C. J., Scherer, G. W., *Sol-Gel Science: The Physics and Chemistry of Sol-Gel Processing*. Academic Press: San Diego, CA, 1990.

17. (a) Towey, T. F.; Khanlodhi, A.; Robinson, B. H., Kinetics and Mechanism of Formation of Quantum-Sized Cadmium-Sulfide Particles in Water Aerosol-Ot Oil Microemulsions. *J. Chem. Soc.-Faraday Trans.* 1990, *86* (22), 3757-3762; (b) Pileni, M. P., The role of soft colloidal templates in controlling the size and shape of inorganic nanocrystals. *Nature Mater.* 2003, *2* (3), 145-150.

18. Lin, P.; Xian, C. Y.; Mao, Z. P.; Zhu, Q.; Chen, X. L.; Zheng, L. M., Synthesis and characterization of titania nanoparticles by microemulsion process. *Indian J. Chem. A* 2006, *45* (9), 2017-2020.

19. Whinton, M. E.; Hughes, T. C.; Peng, S.; Brook, M. A., Silicone Microemulsion Structures Are Maintained During Polymerization Using Reactive Surfactants. *submitted.*

20. Li, Y.; Kim, S. J., Synthesis and Characterization of Nano titania Particles Embedded in Mesoporous Silica with Both High Photocatalytic Activity and Adsorption Capability. *J. Phys. Chem. B* 2005, *109*, 12309-12315.

21. Li, Y. Z.; Kim, S. J., Synthesis and characterization of nano titania particles embedded in mesoporous silica with both high photocatalytic activity and adsorption capability. *J. Phys. Chem. B* 2005, *109* (25), 12309-12315.

5. Chapter 5: General Conclusions

This thesis has discussed the development of silicone-based microemulsions to exploit the unique properties and nanomorphology of the microemulsion template to create novel nanoporous silicone elastomers. The thermal stability and high interfacial area of microemulsions make them attractive towards the development of silicone elastomeric materials with high internal surface area. The tolerance of the microemulsion template to alternative, non-radical based chemical processes was investigated to determine the utility of RTV type cure in the formation of nanoporous elastomers from microemulsion templates. The application of silicone microemulsions as a nano-reactor in the formation of in situ metal oxides was explored towards the development UV protective silicone materials.

In Chapter 2 silicone microemulsions containing non-volatile silicone oil and a trisiloxane PEO surfactant were prepared. Two types of non-volatile silicone oils (15-35 cSt, 45-85 cSt) were formulated into silicone microemulsions, stabilized by either a non-polymerizable or analogous surfactant with polymerizable acrylic group. The non-polymerizable surfactant was more efficient at stabilizing equal weights of water/silicone oil, however, stable, transparent materials were only achieved when microemulsions containing the reactive surfactant were polymerized.

The role of the co-surfactant HEMA in expanding the microemulsion region was investigated and it was found that the microemulsion region could be expanded with increasing content of HEMA. The bicontinuous region of the microemulsion phase diagram was determined using electrical conductivity, in which an oil/surfactant mixture was titrated with water. Formulations residing within the bicontinuous region of the phase diagram were polymerized using two simultaneous cure methods: photopolymerization of the aqueous phase and RTV cure of the silicone phase. The polymerized microemulsions were shown to be permeable to aqueous solutions, indicating that the bicontinuous network was preserved in the elastomeric product.

In Chapter 3, we aimed to understand how the polymerization of each phase affects morphology in the polymeric product. We used SAXS as a tool to evaluate structural transitions from a liquid microemulsion to polymeric material. In order to determine the effects of photopolymerization vs RTV cure on one-to-one microemulsion templating, the water phase and oil phase were polymerized together and independently. The photopolymerization of microemulsions in all cases resulted in an observed increase in the q-peak, indicating an increase in polymeric nanostructuring, regardless of microemulsion composition. Microemulsions that underwent photopolymerization also had a decrease in amphiphilicity factor, indicating more strongly structured microemulsions when compared to the original, unpolymerized microemulsion.

In order to understand the effect of RTV cure on microemulsion structure, the effects of the individual additives required to rigidify the oil phase (TEOS crosslinker or DBDTL catalyst) were investigated. The incorporation of TEOS into a microemulsion resulted in a decrease in q-peak intensity, indicating the presence of an amorphous, unstructured polymeric solution. The incorporation of DBTDL into a microemulsion resulted in a slight decrease in q-peak intensity and a shift to a higher q value. The addition of DBTDL still resulted in a pronounced q-peak, indicating that there is nanophase separation within the microemulsion. However, the morphology had shifted from the original microemulsion, as indicating from the fitting parameter (chi^2 value) obtained from fitting the acquired scattering data to the Teubner-Strey model. The incorporation of both TEOS and DBTDL together within a microemulsions resulted in the RTV cure of the silicone phase. This also resulted in a decrease in q peak intensity, meaning a loss of nanophase separation and therefore, microemulsion structure. This implies that RTV alone does not appear to be sufficient at stabilizing the oil/water interface during polymerization.

The inability of a silicone elastomer, formed by RTV cure, to retain morphology in the polymerized microemulsion was mitigated when photopolymerization was also performed on the microemulsion. The polymerization of both the water phase and the oil phase resulted in retention of microemulsion structure with physical parameters most similar to the original, unpolymerized microemulsion. Anchoring of the surfactant to the interface appears to be key in retaining nanophase morphology, regardless of whether or not the oil phase is also polymerized. However, this suggests that the polymerization of microemulsions could potentially be accomplished with methods other than radical processes if the surfactant could be tethered or physically constrained at the interface to prevent macrophase separation.

The last part of this thesis, Chapter 4, focused on exploiting the microemulsion structure to retard the formation of titania particles from a titanium alkoxide precursor. Titanium was incorporated directly into the microemulsion through the addition of titanium isopropoxide (TTIP), which undergoes raw material interactions with the surfactant (Silsurf A008-UP) via a nucleophilic substitution reaction. Microemulsions containing TTIP formed titania in situ as water was titrated into a mixture of TTIP/A008-UP/OHPDMS to form a microemulsion system. Although, air stable, direct content with water results in the hydrolysis of a TTIP/Silsurf A008-UP mixture, followed by condensation and subsequent TiO_2 formation. The effect of microemulsion structure on the formation of TiO_2 particles was investigated by preparing microemulsions containing the titanium precursor, with varying amounts of water (all in molar excess of titanium). Four water contents were evaluated: 8wt%, 13wt%, 18wt%, and 35wt%. The lowest water content represented the water-in-oil structure type, while 13wt% represented the beginning of the bicontinuous morphology. Increasing water content to 18wt% resulted in a bicontinuous structure with increased water channels while a microemulsion with 35wt% represented an oil-in-water structure type.

The formation of TiO_2 and depletion of the tetracoordinate Ti^{4+} species was monitored using UV absorbance at ~280 nm and ~215 nm, respectively. Despite the huge molar excess of water in all cases, the rate of depletion of Ti^{4+} varied depending on microemulsion water content and therefore, structure. Overall it was very much slower than the reaction of TTIP and particularly slower than in the absence of a bicontinuous microemulsion. The water-in-oil microemulsion structure containing ~8 wt% water showed an increase in absorbance at ~280 nm over the course of 72 hours, indicating the formation of TiO_2. However, after 72 hours, a further increase in absorbance was not observed, indicating that TiO_2 formation has halted. During this time, no visible titania particles were observed and the solution remained optically transparent, consistent with the formation of particles that are well below the wavelength of scattering visible light (<50nm).

The microemulsion formulated with ~13wt% water (bicontinuous structure) showed a gradual and continual increase in absorbance at ~280 nm over the duration of 168 hours, indicating that particles were continually forming. This microemulsion formulation remained optically transparent up until 144 hours, after which they began to turn translucent, indicative of larger particle formation.

Increasing the water content to ~18wt% within the microemulsion still resulted in a bicontinuous structure, however, the amount and size of water channels had increased in comparison to the microemulsion containing ~13wt% water. The absorbance of this microemulsion formulation was not initially as high as the previous formulations, indicating that more of the tetracoordinate titanium-surfactant complex had been consumed prior to the initial measurement. However, a slow and gradual increase of the absorbance peak at ~280 nm was still observed over the course of 168 hours, indicating the continual growth of TiO_2 particles. This formulation remained transparent for 48 hours, after which titania could be observed: the microemulsion turned white/translucent.

The microemulsion formulated with ~35wt% water was of an oil-in-water structure type. Absorbance of this formulation was also not initially high, indicating that most of the tetracoordinate titanium-surfactant compound was consumed prior to the initial measurement. This is similar to what was observed for the bicontinuous structure containing a high content of water (~18wt%), however, in this system, we did not observe a gradual increase in absorbance at ~280 nm. Absorbance at 280 nm remains relatively stable over the course of 168 hours, indicating that TiO_2 formation was mostly completed when the microemulsion was first prepared. This was consistent with visual observations, in which visible TiO_2 particles were observed immediately after microemulsion formation.

All four formulations revealed distinct patterns of TiO_2 formation, dependent on the microemulsion structure type. Developing systems in which TiO_2 formation can be slowed and controlled could ultimately lead to the development of transparent, UV absorbent silicone elastomers.

Within the context of this thesis, we have explored how trisiloxane surfactants affect the microemulsion region of formulations consisting of non-volatile PDMS and water with and without a hydrophilic monomer. It has been demonstrated that the hydrophilic monomer HEMA expands the microemulsion region of silicone microemulsions and that the surfactant functionality also impacts the microemulsion region of the phase diagram. It was also shown that bicontinuous microemulsions could be successfully polymerized into nanostructured, transparent polymeric materials, given that the surfactant could be chemically anchored at the interface.

Investigations using SAXS showed that the stability of microemulsions during polymerization was affected by both the water and oil phase of the microemulsion. Polymerization (RTV cure) within the oil phase, in the absence of water phase polymerization, did not result in the formation one-to-one templated materials, likely a result of the malleability and flexibility of the silicone phase. However, polymerization of the water phase, in which the surfactant is chemically bound at the interface, is able to lock-in structure despite the fluidity of the silicone phase. The importance of chemically anchoring the surfactant was explored by evaluating microemulsion structure when both phases were polymerized. Water phase polymerization in which the surfactant was bound at the interface resulted in bicontinuous polymeric microemulsions, despite the migratory and disruptive effects of physically crosslinking the oil phase. We believe that physical anchoring of the surfactant within the oil phase could lead to development of nano-structured silicone elastomers using industrially common RTV methods.

In summary, this thesis has explored the polymerization, characterization, and application of silicone microemulsions with the aim of developing nanostructured polymeric materials. We have shown that silicone microemulsions can be successfully polymerized through polymerization of either the water phase or both the water/oil phases. Evaluation of the liquid to solid transition using SAXS has provided a greater understanding into the processes that lead to morphology retention or collapse. And finally, utilization of the template in the controlled formation of titanium dioxide has explored new ways in which nanodomains can be used to constrict particle growth, which would be useful towards the development of a new class of silicone elastomer materials with unique optical properties.

6. Chapter 6: Appendix

6.1. Supporting Information for CHAPTER 2: Elastomeric hydrogels by polymerizing silicone microemulsions

Figure 6.1.1.1: Full microemulsion formulations with masses (Surfactant Phase)

Entry	Surfactant	A008-UP (wt%)	Mass (g)	ACR A008-UP (wt%)	Mass (g)
1	**1**	45.0	0.1543	0.0	0.0000
2	**1**	23.9	0.1315	0.0	0.0000
3	**2**	0.0	0.0000	50.0	0.1436
4	**2**	0.0	0.0000	38.0	0.1394
5	**2**	0.0	0.0000	42.0	0.1448
6*	**2**	0.0	0.0000	41.5	0.8002
7	**2**	0.0	0.0000	43.4	1.4595
8	**2**	0.0	0.0000	46.1	0.9416
9*	**1**	38.9	0.1990	0.0	0.0000
10	**1**	40.0	0.1446	0.0	0.0000
11	**2**	0.0	0.0000	45.4	0.2593
12*	**1**	39.2	0.2142	0.0	0.0000
13*	**2**	0.0	0.0000	45.6	1.0233
14	**2**	0.0	0.0000	44.4	0.2301
15	**2**	0.0	0.0000	46.6	0.2484

Full microemulsion formulations with masses continued (Water Phase)

Entry	Water Phase (total wt%)	H_2O (wt%)	Mass (g)	HEMA (wt%)	Mass (g)	HMP (wt%)	Mass (g)	DMPA (wt%)	Mass (g)	%HEMA in HEMA/ H_2O Sol'n
1	25.0	25.0	0.0857	0.0	0.0000	0.0	0.0000	0	0.0000	0.0
2	37.9	33.0	0.1813	3.7	0.0200	1.2	0.0068	0	0.0000	10.1
3	20.0	18.0	0.0517	2.0	0.0057	0.0	0.0000	0	0.0000	10.0
4	30.0	15.0	0.0550	15.0	0.0550	0.0	0.0000	0	0.0000	50.0
5	33.0	23.1	0.0796	9.9	0.0341	0.0	0.0000	0	0.0000	30.0
6*	26.8	18.4	0.3535	7.9	0.1515	0.0	0.0000	0.5	0.0105	30.0
7	28.0	23.8	0.8001	2.6	0.0889	1.6	0.0500	0	0.0000	9.8
8	28.3	24.8	0.5067	3.0	0.0622	0.5	0.0100	0	0.0000	10.0
9*	29.8	20.2	0.1035	8.6	0.0443	1.2	0.0060	0	0.0000	28.6
10	30.0	30.0	0.1085	0.0	0.0000	0.0	0.0000	0	0.0000	0.0
11	27.1	24.4	0.1392	2.7	0.0155	0.0	0.0000	0	0.0000	10.0
12*	29.4	25.4	0.1387	2.8	0.0154	1.2	0.0063	0	0.0000	9.9
13*	26.8	18.4	0.4145	7.9	0.1777	0.0	0.0000	0.5	0.0110	30.0
14	29.4	25.1	0.1298	3.3	0.0172	1.0	0.0050	0	0.0000	11.7
15	27.8	24.0	0.1279	2.9	0.0154	0.9	0.0048	0	0.0000	10.4

Full microemulsion formulations with masses continued (Oil Phase)

Entry	Silicone Phase (wt%)	HO-PDMS (15-35 cSt) (wt%)	Mass (g)	HO-PDMS (45-85 cSt) (wt%)	Mass (g)	TEOS (wt%)	Mass (g)
1	30.0	30.0	0.1029	0.0	0.0000	0.0	0.0000
2	38.2	0.0	0.0000	38.2	0.2102	0.0	0.0000
3	30.0	30.0	0.0862	0.0	0.0000	0.0	0.0000
4	32.0	32.0	0.1174	0.0	0.0000	0.0	0.0000
5	25.0	25.0	0.0862	0.0	0.0000	0.0	0.0000
6*	31.7	0.0	0.0000	28.4	0.5473	2.8	0.0531
7	28.6	0.0	0.0000	25.6	0.8611	1.4	0.0457
8	25.6	0.0	0.0000	22.5	0.4592	2.3	0.0465
9*	31.1	16.3	0.0832	0.0	0.0000	13.5	0.0689
10	30.0	18.0	0.0651	0.0	0.0000	10.2	0.0369
11	27.5	0.0	0.0000	25.2	0.1438	1.3	0.0072
12*	31.4	0.0	0.0000	27.1	0.1480	2.5	0.0135
13*	27.6	15.1	0.3389	0.0	0.0000	12	0.2701
14	26.2	0.0	0.0000	22.6	0.1172	2.7	0.0141
15	25.6	0.0	0.0000	22.1	0.1181	2.3	0.0124

Full microemulsion formulations with masses continued (Catalysts)

Entry	Dibutyltin Dilaurate Catalyst (wt%)	Mass (g)	Benzyl Amine Catalyst (wt%)	Mass (g)	Ingredients total %	Phase total %
1	0.0	0.0000	0.0	0.0000	100.0	100.0
2	0.0	0.0000	0.0	0.0000	100.0	100.0
3	0.0	0.0000	0.0	0.0000	100.0	100.0
4	0.0	0.0000	0.0	0.0000	100.0	100.0
5	0.0	0.0000	0.0	0.0000	100.0	100.0
6*	0.5	0.0100	0.0	0.0000	100.0	100.0
7	1.6	0.0545	0.0	0.0000	100.0	100.0
8	0.8	0.0175	0.0	0.0000	100.0	100.0
9*	1.3	0.0069	0.0	0.0000	100.0	100.0
10	0.0	0.0000	1.8	0.0065	100.0	100.0
11	1	0.0059	0.0	0.0000	100.0	100.0
12*	1.8	0.0099	0.0	0.0000	100.0	100.0
13*	0.5	0.0100	0.0	0.0000	100.0	100.0
14	0.9	0.0047	0.0	0.0000	100.0	100.0
15	1.2	0.0063	0.0	0.0000	100.0	100.0

6.1.1. Characterization

Conductivities of the microemulsion samples were measured using a CDM 83 conductivity meter (Radiometer Copenhagen). Scanning electron microscope (SEM) images of microgels were obtained using a JEOL 7000F SEM at an accelerating voltage of 5 kV. Samples were coated with 30 nm gold using a Gatan precision etching coating system (PECS), model 682 in a process that does not induce morphological changes in the surface. UV-visible absorbance/transmittance were measured using Tecan Safire Multi-mode Spectrophotometer.

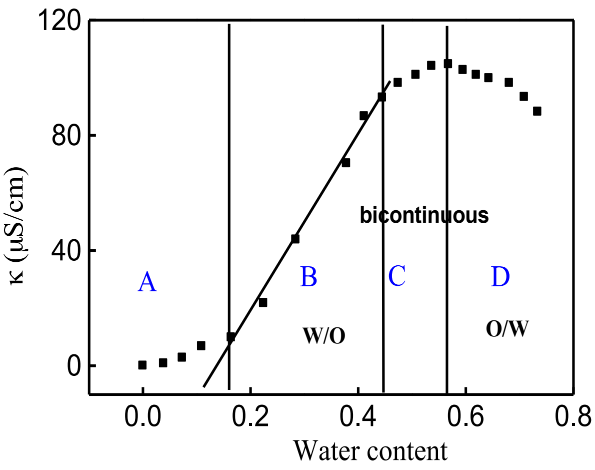

Figure 6.1.1.1: Conductivity plot for μE based on water titration into surfactant/oil mixture using surfactant:oil ratio from formulation 1 (Table 6.1.1, entry 1).

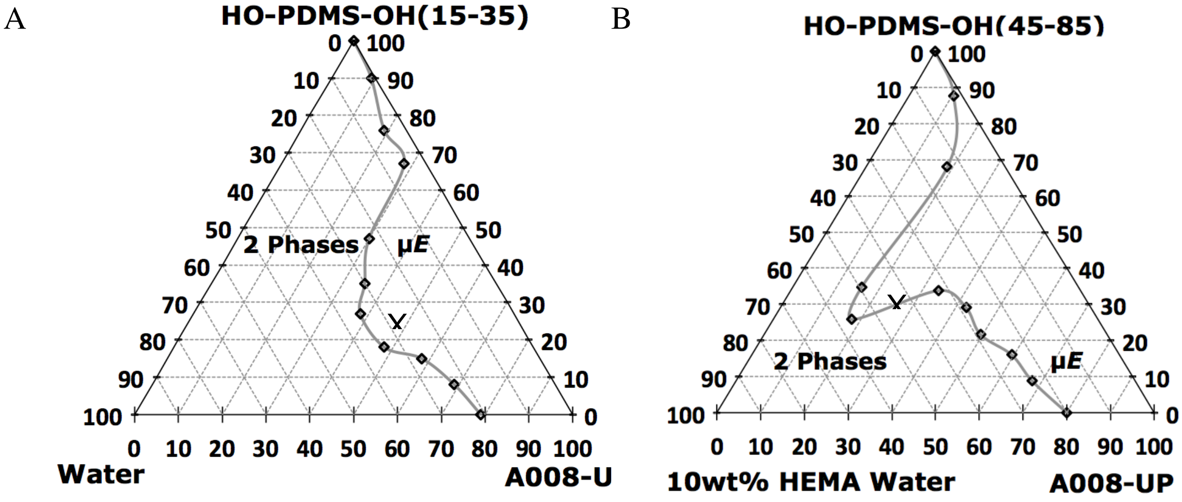

Figure 6.1.1.2: Phase diagrams for μE formed with: A: water, 15-35 cSt silicone oil + 1, B: 10% HEMA in water, 45-85 cSt silicone oil + 1. X indicates high water/low surfactant zones that were seen only with surfactant 1.

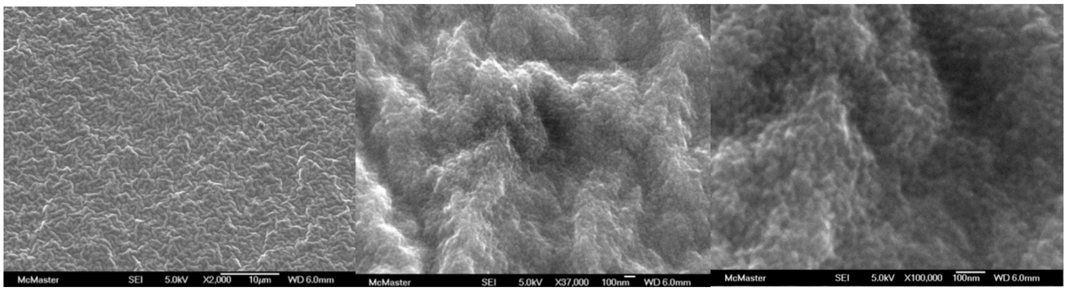

Figure 6.1.1.3: SEM images using gold coating of the microgel (Table 2.5.3.5.1, entry 10) at three magnifications. Scale bar = 10 μm, 100 nm and 100 nm.

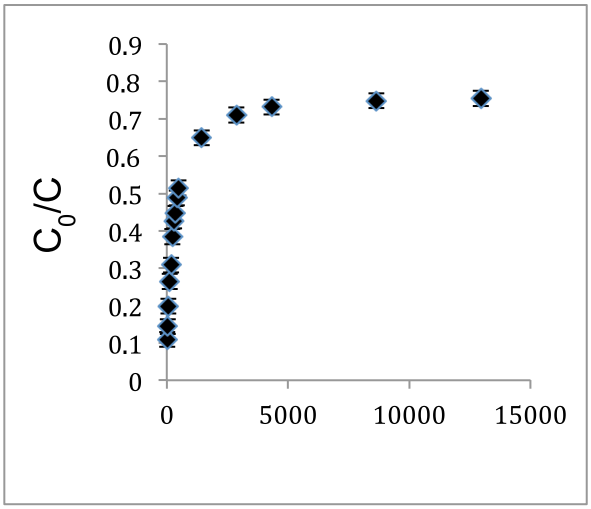

Figure 6.1.1.4: Release curve for phenol red in the microgel (, entry 10). C_0: released concentration; C: total concentration.

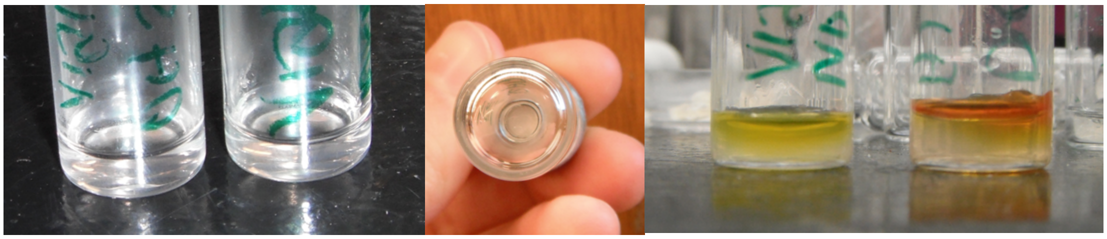

Figure 6.1.1.5: Phenol red pH 7 (left) and pH 9 (right) permeating into formulation after Table 2.3.1, entry 14, 15.

6.2. Supporting Information for CHAPTER 3: Silicone Microemulsion Structures are maintained during Microemulsion Polymerization using Reactive Surfactants

Table 6.2.1: Microemulsion Formulations for SAXS analysis expressed in weight percent and actual mass.

Formulation	ACR A008-UP (wt%)	ACR A008-UP (g)	OHPDMS (25 cSt) (wt%)	OHPDMS (25 cSt) (g)	HEMA-Water Solution (wt%)	HEMA-Water Solution (g)
1	46.83	0.5154	21.75	0.2393	31.42	0.3458
2	46.74	2.9528	21.68	1.3700	31.33	1.9795
3	44.93	2.8338	20.85	1.3154	30.04	1.8946
4	45.07	0.4951	21.05	0.2313	30.05	0.3301
5	44.66	0.9846	21.07	0.4644	29.63	0.6531
6	46.42	1.0209	21.74	0.4780	31.06	0.6830
7	46.43	2.9245	21.60	1.3607	30.97	1.9509
8	44.66	0.9835	20.66	0.4549	29.78	0.6558

Table 6.2.1 continued

Formulation	TEOS (wt%)	TEOS (g)	Irgacure 184 (wt%)	Irgacure 184 (g)	DBTDL (wt%)	DBTDL (g)
1	0.00	0.0000	0.00	0.0000	0.00	0.0000
2	0.00	0.0000	0.00	0.0000	0.25	0.0158
3	3.93	0.2481	0.00	0.0000	0.25	0.0158

4	3.83	0.0421	0.00	0.0000	0.00	0.0000
5	3.89	0.0858	0.75	0.0165	0.00	0.0000
6	0.00	0.0000	0.78	0.0172	0.00	0.0000
7	0.00	0.0000	0.75	0.0473	0.25	0.0158
8	3.90	0.0858	0.75	0.0165	0.25	0.0055

6.3. Supporting Information for CHAPTER 4: Very slow formation of TiO_2 nanoparticles by hydrolysis of an alkoxytitanate within a bicontinuous silicone/water microemulsion

6.3.1. General Methods

NMR spectra were recorded at 25 °C on a Bruker AVANCE 600 MHz spectrometer in $CDCl_3$ solutions. Chemical shifts are reported relative to $CDCl_3$ (^{13}C, 77 ppm) (^{1}H, 7.26 ppm). In order to observe the chemical shift of CH_2 PEG protons in the mixed OiPr/OSilsurf compounds, an analogous, but slightly simpler surfactant (Silsurf A004-UP) was investigated in the reaction with titanium isopropoxide. It differs from Silsurf A008-UP by having only 4 PEG units on average instead of 8.

6.3.1.1. General Procedure for the Synthesis of Titanium-Siloxane Complexes

Siloxane surfactant A004-UP (456 g/mol, 1.1769 g, 2.58 mmol) Gelest) was slowly added to titanium isopropoxide (0.7390 g, 2.6 mmol) over the course of 10 min while mixing. Isopropanol is produced during the course of the reaction and was distilled off at

50 °C under reduced pressure (1 mm Hg). Analogous reactions were used to prepare the di-, tri- and tetra-substituted analogues **1**, **2** and **3**, respectively (Figure 6.3.1.1).

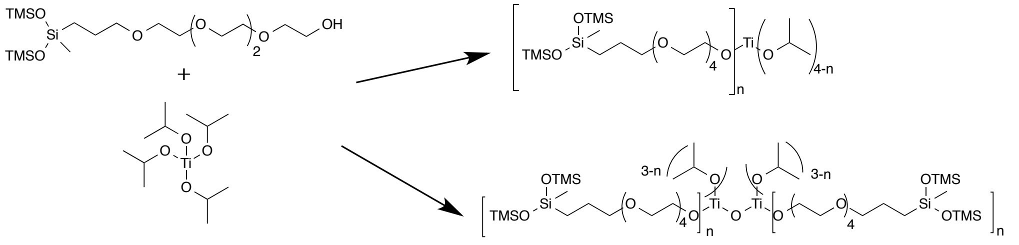

A004-UP-Titanium Alkoxide **1**: n=1
A004-UP-Titanium Alkoxide **2**: n=2
A004-UP-Titanium Alkoxide **3**: n=3

Figure 6.3.1.1: Raw material interactions between TTIP and surfactant monomer resulting in the synthesis of A004-UP-Titanium alkoxides 1-3 with predicted substitution on titanium center.

1 Bright yellow oil (1.5861g, 96.5%); ^{1}H NMR (600 MHz, $CDCl_3$, 25 °C, Figure 6.3.1.2) δ: 0 (s, 3H, Si**CH_3**), 0.08 (s, 18H, **TMS**O-Si-O**TMS**), 0.42 (m, 2H, Si**CH_2**CH_2CH_2), 1.24 (d, 12H, CH(**CH_3)$_2$**, *J* = 6.06 Hz), 1.59 (m, 2H $SiCH_2$**CH_2**CH_2), 3.40 (t, 2H, $SiCH_2CH_2$**CH_2**, *J* =7.14 Hz), 3.57 (m, 2H, OCH_2**CH_2**), 3.64 (broad m, 16H, O**CH_2CH_2**), 4.32 (broad s, 2H, Ti-O**CH_2**), 4.53 (broad s, 2H, Ti-O**CH**$(CH_3)_2$)

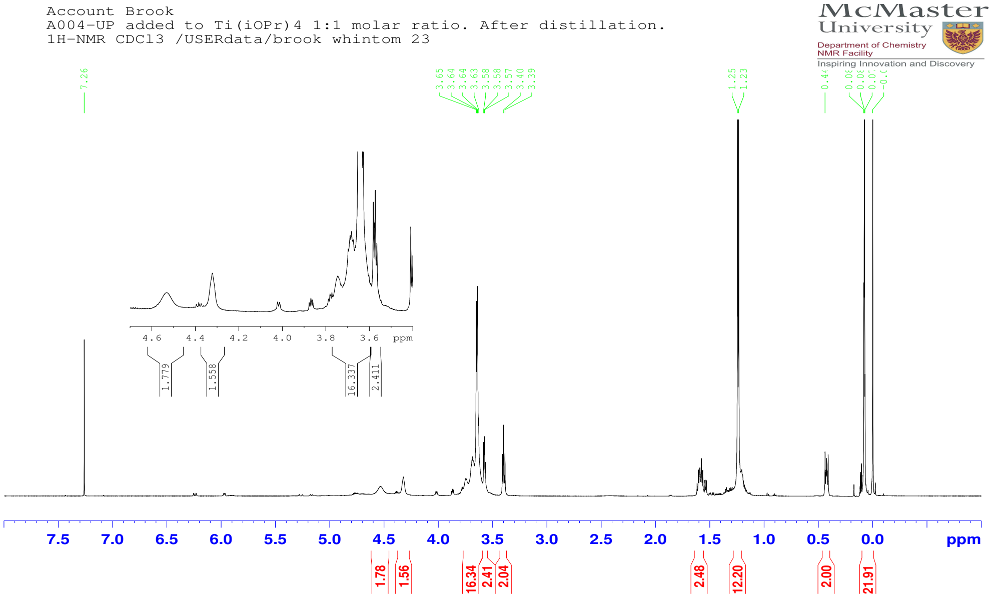

Figure 6.3.1.2: ^{1}H NMR of 1

6.3.1.2. Synthesis of Titanium-Siloxane Complex 2

2 Siloxane surfactant A004-UP (456 g/mol, 1.2865g, 2.82 mmol, Gelest); titanium isopropoxide (0.4003 g, 1.41 mmol). Bright yellow compound (1.3888g, 91.7%); ^{1}H NMR (600 MHZ, $CDCl_3$, 25 °C, Figure 6.3.1.3) δ: 0 (s, 6H, Si$\mathbf{CH_3}$), 0.07 (s, 36H, **TMS**O-Si-O**TMS**), 0.41 (m, 4H, $\mathbf{CH_2}$), 1.21 (d, 5H, CH$\mathbf{(CH_3)_2}$, J = 5.94 Hz), 1.58 (m, 4H, $\mathbf{CH_2}$), 3.39 (t, 4H, $\mathbf{CH_2}$, J = 7.14 Hz), 3.56 (m, 4H, $OCH_2$$\mathbf{CH_2}$), 3.63 (broad m, 32H, O$\mathbf{CH_2CH_2}$), 4.34 (broad s, 3H, Ti-O$\mathbf{CH_2}$), 4.69 (broad s, 1H, Ti-O**CH**$(CH_3)_2$).

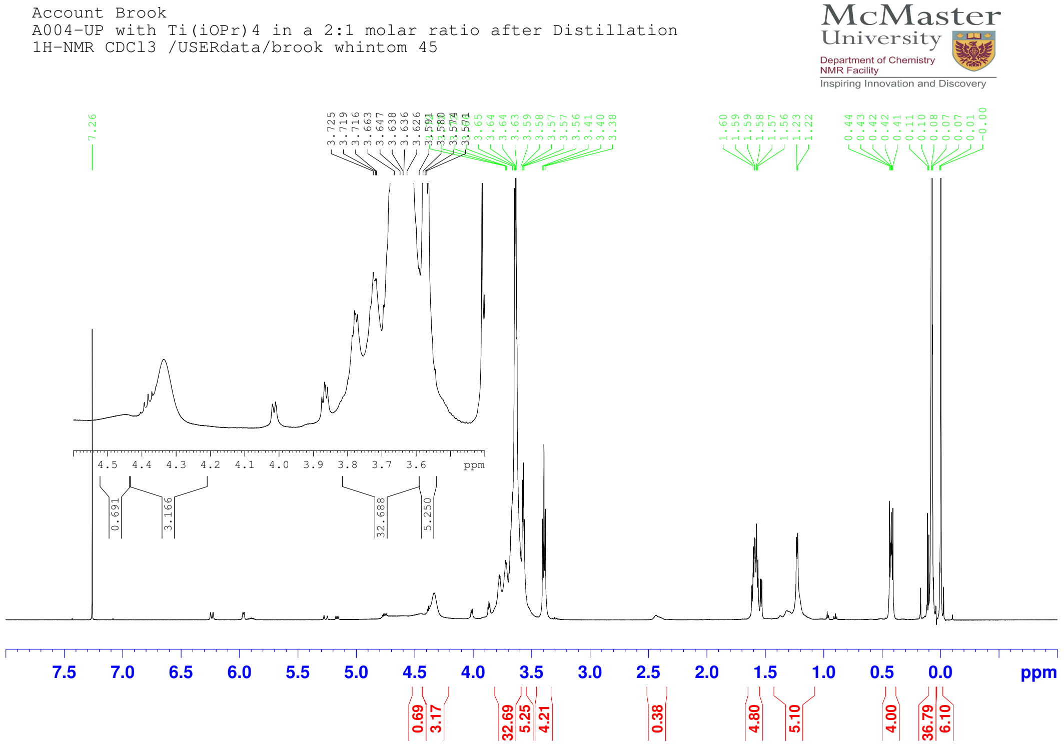

Figure 6.3.1.3: ^{1}H NMR of 2

6.3.1.3. Synthesis of Titanium-Siloxane Complex 3.

Siloxane surfactant A004-UP (456 g/mol, 1.2441g, 2.73 mmol, Gelest), titanium isopropoxide (0.2559 g, 0.9 mmol). Bright yellow compound (1.2644 95.3%); 1H NMR (600 MHZ, CDCl3, 25 °C, Figure 6.3.1.4) δ: 0 (s, 12H, SiCH3), 0.07 (s, 72H, TMSO-Si-OTMS), 0.42 (m, 8H, SiCH2CH2CH2), 1.59 (m, 8H, SiCH2CH2CH2), 3.40 (m, 6H, SiCH2CH2CH2), 3.63 (broad, m, 50H, OCH2CH2), 4.3 (broad s, 4H, Ti-OCH2CH2).

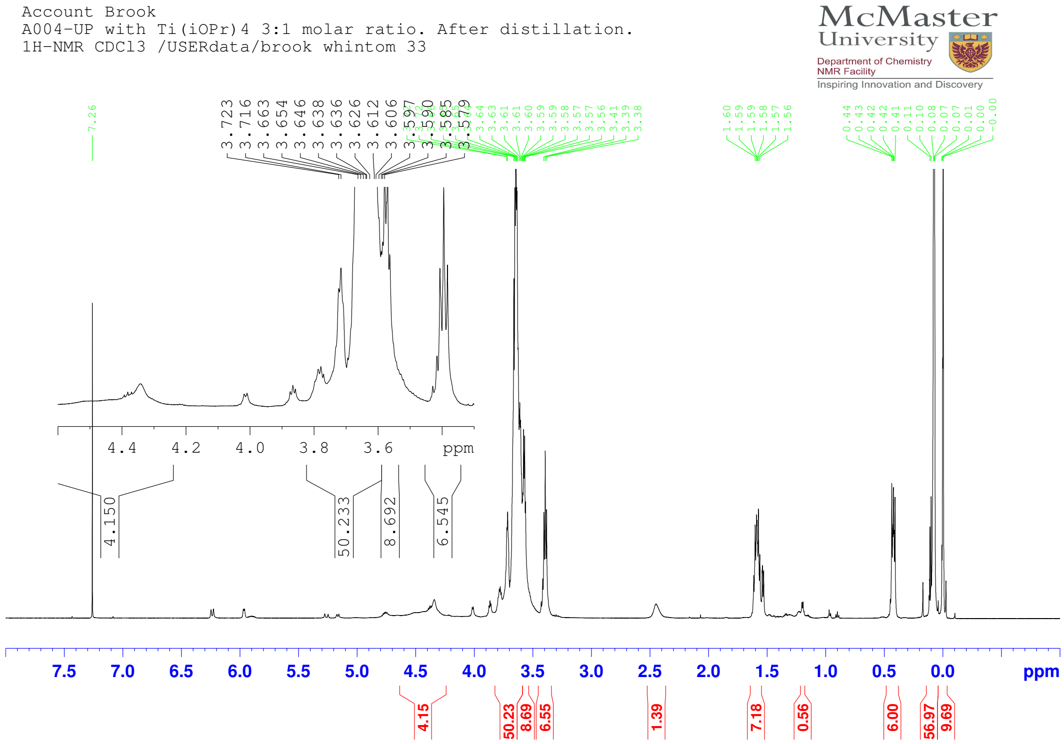

Figure 6.3.1.4: ^{1}H NMR of 3

Siloxane Surfactant A004-UP; ^{1}H'NMR (600 MHZ, CDCl$_3$, 25°C) δ: 0 (s, 3H, Si**CH$_3$**), 0.07 (s, 18H, **TMS**O-Si-O**TMS**), 0.42 (m, 2H, Si**CH$_2$**CH$_2$CH$_2$), 1.59 (m, 2H, SiCH$_2$**CH$_2$**CH$_2$), 2.5 (broad, 1H, OH), 3.4 (m, 2H, SiCH$_2$CH$_2$**CH$_2$**), 3.58 (m, 2H, HO-(CH$_2$CH$_2$O)$_3$CH$_2$**CH$_2$**OCH$_2$), 3.64 (m, 14H, HO-(**CH$_2$CH$_2$**O)$_3$**CH$_2$**CH$_2$O 3.72 (m, 2H, HO-**CH$_2$**CH$_2$(OCH$_2$CH$_2$)$_3$)

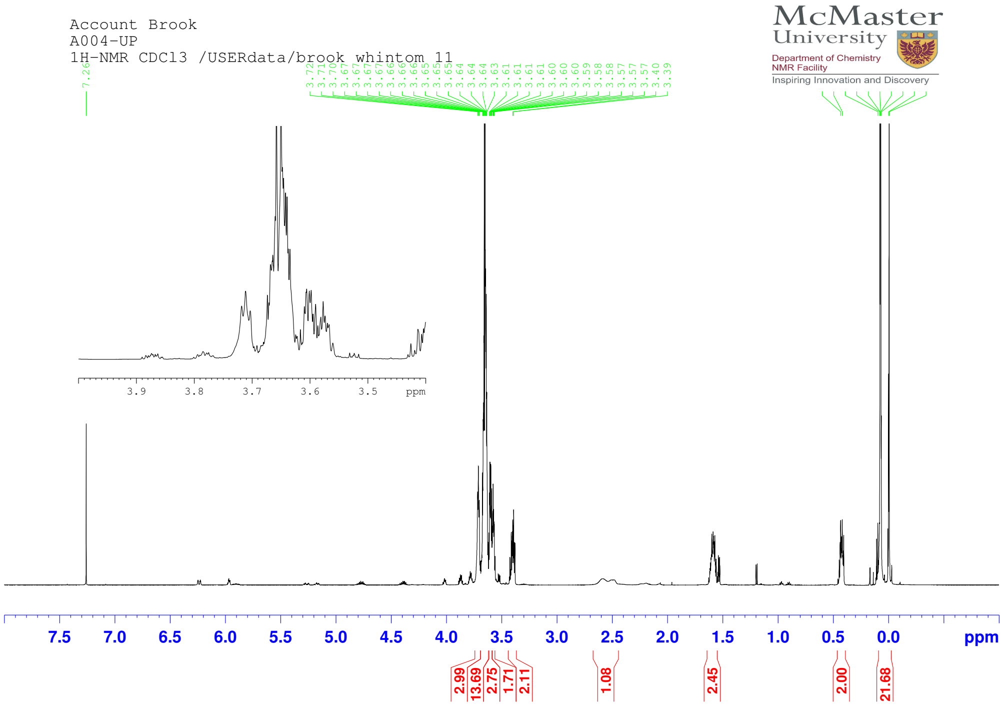

Figure 6.3.1.5: ^{1}H NMR of surfactant A004-UP.

6.3.2. Microemulsion Formulations with Mass Quantities

Table 6.3.1: Formulations and associated masses used for UV absorption measurements between quartz slides following the UV absorption of TTIP and TiO_2

Formulation	TTIP wt% (g)	Silsurf A008-UP wt% (g)	PDMS-OH (DMS S14) wt% (g)	Water wt% (g)
1	3.51 (0.0209g)	49.18 (0.2930g)	39.64 (0.2362g)	7.67 (0.0457g)
2		51.12 (0.4106g)	41.57 (0.3339g)	7.31 (0.0587g)
3	3.31 (0.0442g)	46.32 (0.618g)	37.44 (0.4997g)	12.93 (0.1725g)

4		47.80 (0.7016g)	38.84 (0.5702g)	13.36 (0.1961g)
5	3.04 (0.0702g)	43.36 (1.0007g)	35.35 (0.8158g)	18.25 (0.4211g)
6		44.69 (1.0131g)	36.50 (0.8274g)	18.81 (0.4265g)
7	2.47 (0.0718g)	34.60 (1.0072g)	28.20 (0.8208g)	34.73 (1.0111g)
8		35.55 (0.9964g)	28.92 (0.8105g)	35.54 (0.9961g)

6.3.2.1. SAXS Characterization of Microemulsion Formulation

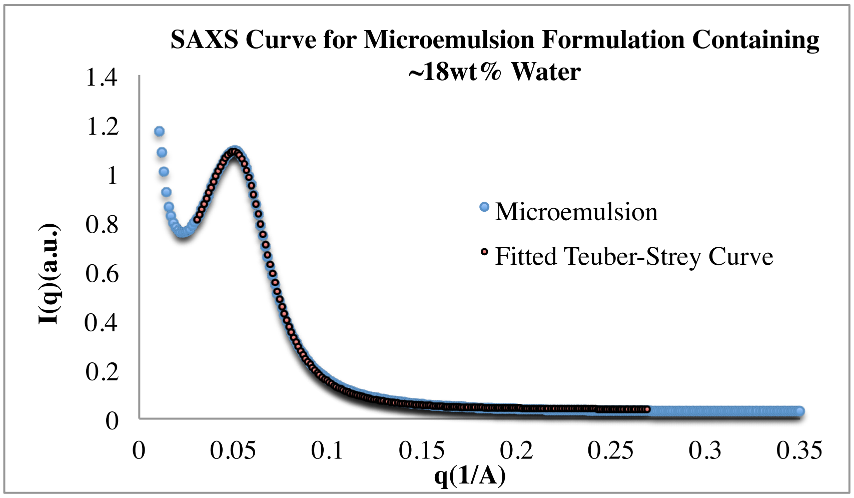

Chart 6.3.1: SAXS characterization of microemulsion formulation 6 of Table 6.3.1.

Formulation	Domain Size (nm)	Correlation Length (nm)	Amphiphilicity Factor
6	9.57	4.24	-0.69

Table 6.3.2: Microemulsion structural parameters determined by Teubner-Strey analysis of acquired scattering data.

6.3.3. Additional UV-Vis Absorbance Spectra

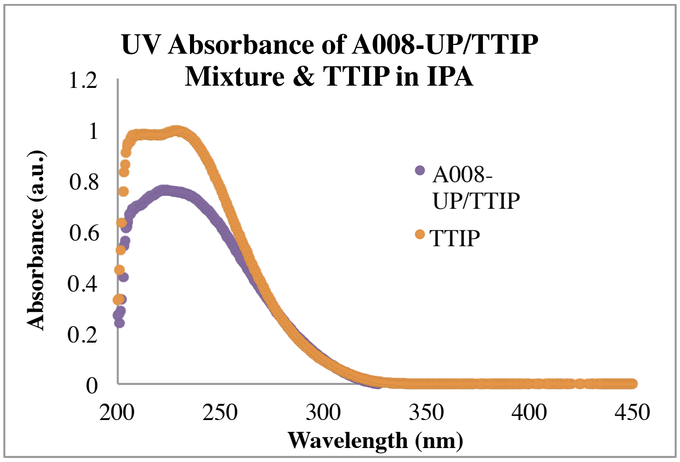

Chart 6.3.2: Differences in UV-Vis Absorption of A008-UP/TTIP mixture and TTIP in IPA.

6.3.4. Transmission Electron Microscopy

Microemulsions were broken by adding a large excess of isopropanol at various timepoints (e.g., 1 mL of IPA was added to ~0.25g of the emulsion). Titania particles were harvested from the TTIP microemulsions after 4 h of initial microemulsion preparation using centrifugation (images were only obtained for the microemulsion formulation containing ~13wt% water). The imaged particles vary in size from a few nanometers to a hundred nanometers. The edges of the particles were not well defined, which could be due to the presence of silicones as indicated by EDX (see below).

Unfortunately, attempts to directly image particles encapsulated within the gel were unsuccessful. Therefore, in order to obtain TEM images, particles had to be separated from the microemulsion and the resulting images represent the densest TiO_2 particles isolated from microemulsions (Figure 6.3.4.1 to Figure 6.3.4.3). There are, therefore, a large number of smaller particles that were could not be isolated from the microemulsion gel. Centrifugation is expected to have some degree of impact on aggregation and structure when compared to particles stabilized in the microemulsion.

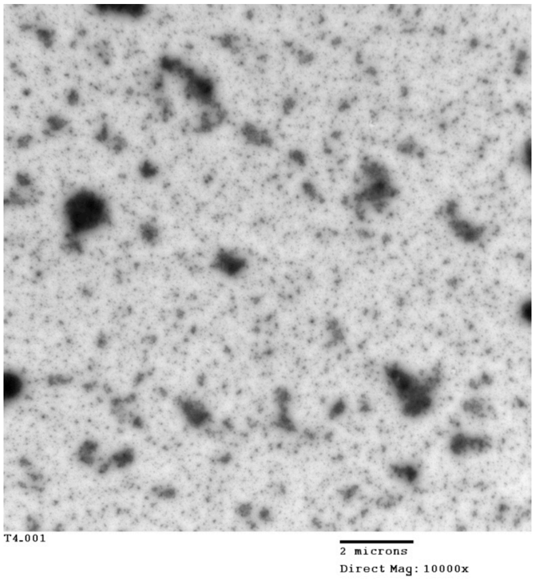

Figure 6.3.4.1: Isolated particles from medium water content microemulsion 4 hours after initial TTIP microemulsion preparation.

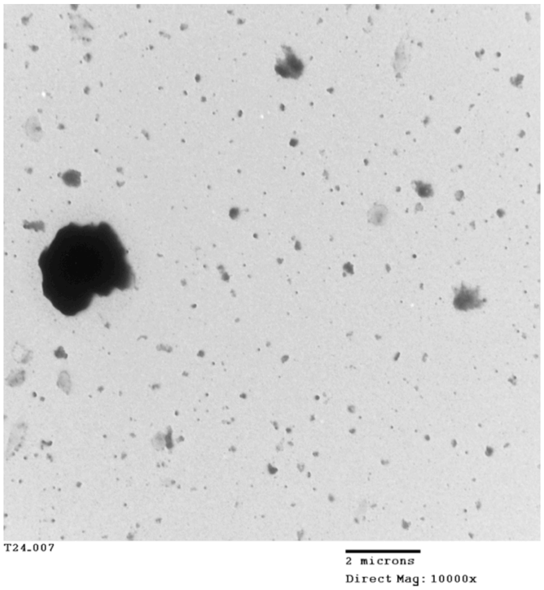

Figure 6.3.4.2: Isolated particles from medium water content microemulsion 24 hours after initial TTIP microemulsion preparation.

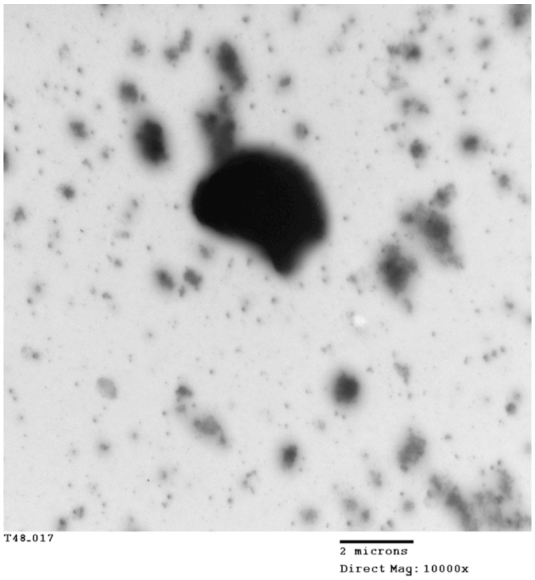

Figure 6.3.4.3: Isolated particles from medium water content microemulsion 48 hours after initial TTIP microemulsion preparation.

6.3.4.1. EDX Spectra

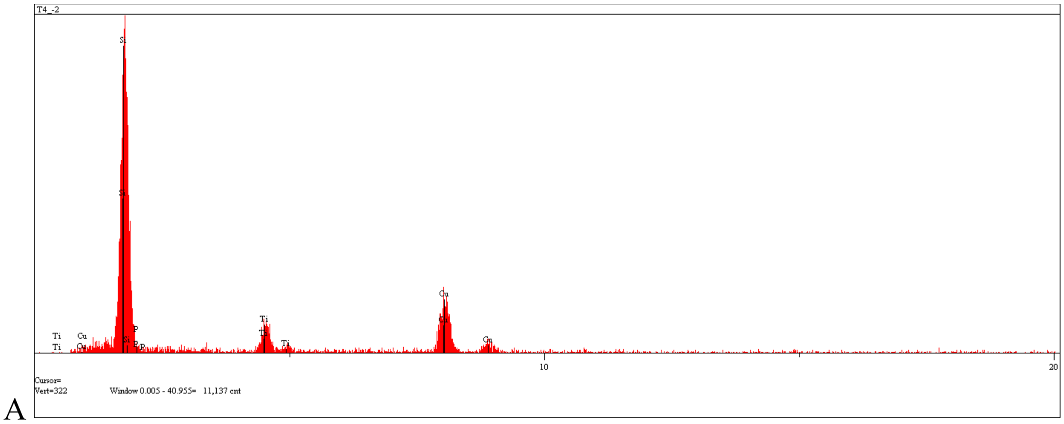

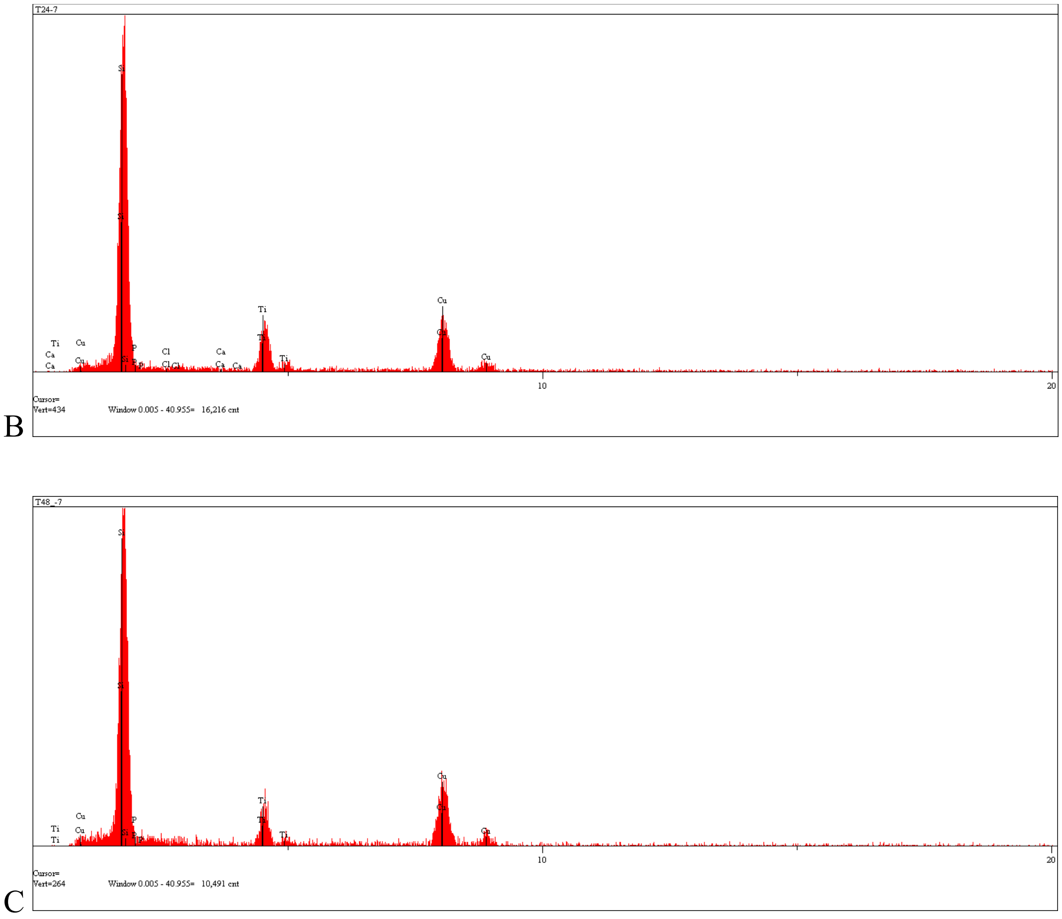

Figure 6.3.4.4: EDX of isolated particles from medium water content microemulsion after A: 4, B: 24 and C: 48 hours.

6.3.4.2. Using Image J for Particle Analysis

Titania particles formed within a silicone microemulsion containing ~13wt% water were imaged at different time points (t=4, 24, 48 h) by TEM, as previously described. Micrographs at the same magnification were analyzed and the minimum particle size cut off was kept consistent between images in order to obtain directly comparable data. The rows in the above image represent a stage in the particle analysis. The analysis assumes perfectly round particles and the diameter was calculated and reported from the resulting particle area data.

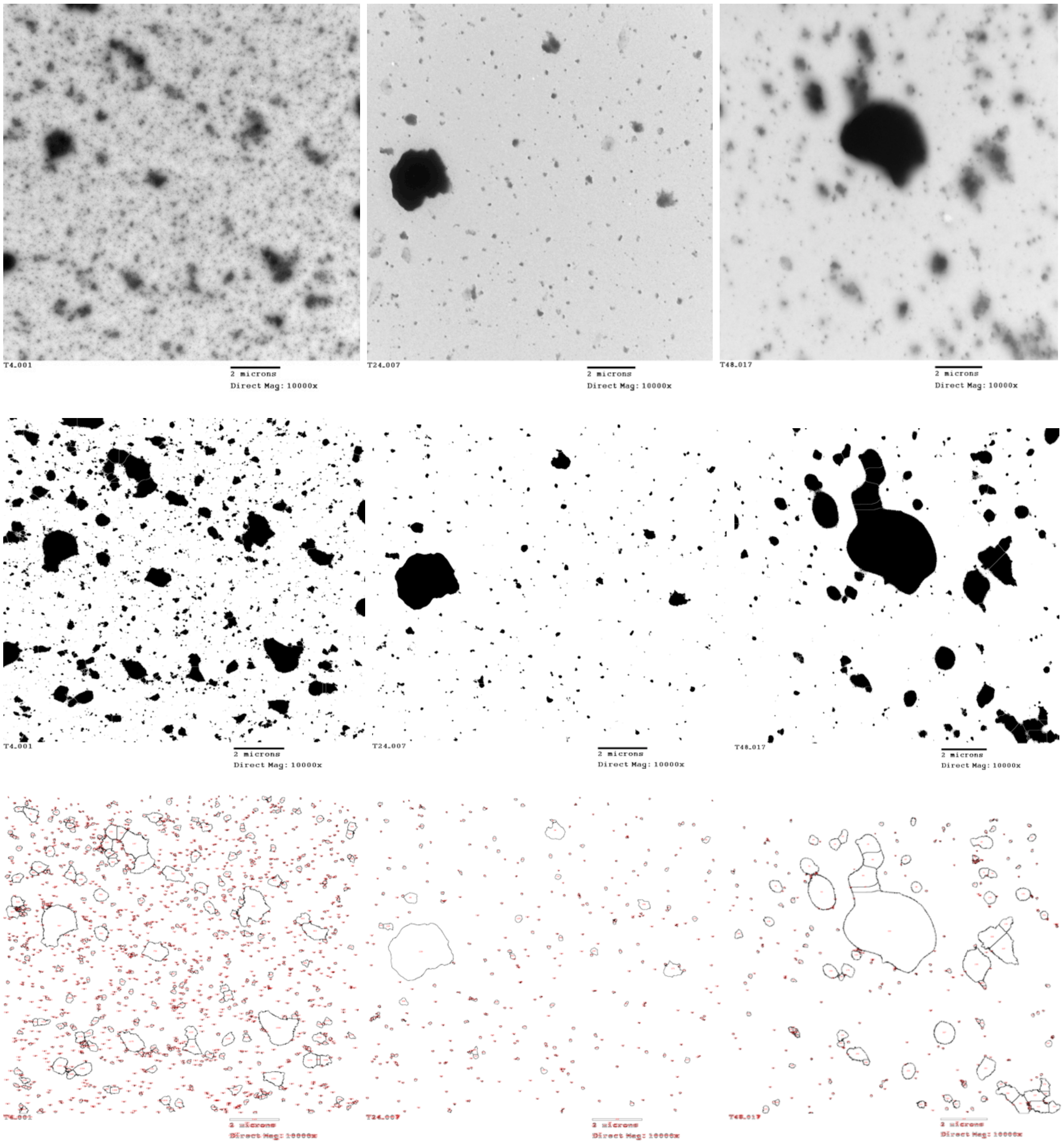

Figure 6.3.4.5: Image Analysis Steps for particle size determination at 10000X magnification.